AD-A111 513 DAVID W TAYLOR NAVAL SHIP RESEARCH AND DEVELOPMENT CE--ETC F/6 19/3
INVESTIGATION OF SMALL ROADWHEELS FOR USE ON TRACKED VEHICLES.(U)
OCT 81 D P KIHL, R A SWANEK
UNCLASSIFIED DTNSRDC-81/061 NL

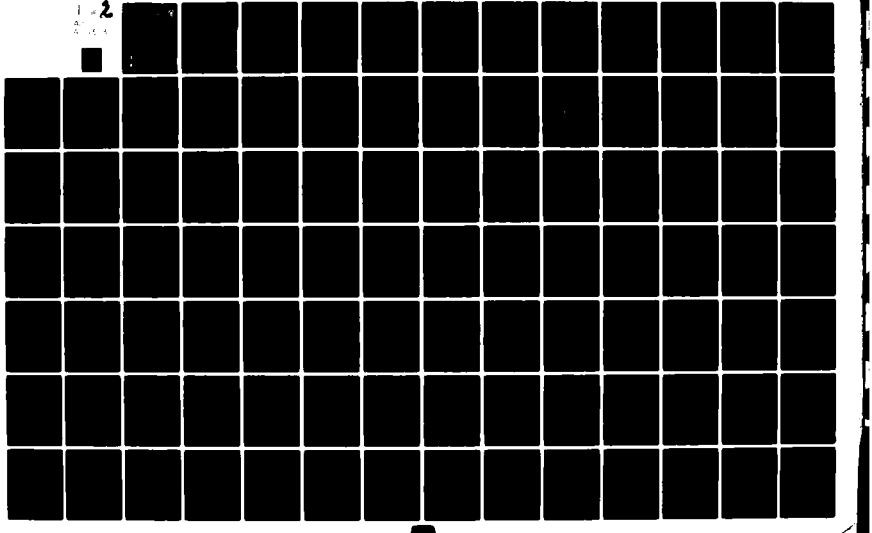

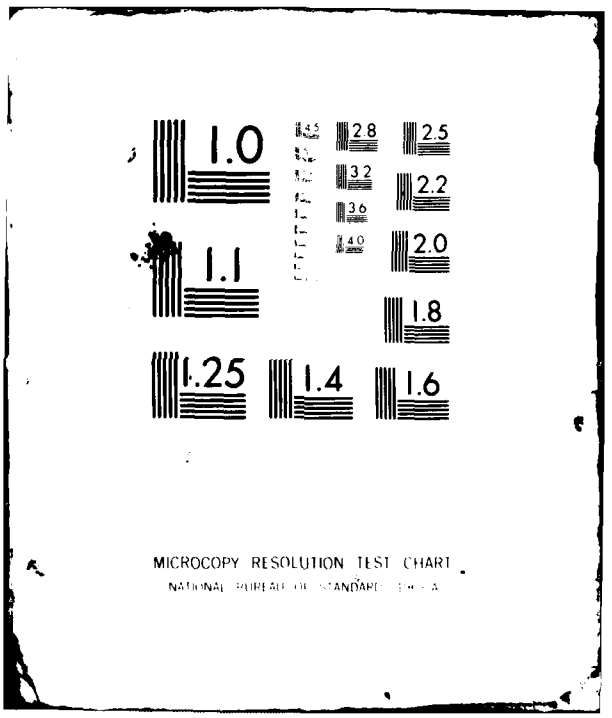
1.0
1.1
1.25
1.4
1.6
1.8
2.0
2.2
2.5
2.8
3.2
3.6
4.0
4.5
MICROCOPY RESOLUTION TEST CHART
NATIONAL BUREAU OF STANDARDS

DAVID W. TAYLOR NAVAL SHIP RESEARCH AND DEVELOPMENT CENTER

Bethesda, Maryland 20084

12

INVESTIGATION OF SMALL ROADWHEELS FOR USE ON TRACKED VEHICLES

by

David P. Kim
Richard A. Siuru

APPROVED FOR PUBLIC RELEASE: DISTRIBUTION UNLIMITED

October 1981

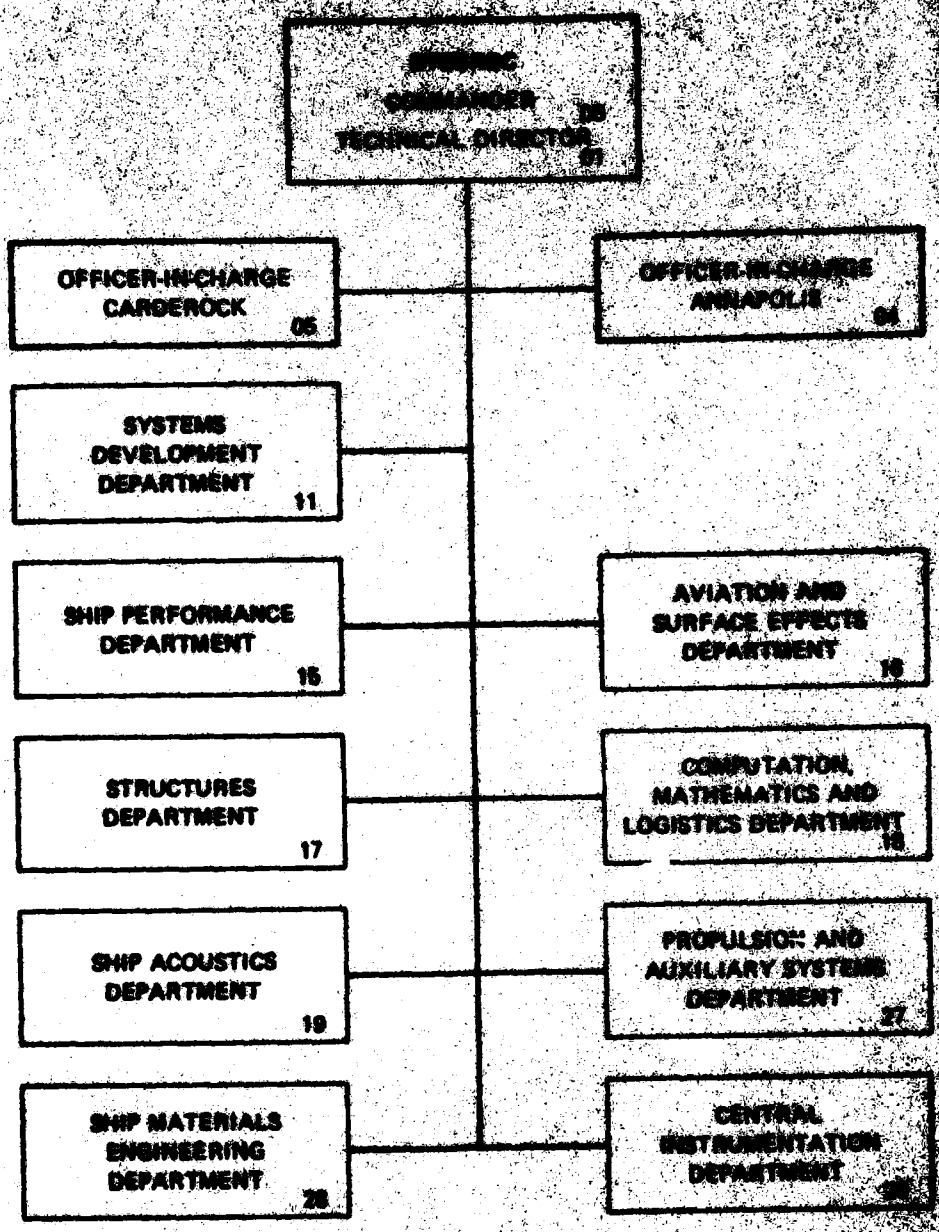
TECHNICAL DIRECTOR
01
OFFICER-IN-CHARGE
CARDEROCK
05
OFFICER-IN-CHARGE
ANNAPOLIS
04
SYSTEMS
DEVELOPMENT
DEPARTMENT
11
SHIP PERFORMANCE
DEPARTMENT
15
AVIATION AND
SURFACE EFFECTS
DEPARTMENT
16
STRUCTURES
DEPARTMENT
17
COMPUTATION,
MATHEMATICS AND
LOGISTICS DEPARTMENT
18
SHIP ACOUSTICS
DEPARTMENT
19
PROPULSION AND
AUXILIARY SYSTEMS
DEPARTMENT
27
SHIP MATERIALS
ENGINEERING
DEPARTMENT
28
CENTRAL
INSTRUMENTATION
DEPARTMENT

UNCLASSIFIED

SECURITY CLASSIFICATION OF THIS PAGE (When Data Entered)

REPORT DOCUMENTATION PAGE	READ INSTRUCTIONS BEFORE COMPLETING FORM
1. REPORT NUMBER: DTNSRDC-81/061	2. GOVT ACCESSION NO.: AD-A111 513
3. RECIPIENT'S CATALOG NUMBER	
4. TITLE (and Subtitle): INVESTIGATION OF SMALL ROADWHEELS FOR USE ON TRACKED VEHICLES	5. TYPE OF REPORT & PERIOD COVERED: Final
	6. PERFORMING ORG. REPORT NUMBER
7. AUTHOR(s): David P. Kihl, Richard A. Swanek	8. CONTRACT OR GRANT NUMBER(s)
9. PERFORMING ORGANIZATION NAME AND ADDRESS: David W. Taylor Naval Ship Research and Development Center, Bethesda, Maryland 20084	10. PROGRAM ELEMENT, PROJECT, TASK AREA & WORK UNIT NUMBERS: (See reverse side)
11. CONTROLLING OFFICE NAME AND ADDRESS	12. REPORT DATE: October 1981
	13. NUMBER OF PAGES: 96
14. MONITORING AGENCY NAME & ADDRESS (if different from Controlling Office)	15. SECURITY CLASS. (of this report): UNCLASSIFIED
	15a. DECLASSIFICATION/DOWNGRADING SCHEDULE

16. DISTRIBUTION STATEMENT (of this Report)

APPROVED FOR PUBLIC RELEASE: DISTRIBUTION UNLIMITED

17. DISTRIBUTION STATEMENT (of the abstract entered in Block 20, if different from Report)

18. SUPPLEMENTARY NOTES

19. KEY WORDS (Continue on reverse side if necessary and identify by block number)

Amphibian Tracked Landing Vehicle
Torsion Bar Suspensions
Small Roadwheels

20. ABSTRACT (Continue on reverse side if necessary and identify by block number)

The feasibility of using small roadwheels for future tracked vehicles was investigated by first analyzing an existing LVTP7 suspension and then designing a small roadwheel and roadarm assembly compatible with the LVTP7 track and suspension. Small roadwheel and roadarm assemblies will later be fabricated and placed on an existing LVTP7 for verification of design assumptions and demonstration of mechanical feasibility. The LVTP7 is an armored assault amphibious full-tracked landing vehicle.

(Continued on reverse side)

DD FORM 1 JAN 73 1473 EDITION OF 1 NOV 65 IS OBSOLETE
S/N 0102-LF-014-6601

UNCLASSIFIED

SECURITY CLASSIFICATION OF THIS PAGE (When Data Entered)

(Block 10)

Program Element 62543N
Task Area ZF43461280
Work Unit 1120-021

(Block 20 continued)

The primary benefit from using small roadwheels is a considerable internal volume gain. This internal volume can be employed either to gain buoyancy or to lower the land silhouette by redistributing the internal volume. An additional potential benefit is a more uniform ground pressure distribution.

Although small roadwheels can contribute considerable internal volume gain, they produce an undesirable vehicle vertical spring stiffness-deflection relationship when used solely with torsion bar suspensions. Auxiliary bump springs or a hydropneumatic suspension would be needed to stiffen the suspension against vertical deflections above static and produce a more desirable spring stiffness-deflection relationship.

A suspension weight study indicates that the total suspension weight should be relatively insensitive to roadwheel diameter.

Roadarm and torsion bar analysis and design procedures developed, provide a methodology for carrying out parametric studies relating roadwheel diameter to weight, buoyancy gain, and vehicle ride characteristics.

TABLE OF CONTENTS

LIST OF FIGURES

LIST OF TABLES

NOTATION

A	Cross sectional area of roadarm	(square inches)
a	Ratio of γ_{yp}/γ_p or r_i/r	
b	Width of roadarm cross section	(inches)
C_w	Torsional warping constant	(sextuple inches)
D	Roadwheel diameter	(inches)
D_T	Torsion tube outer diameter	(inches)
d	Torsion bar diameter	(inches)
d_T	Torsion tube inner diameter	(inches)
E	Modulus of elasticity	(kips per square inch)
F.S.	Factor of Safety	
f	Frequency	(Hz)
G	Shear modulus of rigidity	(kips per square inch)
h	Height of roadarm cross section	(inches)
J	Torsional constant	(quadruple inches)
K	Vertical spring rate of each roadwheel	(kips per inch)
K_{TOTAL}	Total vertical spring rate of vehicle	(kips per inch)
k	Rotational spring rate	(inch-kips per radian)
k_{BAR}	Rotational spring rate torsion bar	(inch-kips per radian)
k_{eq}	Equivalent rotational spring rate of torsion tube over bar	(inch-kips per radian)
k_{TUBE}	Rotational spring rate of torsion tube	(inch-kips per radian)
L_A	Allowable load per inch of nominal tire width	(pounds per inch)
L_B	Active length of torsion bar	(inches)
L_{eff}	Effective length of roadarm between hubs	(inches)
L_T	Active length of torsion tube	(inches)
M_x	Torsional moment about x-axis of roadarm	(inch-kips)

M_y	Bending moment about y-axis of roadarm	(inch-kips)
M_z	Bending moment about z-axis of roadarm	(inch-kips)
N	Number of roadwheels per vehicle	
P_h	Horizontal wheel load, positive outward	(kips)
P_v	Vertical wheel load, positive upward	(kips)
P_{v_s}	Vertical wheel load at the static position	(kips)
R	Length of roadarm	(inches)
r	Radius of torsion bar	(inches)
r_i	Intermediate radius locating elastic-plastic core of torsion bar during presetting	(inches)
SM_y	Section modulus of roadarm cross section about y-axis of roadarm	(cubic inches)
SM_z	Section modulus of roadarm cross section about z-axis of roadarm	(cubic inches)
T	Torque applied on torsion bar	(inch-kips)
T_{PRESET}	Torque required to preset torsion bar	(inch-kips)
$T_{PRESET\ UNLOAD}$	Torque required to unload torsion bar from preset torque	(inch-kips)
T_{yp}	Torque required to initiate yielding of torsion bar during presetting	(inch-kips)
V_x	Axial force along x-axis of roadarm	(kips)
V_y	Shear force along y-axis of roadarm	(kips)
V_z	Shear force along z-axis of roadarm	(kips)
W	Weight of combat equipped vehicle	(kips)
W_B	Weight of torsion bar	(pounds)
W_H	Weight of roadwheel hub and spindle	(pounds)
W_R	Weight of roadwheel rubber tire tread	(pounds)
W_{RA}	Weight of roadarm	(pounds)
W_S	Weight of steel wear ring	(pounds)

W_T	Weight of torsion tube	(pounds)
W_{TA}	Weight of trunnion and torsion bar anchors	(pounds)
W_W	Weight of roadwheel rim and web	(pounds)
X,Y,Z	Coordinate axes used in roadarm design	
X_o, Y_o, Z_o	Coordinates locating centroid of roadarm cross section when roadarm is in the horizontal position	
α	Roadarm angle of inclination toward or away from vehicle hull. Positive away from vehicle.	(radians)
β	Angle roadarm makes with horizontal under zero load. Positive below horizontal.	(radians)
γ_{max}	Maximum torsional shear strain in torsion bar	
γ_p	Torsional shear strain required to preset torsion bar	
γ_{yp}	Torsional yield shear strain in torsion bar	
Δ	Vertical deflection of the end of the roadarm from the static load position. Positive upward.	(inches)
ΔB	Change in buoyancy associated with dropping sponson	(pounds)
ΔW	Change in total suspension weight	(pounds)
$\Delta\tau$	Residual shear stress remaining after presetting	(kips per square inch
δ	Vertical deflection of the end of the roadarm from the zero load position. Positive upward.	(inches)
θ	Angle roadarm makes with horizontal reference line under vertical wheel load P_v. Positive above reference line.	(radians)
θ_s	Angle roadarm makes with horizontal reference line under static wheel load P_s. Positive above reference line.	(radians)
θ_{10}	Angle roadarm makes with horizontal reference line when Δ = 10 inches. Positive above reference line.	(radians)
μ	Poisson's ratio	
σ_{Ax}	Axial stress in x-direction of roadarm	(kips per square inch

σ_{My}	Bending stress in x-direction of roadarm due to moment M_y	(kips per square inch)
σ_{Mz}	Bending stress in x-direction of roadarm due to moment M_z	(kips per square inch)
σ_y	Tensile yield stress	(kips per square inch)
σ_W	Warping stress in x-direction of roadarm due to torque M_x	(kips per square inch)
σ_1	Combined longitudinal stress at corner 1 of roadarm cross section	(kips per square inch)
σ_2	Combined longitudinal stress at corner 2 of roadarm cross section	(kips per square inch)
σ_3	Combined longitudinal stress at corner 3 of roadarm cross section	(kips per square inch)
σ_4	Combined longitudinal stress at corner 4 of roadarm cross section	(kips per square inch)
τ_{BAR}	Shear stress in torsion bar	(kips per square inch)
$\tau_{BAR_{10}}$	Shear stress in torsion bar when Δ = 10 inches	(kips per square inch)
$\tau_{BOTTOM\ EDGE}$	Combined shear stress along bottom edge of roadarm cross section	(kips per square inch)
$\tau_{INBOARD\ EDGE}$	Combined shear stress along inboard edge of roadarm cross section	(kips per square inch)
$\tau_{OUTBOARD\ EDGE}$	Combined shear stress along outboard edge of roadarm cross section	(kips per square inch)
τ_p	Shear stress in torsion bar during presetting	(kips per square inch)
$\tau_{TOP\ EDGE}$	Combined shear stress along top edge of roadarm cross section	(kips per square inch)
τ_{TUBE}	Shear stress in torsion tube	(kips per square inch)
τ_{Vy}	Shear stress on roadarm cross section due to shear force V_y	(kips per square inch)
τ_{Vz}	Shear stress on roadarm cross section due to shear force V_z	(kips per square inch)
τ_{Wb}	Shear stress along width of roadarm cross section due to torque M_x	(kips per square inch)
τ_{Wh}	Shear stress along depth of roadarm cross section due to torque M_x	(kips per square inch)

τ_{yp}	Shear stress yield point	(kips per square inch)
ϕ	Torsion bar windup angle ($\theta+\beta$)	(radians)
ϕ_{max}	Maximum torsion bar windup during presetting	(radians)
ϕ_p	Torsion bar windup required to preset torsion bar	(radians)

ABSTRACT

The feasibility of using small roadwheels for future tracked vehicles was investigated by first analyzing an existing LVTP7 suspension and then designing a small roadwheel and roadarm assembly compatible with the LVTP7 track and suspension. Small roadwheel and roadarm assemblies will later be fabricated and placed on an existing LVTP7 for verification of design assumptions and demonstration of mechanical feasibility. The LVTP7 is an armored assault amphibious full-tracked landing vehicle.

The primary benefit from using small roadwheels is a considerable internal volume gain. This internal volume can be employed either to gain buoyancy or to lower the land silhoue redistributing the internal volume. An additional potential benefit is a more uniform ground pressure distribution.

Although small roadwheels can contribute considerable internal volume gain, they produce an undesirable vehicle vertical spring stiffness-deflection relationship when used solely with torsion bar suspensions. Auxiliary bump springs or a hydropneumatic suspension would be needed to stiffen the suspension against vertical deflections above static and produce a more desirable spring stiffness-deflection relationship.

A suspension weight study indicates that the total suspension weight should be relatively insensitive to roadwheel diameter.

Roadarm and torsion bar analysis and design procedures developed, provide a methodology for carrying out parametric studies relating roadwheel diameter to weight, buoyancy gain, and vehicle ride characteristics.

ADMINISTRATIVE INFORMATION

The work described herein was performed by the Ship Structures Division of the Structures Department for the Marine Corps Program Office of the Systems Development Department at the David W. Taylor Naval Ship Research and Development Center (DTNSRDC) under Program Element 62543N, Task Area ZF43461280, and Work Unit 1120-021 during calendar year 1980.

METRIC CONVERSION

1 inch (in) = 2.54×10^{-2} meters

1 inch-kip = 112.98 newton-meters

1 inch-kip per radian = 112.98 newton-meters per radian

1 kip = 4.448×10^{3} newtons

1 kip per square inch = 6.895×10^{6} pascals

1 pound (lb) = 4.448 newtons

INTRODUCTION

The feasibility of small roadwheels was investigated for use on amphibious tracked vehicles. Although both land and amphibious tracked vehicles can use small roadwheels, the primary benefit can be more effectively realized by an amphibious vehicle. This primary benefit is a considerable internal volume gain, which can result in either a lower land silhouette with the same vehicle buoyancy or an increase in buoyancy with the same vehicle silhouette. The prominent features of the LVTP7 associated with this study are given in Figure 1. The internal volume gain results from an increased clearance or cavity created between the sponson (the part of the hull directly above the roadwheels, and the roadwheels when smaller roadwheels are used. When the sponson is dropped over this cavity, an increase in interval volume is achieved. This internal volume increase can then be employed as either a gain in buoyancy and the ability to carry more waterborne payload, or as a redistribution of the internal volume to reduce the land silhouette while maintaining the same amount of vehicle waterborne freeboard.

Also, by using more smaller roadwheels in place of fewer larger roadwheels, a more uniform ground pressure distribution can be obtained to reduce local track sinkage. The resulting ride quality change is assessed in terms of vehicle spring rate,* and can be evaluated with full-scale tests.

The approach was, therefore, aimed at designing small roadwheels for an existing LVTP7 in order to assess their feasibility. If the design concept was feasible, and the resulting vehicle spring rate was acceptable, then a pair of small roadwheels

---

*Spring rate is defined as the change in wheel load as a function of vertical wheel deflection.

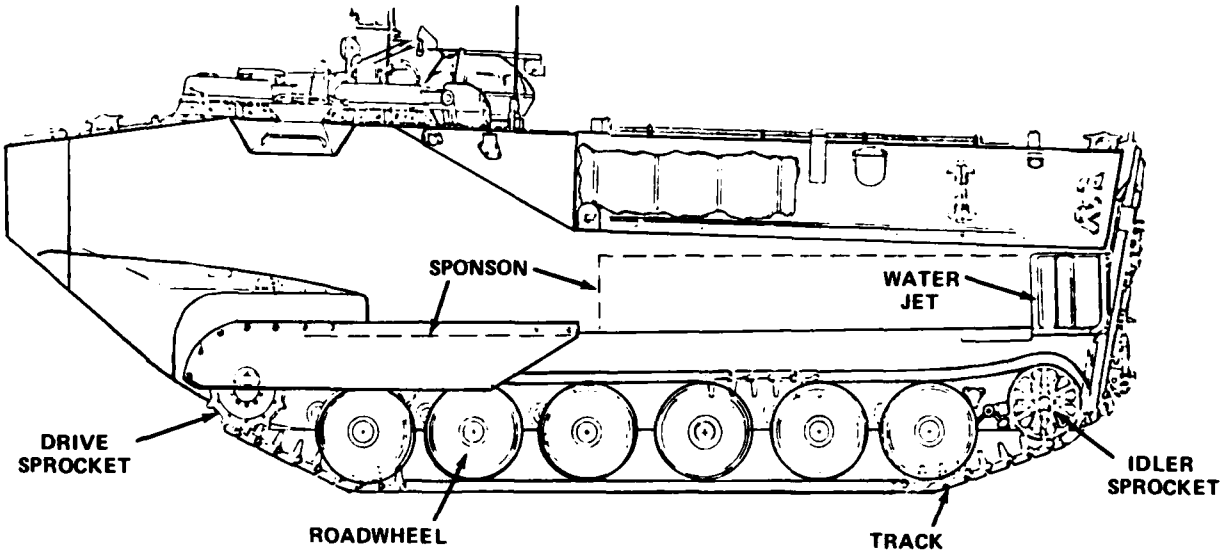

Figure 1 - Prominent Features of LVTP7

could be fabricated and placed on an LVTP7 for full-scale evaluation. The intent of this approach is not to modify the LVTP7, but to test the feasibility of small roadwheels as opposed to the larger existing roadwheels.

The design process proceeded in two stages. First, a pair of roadarms and small roadwheels was designed for installation on an LVTP7 as it exists without modifications to the existing track and suspension system (as indicated in Figure 2). This was done in order to conduct full-scale evaluations to validate the design procedures and to demonstrate structural and mechanical feasibility. Second, a set of roadarms and small roadwheels was designed to be installed on the LVTP7 as a complete set, making any modifications to the track and suspension system necessary to accommodate a final usable design. This design would represent how small roadwheels could best be configured on a vehicle like the LVTP7.

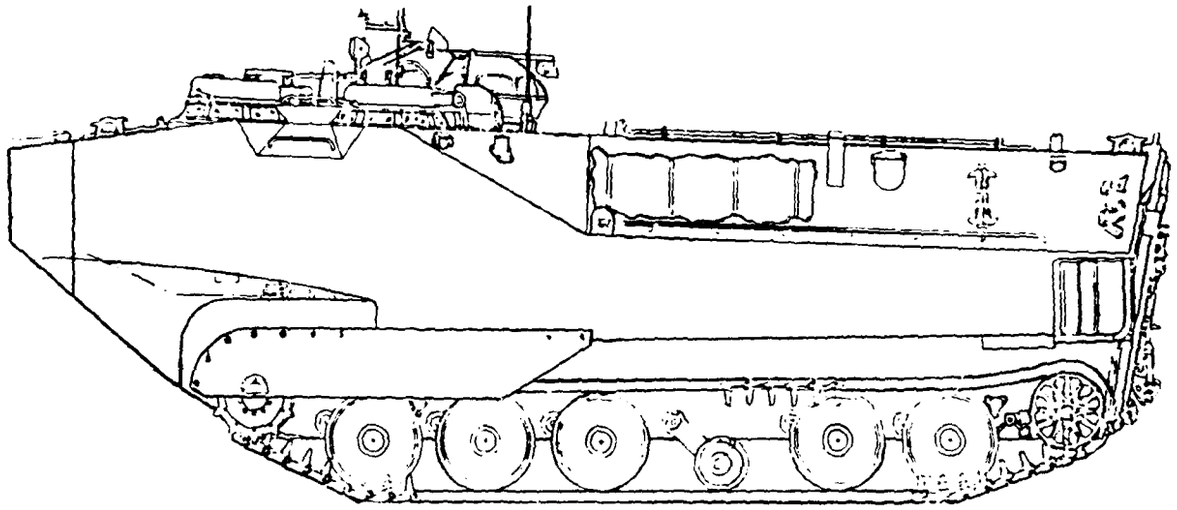

Figure 2 - Small Roadwheel Installed for Full-Scale Evaluation

EXISTING LVTP7 ROADWHEEL

To be adaptable to an existing LVTP7, the roadwheel and roadarm assemblies must conform to the existing track and suspension in much the same way as the existing assemblies. The existing LVTP7 suspension with the roadarm fully extended is shown in Figure 3. The existing wheel is made up of two symmetrical halves of forged aluminum. These halves are mounted onto a hub and held in place by ten studs bolted through the hub and wheel web. Rubber tire tread, vulcanized to the outside wheel flange, serves as a cushion between the steel track and roadwheel to reduce noise, provide a smoother ride, and prevent metal to metal contact between the wheel and track. The track blocks are also rubber padded in the area along which the wheels ride. When assembled back to back the wheel halves form a cavity near the outer wheel edge which accommodates the track guide. This cavity is deeper than the height of the track guide so that in the event of a tire tread loss, metal to metal contact between the top of the track guide and the wheel can be avoided. Also, to prevent the steel track guide from damaging the aluminum wheel, steel wear rings are riveted to the insides of this cavity.

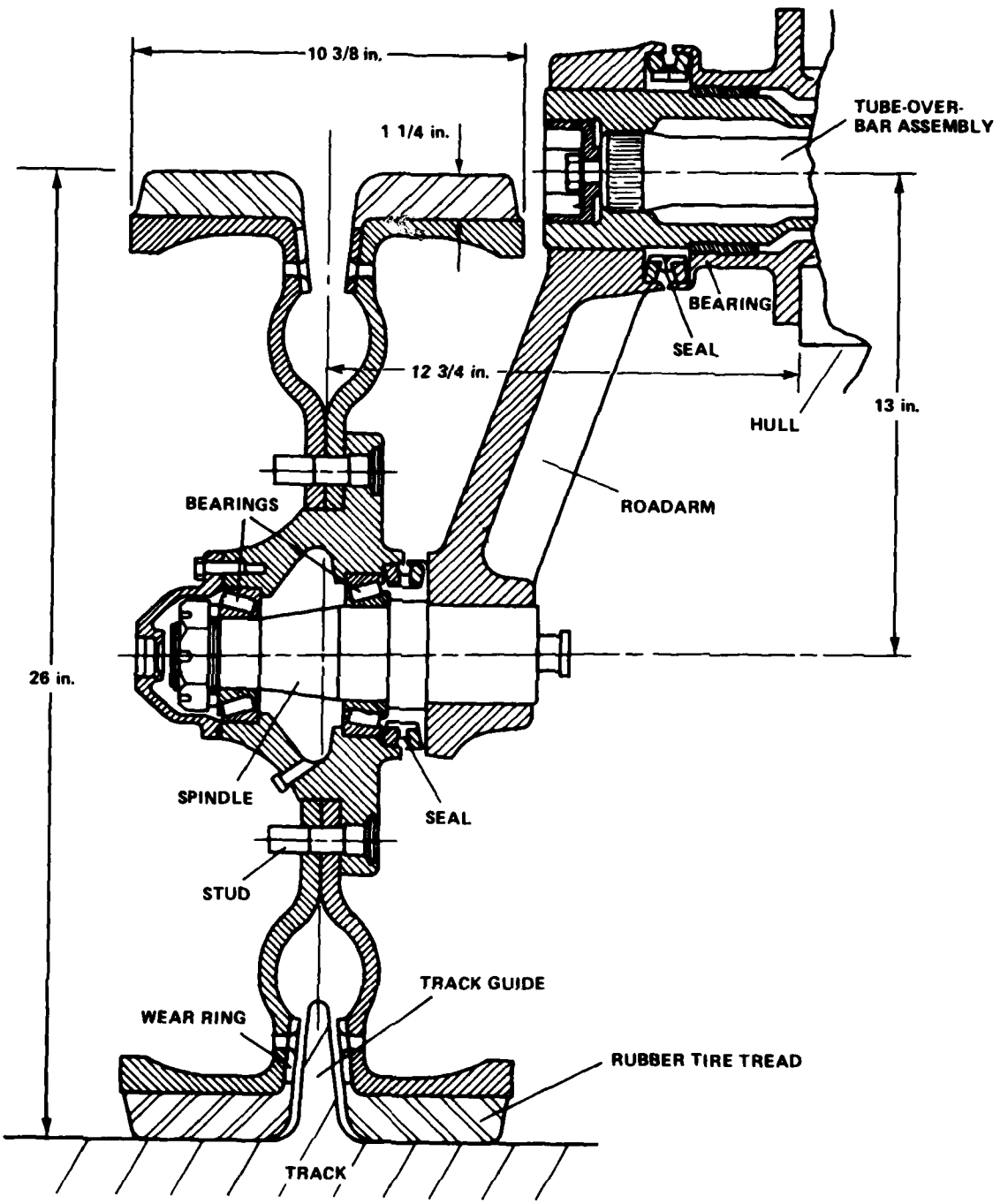

Figure 3 - Existing LVTP7 Suspension

The roadwheels are mounted on a cast aluminum hub which holds the studs in place. The hub contains the wheel bearings and bearing lubricant, and is held in place on a spindle with a retaining nut and cotter pin. The bearings are seated on the spindle and positioned on either side of the roadwheel centerline to evenly distribute the wheel load.

Lubricant seals are included between the spindle and hub to contain the lubricant inside the hub and keep out contaminants, such as sand, saltwater, snow, etc. The spindle is shrunk fit rigidly into a roadarm connected to a torsion tube-over-bar type suspension.

SMALL ROADWHEEL DESIGN

A smaller roadwheel requires the same basic shape as that of the existing roadwheel to be compatible with the track and track guide dimensions. The diameter of the smaller roadwheel is a function of the track guide height, tire tread thickness, and a certain amount of "usable diameter" to mechanically attach the roadwheel to the rest of the suspension system.

Blowout occurs when heat, produced by flexing, breaks down the rubber in the center of the tire tread. The tire tread must, therefore, be sized to overcome the danger of blowout.[1*] The tread thickness used in the small roadwheel design is the same as that of the existing tire tread, and within recommended thicknesses for vehicles of this type. Further, the rubber is assumed to exhibit the same level of performance under similar operating conditions.[2] Even though blowout has been accounted for, loss of the rubber tread can still occur through contact with rock and other debris caught between the tire and track (chunking). The small roadwheel must, therefore, be designed to accommodate the track guide in the event of tread loss.

As shown in Figure 4, the amount of "usable diameter" (to accommodate the spindle, bearings, etc.) remaining for mounting is, therefore, reduced by 10 inches from any diameter wheel selected, because of the LVTP7 track guide height and the necessary thickness of rubber required. To realize the most internal volume gained by lowering the sponson, a roadwheel with as small a diameter as possible must be incorporated into the suspension system. Therefore, the philosophy followed was to

*A complete listing of references is given on page 83.

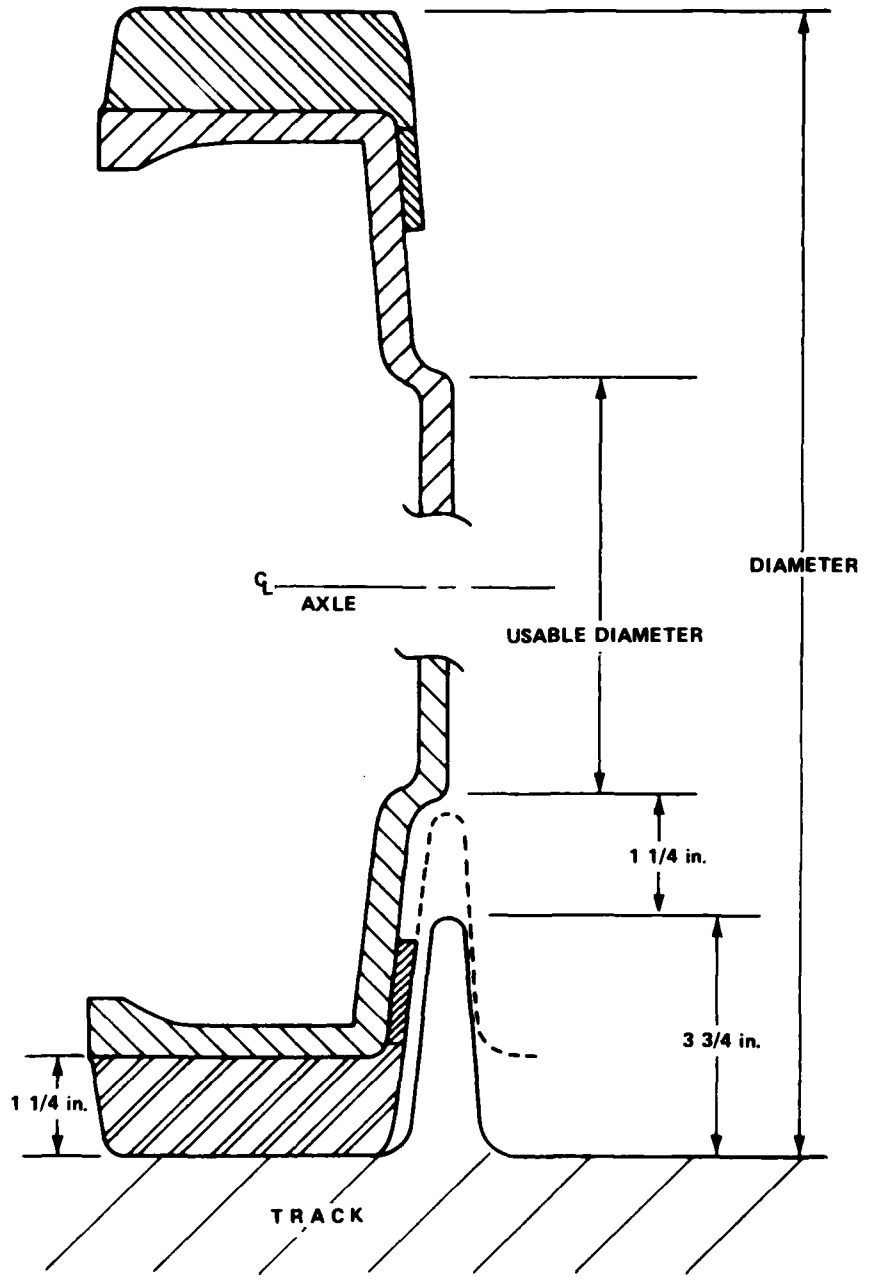

Figure 4 - Usable Diameter of Small Roadwheel

design a roadwheel as small as possible to maximize this internal volume gain, but compatible with the existing track guide and suspension dimensions.

The existing roadwheel, because of its large diameter, has ample usable diameter with which to mount the roadwheel. Unfortunately, to design a small roadwheel, very little usable diameter is available to accommodate a roadwheel hub.

To minimize the amount of usable diameter required, a first design concept was proposed employing the roadarm to house the spindle, bearings, seal, etc., similar to the way the hub was employed on the existing design. Figure 5 illustrates a conceptual drawing of this first design attempt. With the bearings, spindle, etc. relocated in the roadarm, the diameter of the wheel required for mounting decreases considerably. The spindle can be extended through the wheel web and the wheel mounted in place with a knock-off nut. The bearings and spindle are accessible from the inboard side of the roadarm hub and can be replaced by removing a hub cap. The bearings are held in place by a retaining nut and cotter pin. Selection of bearings presented a problem in this type of design because the bearings are not centered about the wheel centerline (line of load application), but rather, are placed on one side of the wheel centerline inside the roadwheel hub. This off-centered type of configuration induces larger loads into the bearings than the centered configuration does. Bearings of sufficient load carrying capacity were found to have an outside diameter on the order of 8 inches, requiring an even larger roadarm hub to contain them. Although this design is feasible, the size of the roadarm hub and spindle to accommodate the bearings considerably increases the weight of the assembly and results in the wheel diameter approaching that of the existing roadwheel.

An alternative approach which also attempted to eliminate the hub and bearings from the usable diameter of the roadwheel proved to be a more practical design. Figure 6 illustrates the basic configuration of this design. The design basically involves building up the wheel web and using the roadwheel itself as the hub. The bearings, in this design, are centered about the roadwheel centerline, greatly reducing the wheel bearing load, and consequently, the bearing size. Bearings on the order of 5 inch outside diameter and 2 inch inside diameter can be selected which are suitable in size and load carrying capacity. Because only the spindle passes through the usable wheel diameter dimension, a 14 inch wheel diameter can be obtained. As before, existing tire tread thickness, bearing seal, and steel wear rings are included in the design. The inboard end of the spindle is shrunk fit into

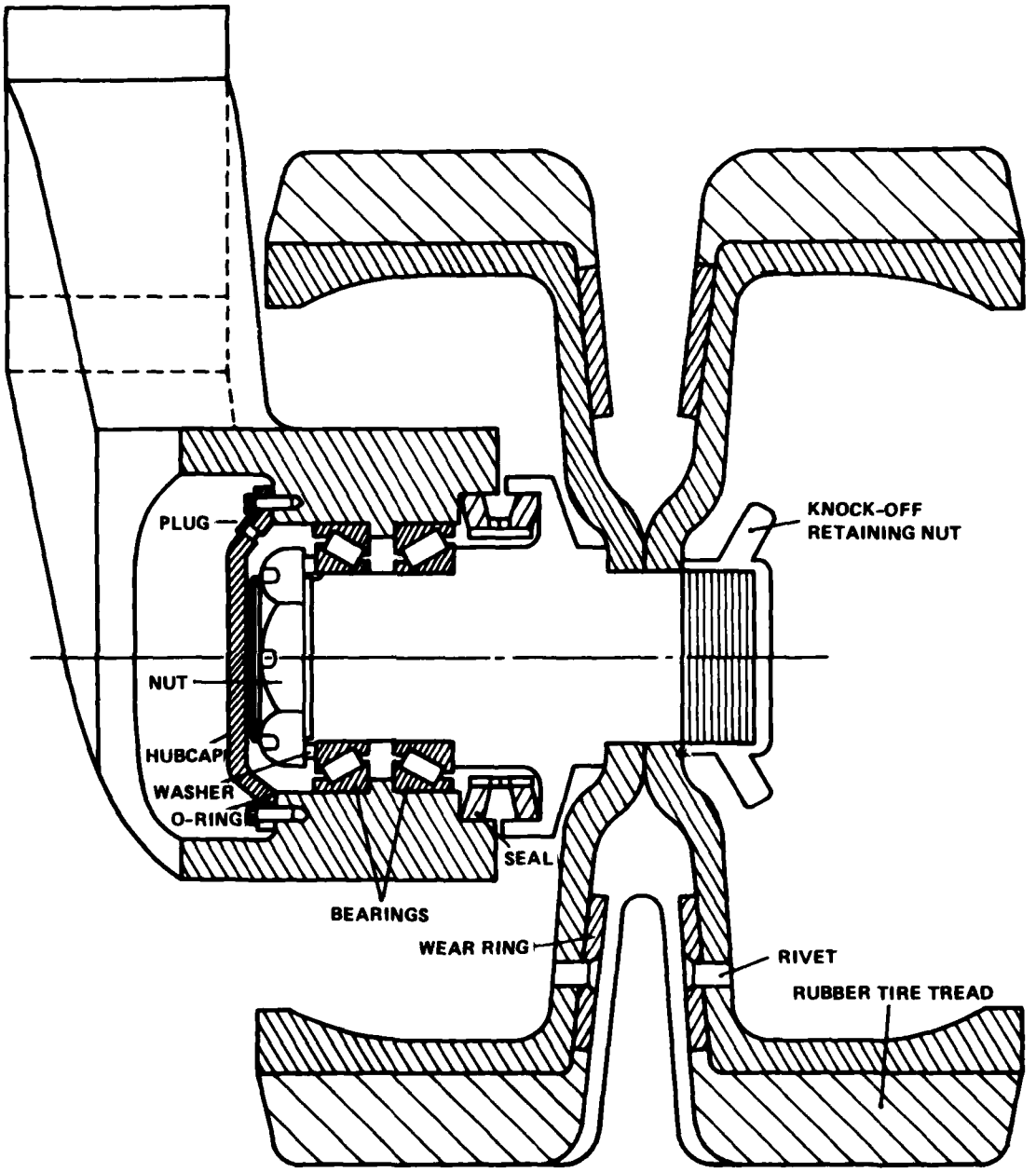

Figure 5 - Roadarm Used as Hub

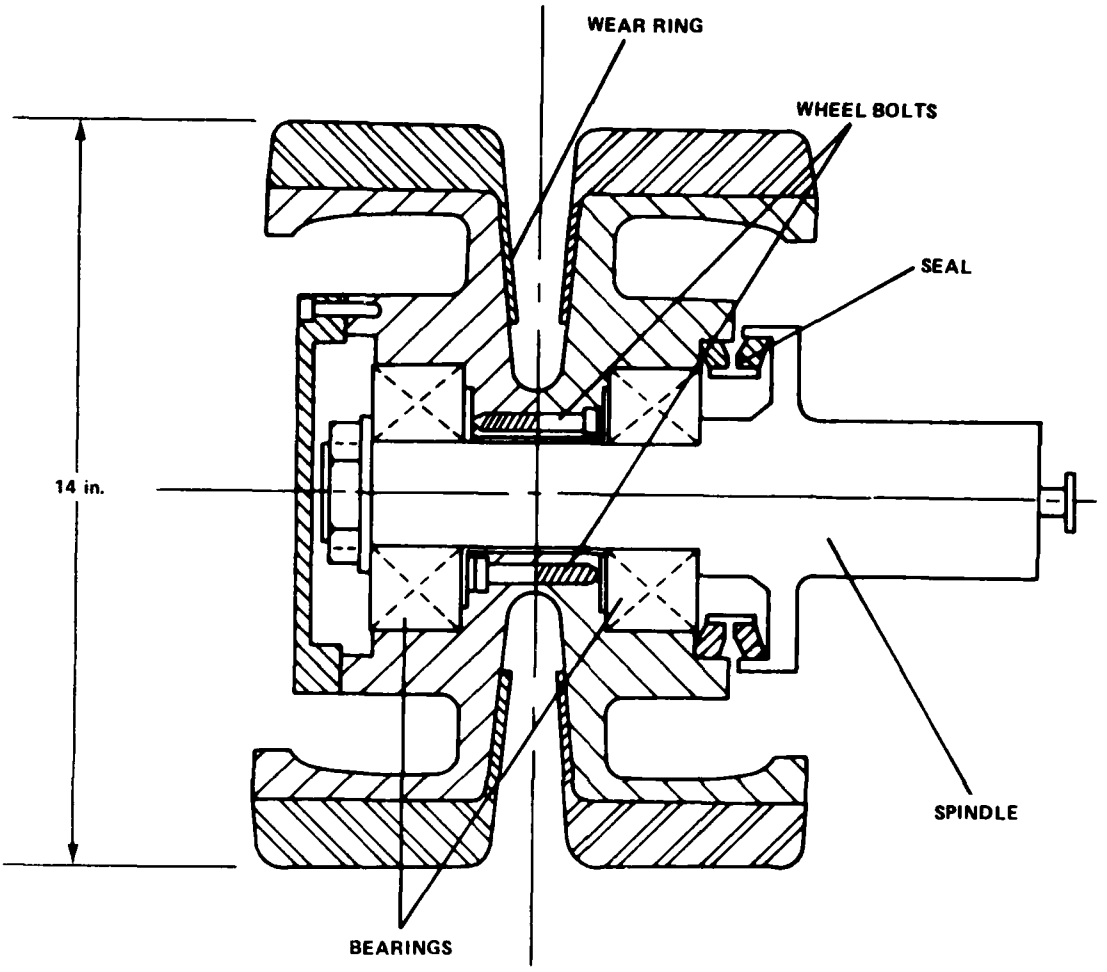

Figure 6 - Roadwheel Used as Hub

the lower end of the roadarm, extends through the wheel, and is held in place by a retaining nut and cotter pin. The wheel halves are made of cast aluminum and are symmetric; each half being used interchangeably as either an inboard or an outboard wheel half. Before being mounted onto the vehicle, the two wheel halves must be joined together by alining and bolting six wheel bolts. The wheel can then be mounted onto the vehicle as a single unit. Wheel studs, as used in the existing design, are not needed because the wheel load is transmitted directly to the bearings and into the spindle. The bearing lubricant is contained by a wheel cover which extends over the retaining nut. The lubricant can be inserted or drained through a plug located in the wheel cover.

The bearings selected* for this design were based on bearing load-carrying capacity scaled from the existing bearing specifications and vehicle revolutions per minute requirements. The scaled load-carrying capacity reflects the ratio of existing number of roadwheels to the number of smaller roadwheels per vehicle; and the increase in revolutions per minute similarly reflects the decrease in diameter from the larger existing roadwheel to the smaller roadwheel. The new bearings have a greater operating life expectancy than the existing wheel bearings.

SINGLE AND TANDEM SMALL ROADWHEEL CONFIGURATIONS

The small roadwheel concept can be used individually or in a tandem set configuration, as shown in Figure 7. The tandem set configuration was designed to evaluate the relative weights of each concept. The same 14 inch diameter roadwheel, which can be used in the single wheel per suspension unit design, can also be linked to another identical roadwheel to form a tandem set of roadwheels connected to the same suspension unit. The two roadwheels are joined by a lower roadarm having a hub at either end to accept the wheel spindles and a third hub at the center where an upper roadarm connects it to the torsion bar. A large spindle, shrunk fit into this center hub of the lower roadarm, extends through the hub at the end of the upper roadarm containing sleeve bearings. The upper roadarm and sleeve bearings are held in place by a cap bolted to the inboard side of the spindle. The lower roadarm is, therefore, free to pivot with respect to the upper roadarm. There are presently no damping or shock absorbing devices included in this tandem roadwheel design. Due to their location, roadwheels at or near the center of the vehicle are usually not equipped with shock absorbers because shock control at these locations is of minimal value. However, if this design is to be used effectively, the extreme front and rear roadwheel set should be equipped with direct acting shock absorbers attached between the hull and upper roadarm.

The relative size and location of the single and tandem roadwheels can be seen in their proper perspective with respect to the larger existing roadwheel in Figure 8.

---

*Timken bearing 619 cone 613X cup or equivalent.

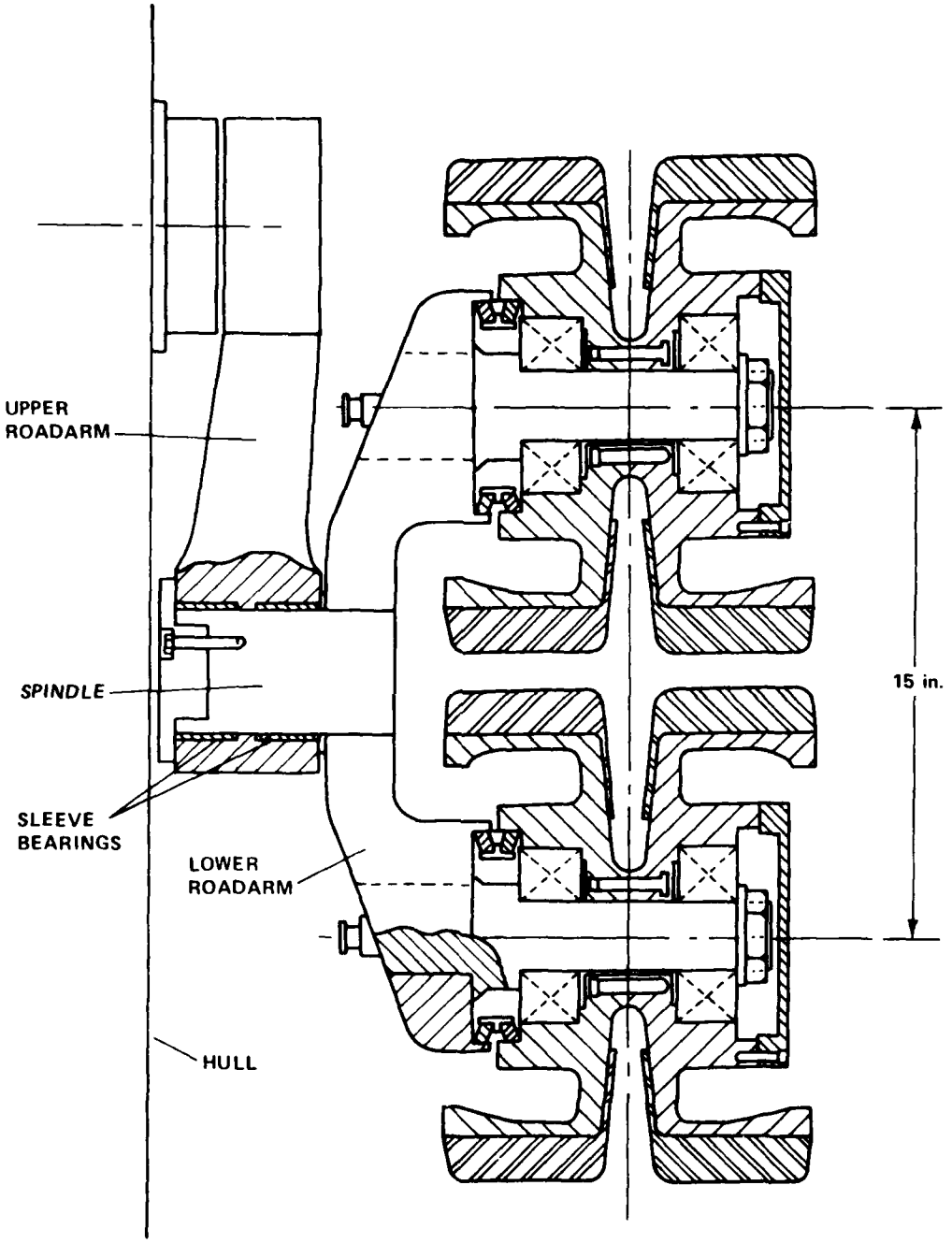

Figure 7 - Tandem Roadwheel Configuration

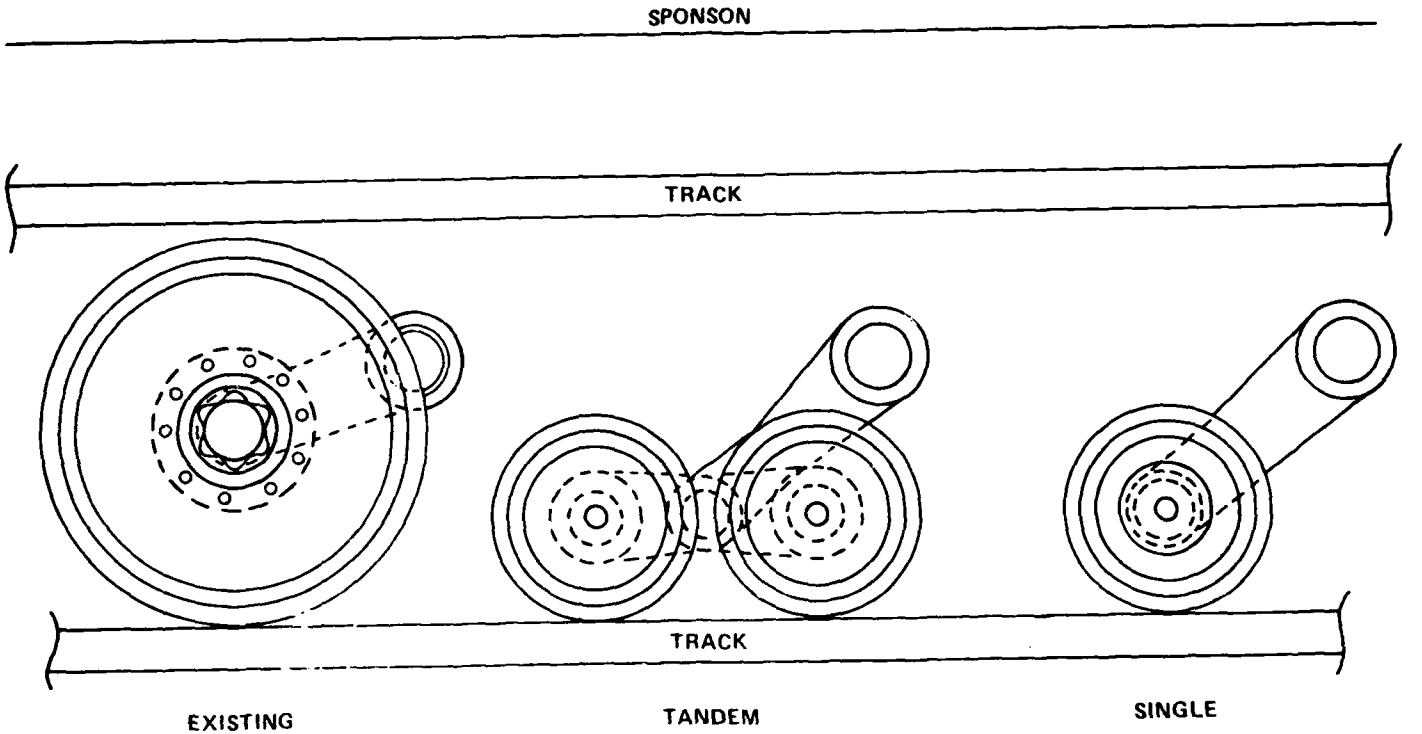

Figure 8 - Relative Size and Location of Existing Small Tandem, Small Single Roadwheels

Because the design objective was to replace one or more wheels per side with the smaller roadwheels (single or tandem), certain constraints were imposed on the placement and location of the roadwheels. Basically, the same suspension geometry and track envelope were to be preserved. By replacing a larger roadwheel with a smaller one, in the design for evaluation, the roadarm length increases 13 to 16 inches to arrive at the same point of contact with the track as the larger wheel. In so doing, the angle the roadarm makes with the horizontal in a statically loaded condition changes from -19.2 degrees to -39.96 degrees. A complete set of small roadwheels would require a slightly smaller roadarm so that no part of the wheel or roadarm assembly would strike an adjacent assembly in the horizontally deflected position. Based on the number of roadwheels per side, the roadarm to be used with a complete set of single roadwheels would be 13 inches. The angle the roadarm makes with the horizontal in the statically loaded condition increases from -19.2 degrees to -52.2 degrees. These increases in angle require the torsion bar to be re-indexed to account for the change in torsion bar windup for the design for evaluation.

Also, the increase in angle and length of roadarm may affect ride quality because surge and heave coupling will be enhanced and may tend to lurch the vehicle forward as the wheels deflect vertically, (this lurching forward can be minimized if the vertical travel between static and bump is centered equidistant from the horizontal position). Further, the vertical stiffness as a function of roadwheel deflection will change, and will effect ride quality (this effect will be discussed later). The resultant ride quality will not be evident with only one small roadwheel per side, and the effect on ride quality would have to be assessed through full-scale testing with a complete set of roadwheels installed on the vehicle.

The number of roadwheels per side was determined by examining the existing track envelope, preserving the same length of track in contact with the ground and maintaining the same angle of attack at the front of the track. Nine, 14-inch single roadwheels per side were found to best fit the existing track envelope and still have ample room remaining to space the roadwheels.

An added advantage of using more small roadwheels could be a reduction in chunking caused by the track guides hitting the rubber tire tread. To reduce the individual wheel load, more small roadwheels are needed to replace the larger roadwheels. Because more small roadwheels are in contact with the track guides, the

track will meander less and reduce the likelihood of the guides hitting the tire tread as the track passess under the roadwheels.

Figure 9 illustrates the 14 inch single and tandem roadwheels placed within the existing track envelope. The roadwheels are nonuniformly spaced to avoid producing a track resonance problem. The spacing is patterned after the existing wheel spacing as an increasing, then decreasing, function of the length between the leading and trailing roadwheels. For the single roadwheels, the first two spacing increments are 5 inches between roadwheels, and increases between each successive pair of roadwheels, except for the last pair which are again spaced 5 inches apart (e.g., spacing is 5, 5, 5.5, 5.5, 6.5, 6.5, 5 and 5 inches between roadwheels from the leading to trailing roadwheel).

The tandem roadwheels, which are arranged in pairs, require an even number of roadwheels per side. The spacing between roadwheels of the same set is 15 inches from center to center. Because this dimension is the same for all sets of tandem roadwheels, only the spacing between sets can be varied along the length of the vehicle. As before, with the single roadwheels, the existing vehicle ground clearance and track envelope are preserved. For the tandem concept, five sets of 14-inch diameter tandem roadwheels per side were found to best fit within the existing track envelope. The spacing between sets is also nonuniform and is similar to that of the existing vehicle, with linearly increasing then decreasing spacing of roadwheel sets between the leading and trailing sets. The first spacing is 5.5 inches, and increases by 1 inch between each successive set of roadwheels, except for the last set which is spaced 4.5 inches (i.e., spacing is 5.5, 6.5, 7.5, 4.5 inches between tandem roadwheel sets from the leading to trailing set).

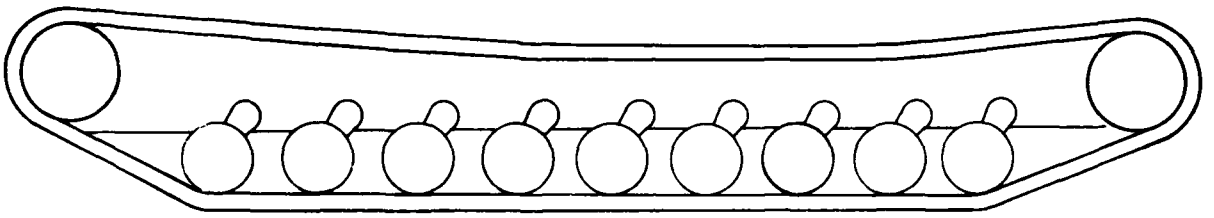

9 SINGLE ROADWHEELS

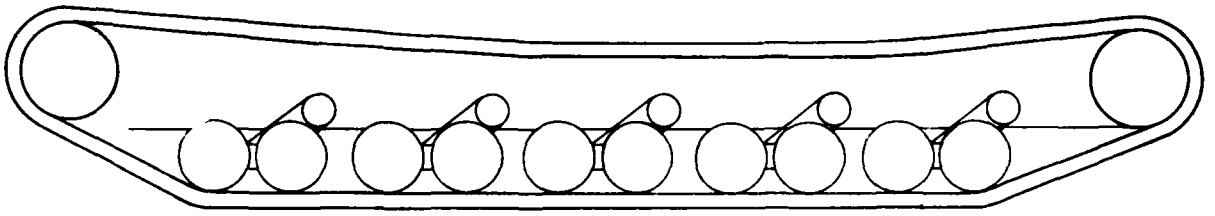

5 SETS OF TANDEM ROADWHEELS

Figure 9 - Single and Tandem Roadwheels in Track Envelope

SMALL ROADWHEEL RUBBER TO TRACK INTERFACE

Before this roadwheel concept (in either single or tandem configuration) can be used on a tracked vehicle, the required rubber tire tread width must be determined to conform with the reduced wheel load and configuration. As stated before, the tire tread thickness was kept the same as that of the existing tire tread to minimize the chance of tread blowout caused by heat buildup. However, heat buildup is also a function of tread width, wheel diameter, and wheel load. The allowable load per inch of rubber tread required to minimize the probability of blowout decreases with decreasing wheel diameter. In addition, the wheel load on the 14-inch diameter roadwheels is decreased from that of the existing 26-inch diameter roadwheels to reflect the 18 smaller roadwheels per vehicle rather than the existing 12 larger roadwheels.

The existing roadwheels are subject to a static load of 4400 pounds per roadwheel, which is the vehicle loaded weight (52,770 pounds) divided by the number of roadwheels (12). Having an overall dual tread width of 8 inches, the existing roadwheels are, therefore, subjected to a static wheel load of 550 pounds per inch of nominal tire width. The existing 26-inch diameter roadwheel can sustain an average cruising speed of approximately 30 miles per hour without fear of blowout.[2] Correspondingly, to avoid blowout in a 14-inch diameter tire (which is rated at 255 pounds per inch of nominal tire width at a cruising speed of 30 miles per hour) requires an overall dual tire width of 11.5 inches, based on an eighteen wheel configuration. The rubber tread width must therefore, be increased to reduce the load per inch on the 14-inch diameter roadwheels. This results in an overall wheel width of 14 inches for the single roadwheels as shown in Figure 10. Typical design practices give this as the maximum allowable tire width.[7] The tandem roadwheels result in a slightly narrower width because 20 wheels (10 sets) per vehicle are used instead of 18 single roadwheels. The overall dual-tire width required for the tandem roadwheels is 10.3 inches, or an overall wheel width of 12.8 inches.

These required wheel widths, although necessary to decrease the probability of tire blowout, are not completely compatible with the existing suspension and track. In the horizontally deflected position, the edge of the single wheel would strike an adjacent torsion bar hub. The wheel must, therefore, either be moved outboard or

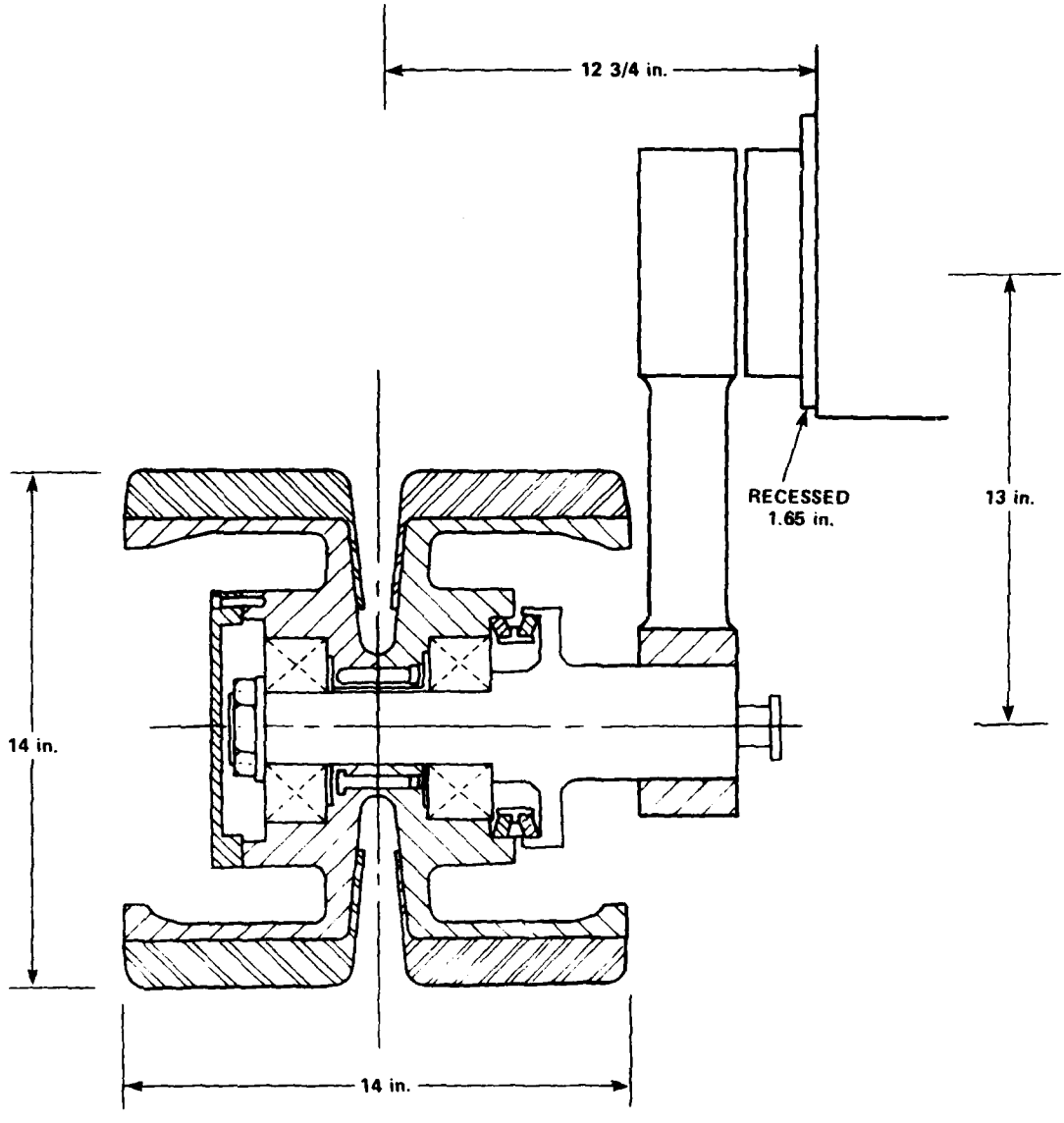

Figure 10 - Required Wheel Width to Preclude Blowout

the torsion bar hub recessed inboard, to allow clearance for the roadwheel to swing in front of an adjacent torsion bar hub. If the wheel were moved outboard, the idler, drive sprocket, and track would also have to be moved outboard. If the torsion bar hub were recessed, the only necessary modification would be to move the flange, through which the hub is mounted to the hull, outward. The torsion bar assembly would then, in effect, extend further inside the hull. Presently there is about 17 inches between the inboard end of the torsion bar assembly and the hull on the other side of the vehicle, posing no major problem with recessing the torsion bar assembly.

The wider wheel widths also cause an incompatibility with the existing track, which was designed to carry a wheel with the existing tire width.

The existing track is made up of steel blocks with rubber backed bearing surfaces upon which the roadwheel tread rides. As illustrated in Figure 11, rectangular cutouts are located on either side of the bearing surface where the drive sprocket engages and drives the track. A wheel wider than the existing wheel does not come in contact with all of the track bearing surface, but will ride over the rectangular cutouts in the track. The track incompatibility cannot be resolved as easily as recessing the torsion bar assembly. If the wider wheel width is to be used, some type of modification of the tire track interface will be required.

Similar incompatibility problems are associated with the tandem wheel configuration. The tandem wheels require two separate roadarms to connect them to the torsion bar; a lower roadarm to link the wheels together and an upper roadarm to connect the lower roadarm to the torsion bar. The incompatibility arises because the space between the inboard wheel edge and the hull is not large enough to accommodate the two roadarms. Because recessing the torsion bar will not resolve this problem, the track must be moved outboard to provide enough room for the two roadarms. The track bearing surface incompatibility, as in the single roadwheel design, must also be taken into account.

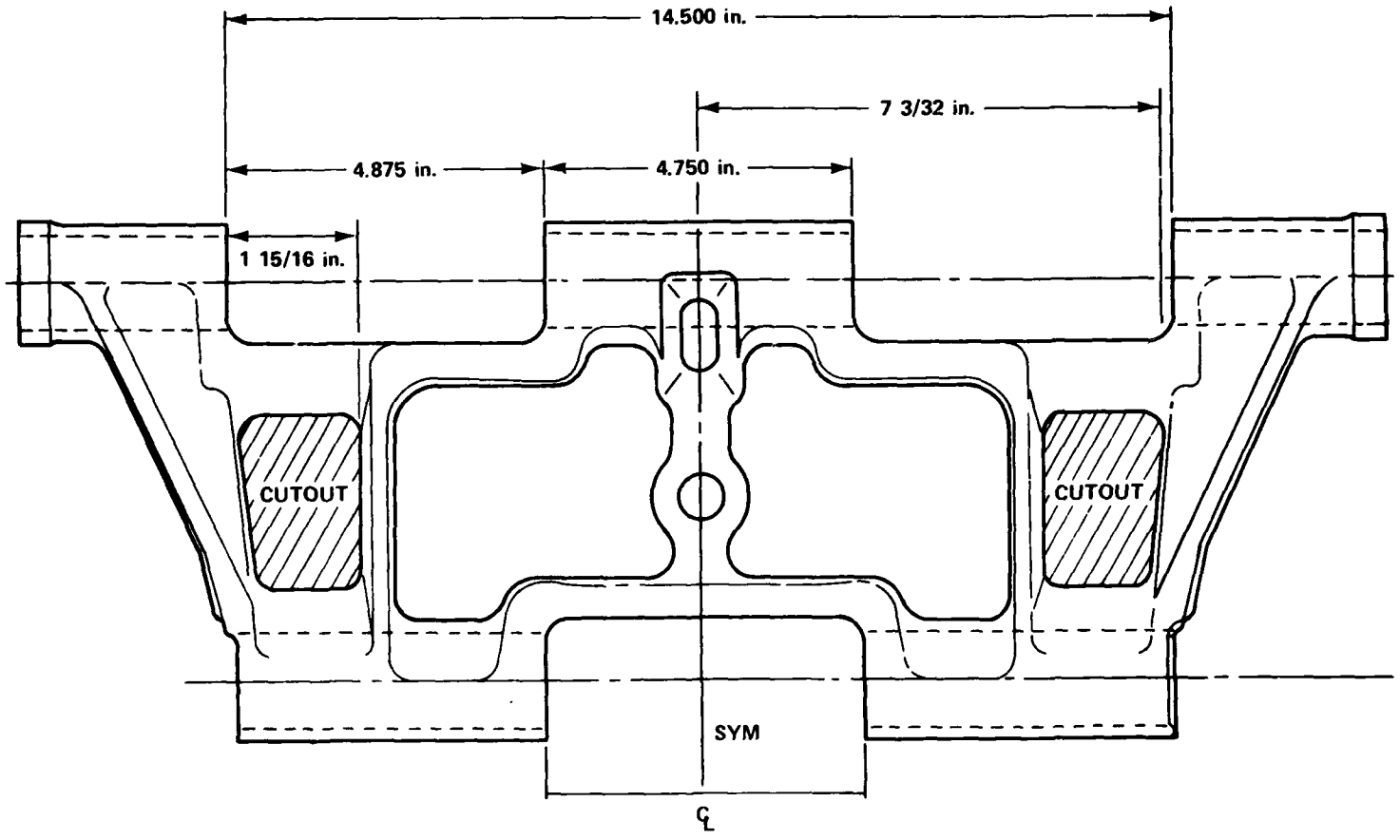

Figure 11 - Existing Track Block Configuration

DESIGN FOR EVALUATION

In service evaluation of the tandem roadwheels on the existing vehicle would be impracticle because the track (and drive and idler sprockets) must be moved outboard to accommodate the roadarms between the hull and wheel. Also, without any torsional stiffness between the upper and lower roadarms of the tandem roadwheels, their response under full-scale testing would be uncertain. Therefore, to avoid unnecessary complications and still provide a design for concept evaluation which is compatible with the existing track and suspension, a single 14-inch diameter roadwheel with the existing wheel width (as shown in Figure 12) can be employed for the evaluation tests.

For these tests, one of the center roadwheels on each side would be selected for replacement by the small roadwheels, as was shown in Figure 2. The applied wheel load on these two roadwheels would be reduced to simulate an 18 rather than 12 wheel configuration in the static position by re-indexing the torsion bar. For these evaluations, vehicle speed must be restricted to 15 miles per hour to avoid tire blowout. Strength calculations for the roadarm of the evaluation design are given in Appendix A.

By replacing only two of the existing twelve roadwheels, for the evaluation tests, the small roadwheels can be fitted onto the vehicle using the same torsion bar to which the large wheel was connected. With the two smaller roadwheels in place, design procedures can be validated, and small roadwheel feasibility evaluated by running the vehicle over various terrains and assessing performances. Provided feasibility is demonstrated from these evaluation tests, the next logical step would be to fabricate an entire set of small roadwheels (18) for evaluation on an existing LVPT7. Although this would involve relocating and adding six torsion bar assemblies, reducing the roadarm length from 16 inches to 13 inches, and running the vehicle in a light or noncombat equipped configuration for these tests, potential handling and ride quality changes would be evaluated. In addition, the effect of the surge and heave coupling, due to the increase in static roadarm angle on ride quality also could be evaluated. The running of the vehicle in the light configuration results from the need to maintain the specified load per inch of tire width without modifying the track blocks for these evaluations.

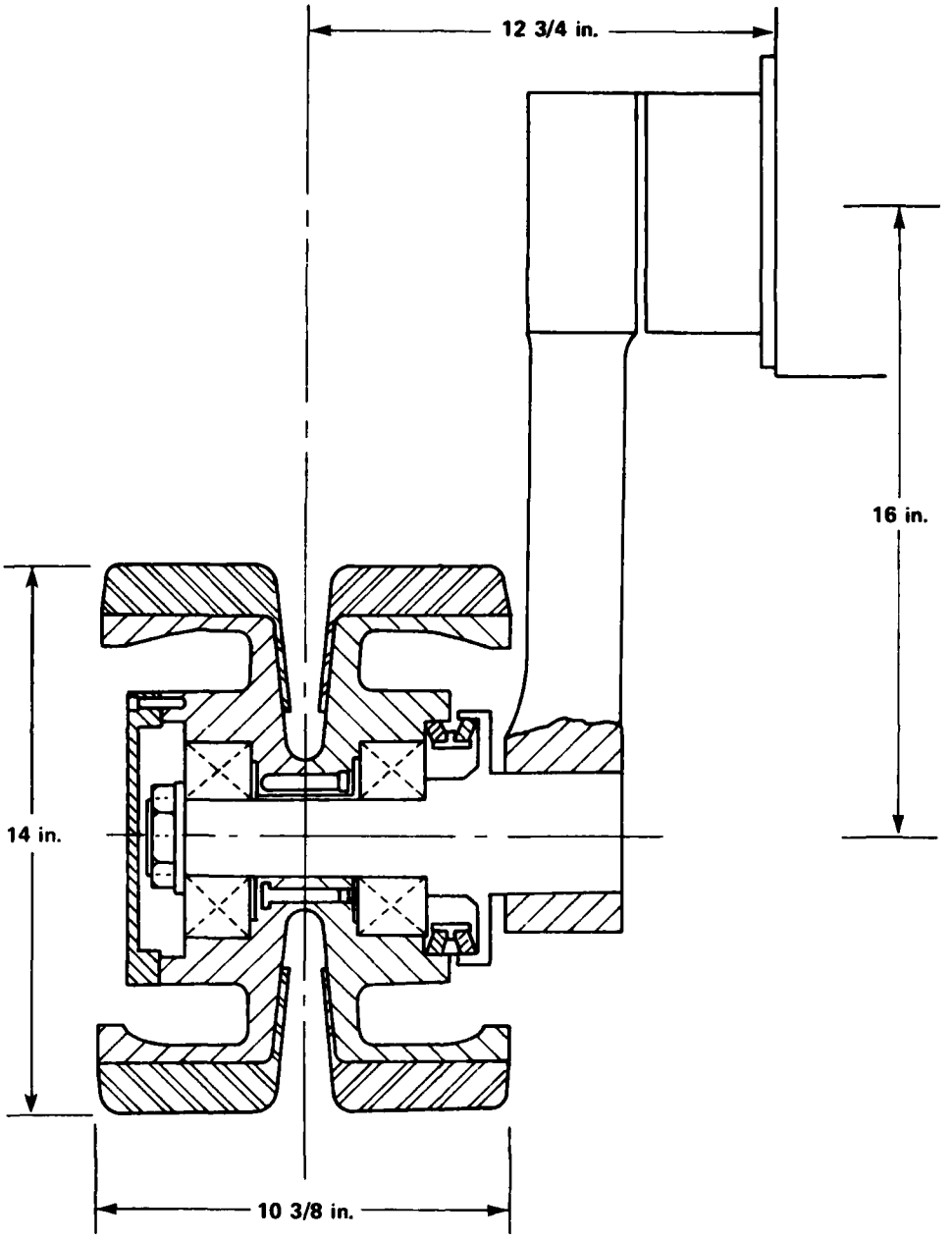

Figure 12 - Single Roadwheel Design for Evaluation

BOUYANCY GAIN

The most meaningful benefit obtained from small roadwhee s the internal volume gained from dropping the sponson over the cavity formed between the track and the existing sponson.

Differences in total suspension weight between the existing, tandem and single suspensions are, therefore, important in comparing the net buoyancy gain or land weight penalty for the same buoyancy with reduced silhouette for each configuration. Total weight estimates for each of these three configurations were calculated and are presented in Table 1. The weight estimates for the single and tandem roadwheels reflect the wide flanged roadwheel design. Weight estimates for the evaluation design are not included because they will be used only to demonstrate feasibility and to validate design procedures. Actual buoyancy gain and silhouette reduction were determined with the final wider wheel design.

TABLE 1 - WEIGHT ESTIMATE COMPARISONS OF EXISTING, TANDEM, AND SINGLE ROADWHEEL CONFIGURATIONS

	Weight Estimates (lb)		
	Existing	Tandem	Single
Roadarm	40	190	41
Torsion Bar	102	125	80
Road Wheel (hub, spindle, etc.)	165	205	104
Weight per Station	307	520	225
Total Suspension Weight	3684	5200	4050

Because the single roadwheels are independently attached to separate suspension units, and the applied wheel loads are not excessive, the torsion tube over-bar suspension will be replaced by a "bar only" torsion bar to be used with the wide flanged roadwheel design. By using a torsion bar alone, additional weight savings can be obtained and a greater net buoyancy gain can be realized. An equivalent torsion bar was, therefore, designed (see Appendix A) and is included in the weight estimate for the single roadwheel suspension. The load the tandem roadwheel set applies to each suspension unit is greater than the load on the suspension when the single roadwheels are used, because ten sets of tandem roadwheels are supporting the same weight as the eighteen single roadwheels. A "bar only" torsion bar cannot

sustain sufficient strength under this load, and a tube over bar must be used. The weight estimates for the three configurations, in Table 1, are divided into three categories: roadarm weight, torsion bar weight, and roadwheel weight. The three categories are subtotaled for each configuration to express the weight at each station. The total suspension weight is the subtotaled station weight multiplied by the number of stations in each roadwheel configuration.

Although the total suspension weight of either of the two small roadwheel configurations is heavier than the existing suspension weight, the buoyancy gain associated with the small roadwheels more than compensates for the increase in total suspension weight when considering waterborne operations.*

The sponson as it exists now is composed of a forward and an aft section. The forward section is located just above the track and extends from the front of the vehicle to just above the third roadwheel from the front.

The aft section extends from this point back toward the aft of the vehicle and is higher than the forward section. The reason for the aft section of the sponson being higher above the track than the forward section is to provide room for water to enter the water jets. The water jets are located at the rear outboard corners of the vehicle.

To effectively use the added inboard volume provided by using small roadwheels, the returning track must be lowered by support rollers located near the drive and idler sprockets as shown in Figure 13. Although these rollers effectively lower the track, they are also a source of horsepower loss and additional track wear. Also, a roller is needed to support the returning track and prevent it from flapping against the lowered sponson. As Figure 13 illustrates, potential buoyancy gain exists in any one or all of the three volume sections shown, depending upon how much water flow is required to enter the water jets (a flow analysis is beyond the scope of this investigation). The buoyancy given for each volume section is shown in parentheses next to the volume number. These buoyancy gains represent the effect of dropping corresponding sections of the sponson on both sides of the vehicle. Volume 1 can be obtained by lowering the track and forward section of the existing sponson, and can

---

*This additional suspension weight (366 pounds), of the single roadwheels and suspension compared to existing roadwheels and suspension, is negligible compared to the static wheel load, and does not effect the required wheel width calculation, or calculations presented in the appendixes.

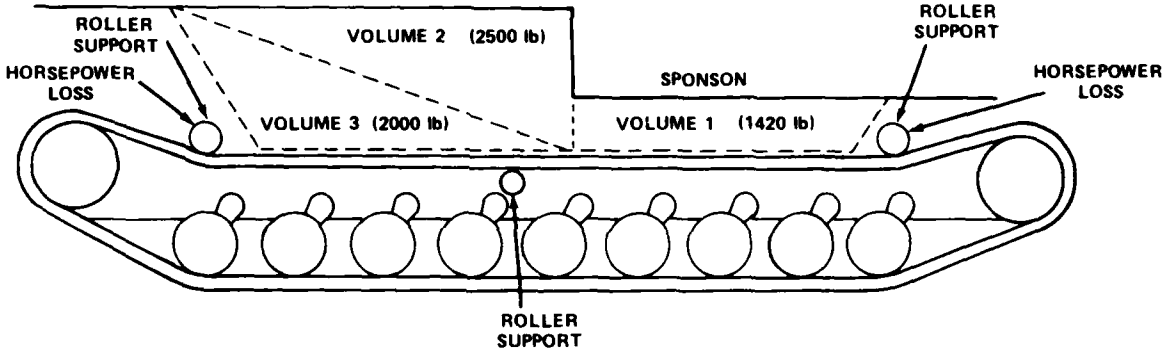

Figure 13 - Buoyancy Gained by Dropping Sponson

be introduced most likely without interrupting the flow of water into the water jets. Volume 1 alone will compensate for the increase in weight gained from using more small, rather than fewer large roadwheels. Volume 2 is obtained by fairing in the forward and aft sections of the sponson. Water flow into the water jets may be affected by the addition of Volume 2. Volume 3 is a further elongation of the aft sponson section up to the aft track support roller. All three volume sections together represent the most interval volume that can be gained by using small roadwheels.* It should be pointed out, however, that portions of Volumes 2 and 3 can be used to achieve a buoyancy gain by fairing in the sponson discontinuity even for the existing large roadwheel configuration.

EFFECT OF WHEEL DIAMETER ON VERTICAL SPRING STIFFNESS

The 14 inch roadwheel was found to be the smallest roadwheel which would be mechanically adapted to the existing vehicle. However, mechanical feasibility does not imply total feasibility. This section assesses the effect on ride quality of reducing the wheel diameter to 14 inches in terms of the vehicle vertical spring stiffness. To provide a full range of wheel diameters for comparison, 20- and 30-inch diameter roadwheels are included in addition to the 14- and existing 26-inch roadwheels. Further, for each wheel diameter, different roadarm lengths are used to see how the total vertical spring stiffness of the vehicle changes as a function of roadwheel and roadarm dimensions.

This assessment is only valid for vehicles with torsion bar suspensions. Further, this is a comparative study and, for simplicity, the total vehicle loaded weight was assumed to represent the total sprung weight. A more rigorous analysis would require a distinction between the sprung and unsprung weight. The validity of the comparisons made are in no way affected by this distinction.

The objective of the parametric study was to try to obtain specific roadwheel and roadarm combinations for a given wheel diameter such that the total vertical stiffness over the service range from static to 10 inches of deflection would approximate the existing total vertical stiffness over the same service range.**

---

*If this interval volume gain were to be employed to lower the land silhouette, a reduction in height of approximately 2 1/4 inches can be realized.

**It should be noted that a torsion bar suspension is a nonlinear system, and the vertical spring stiffness (rate at which wheel load changes with vertical deflection) is not constant as a function of vertical deflection.

(The total vertical spring stiffness of the vehicle is obtained by multiplying the vertical stiffness of each individual suspension unit by the number of roadwheels.) By approximating the existing total vertical spring stiffness, an attempt to match, or even improve the ride quality of the existing vehicle was made, because similar natural frequencies would be obtained.

The study proceeded in two phases to determine how varying wheel diameters and roadarm lengths affect the shape of the total stiffness curve for a specified stiffness, as the vehicle deflects from static to 10 inches of travel; the total stiffness curve being a plot of vehicle spring rate as a function of vertical wheel deflection. In both phases the vehicle clearance was kept constant, which is an important parameter for this particular vehicle. Any change in vehicle clearance will, of course, change the nature of these curves somewhat.

The first phase equates the total stiffness to the existing total stiffness at the static position (10.342 kips per inch); the static position being the vehicle fully loaded and at rest. The second phase equates the total stiffness to the existing total stiffness at 10 inches of wheel travel (20.515 kips per inch). Each specified total stiffness at some deflection generates a family of curves for a given wheel diameter, which pass through the common specified point; each curve representing a different length roadarm. The procedure for generating these curves is given in Appendix B.

Figure 14a illustrates the first phase family of curves generated for a 14-inch diameter wheel. Eighteen roadwheels were found to best fit the track envelope. (Sixteen roadwheels would have fit inside the track envelope, but would have exceeded the maximum load per inch of tire tread previously obtained.) The maximum roadarm length is limited to 13 inches to prevent adjacent roadwheel units from striking one another when the roadarm is in a horizontal position. The resulting curves indicate a very stiff suspension as the roadarm rebounds below the static position and rapidly decreases as deflection increases. The curves attain their lowest stiffness (softest) at about 6 inches of travel, and then begin to gradually increase. It is interesting to note that the stiffness at 10 inches of travel is less than the static stiffness. As the roadarm length decreases, the suspension becomes much stiffer as the roadarm rebounds below the static position and becomes slightly softer for deflections between static and 10 inches.

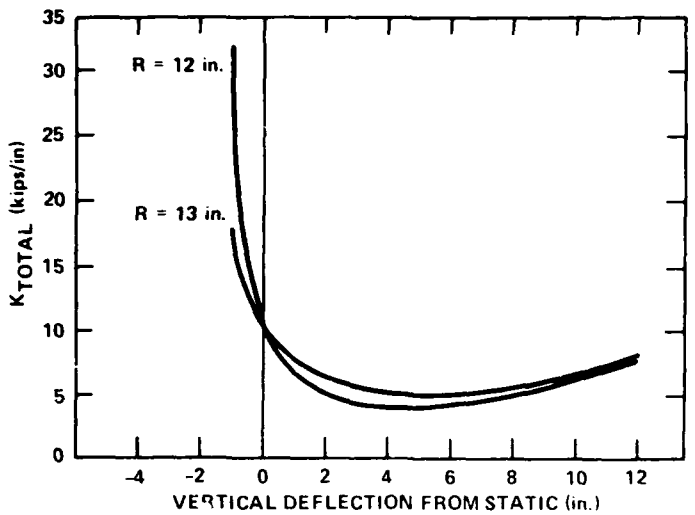

Figure 14a - 14-Inch Diameter

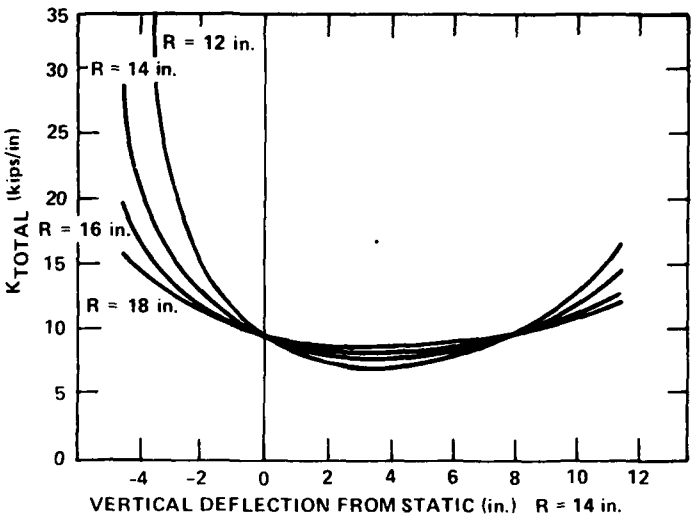

Figure 14b - 20-Inch Diameter

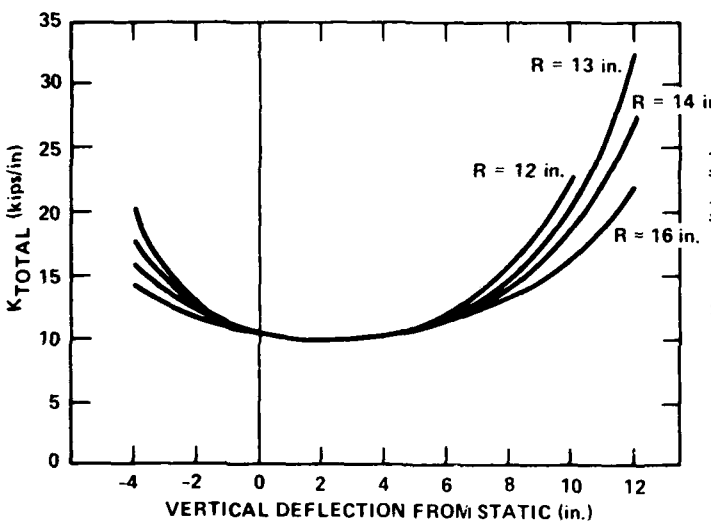

Figure 14c - 26-Inch Diameter

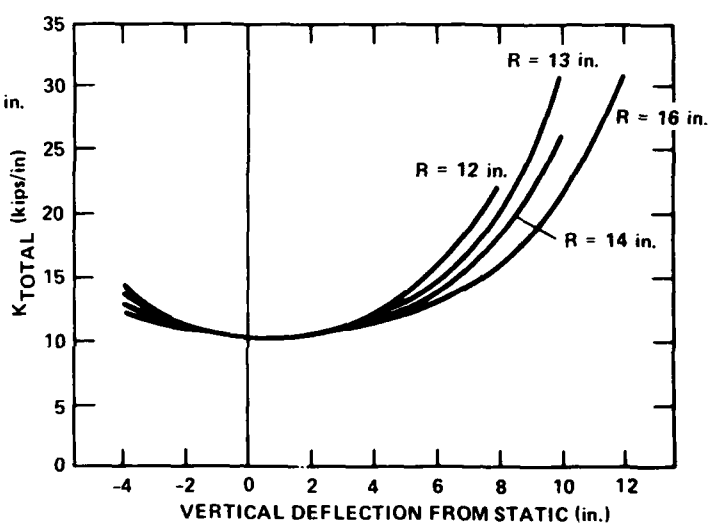

Figure 14d - 30-Inch Diameter

Figure 14 - Spring Rate versus Deflection with Stiffnesses Equated at Static Condition

The 20-inch diameter roadwheel curves, shown in Figure 14b exhibit the same basic suspension response as the 14-inch roadwheel except that they are softer through rebound deflections. The maximum length* roadarm for the 20-inch diameter wheel is 19 inches, and there are 14 roadwheels per vehicle. The curves attain their lowest stiffness at about 4 inches of travel and then increase more rapidly than the 14-inch diameter roadwheel curves. As the roadarm length increases the stiffness curves tend to flatten throughout the service range.

The 26-inch wheel stiffness curves (including the existing R = 13 inch curve) is shown in Figure 14c where the maximum roadarm length is 25 inches, and there are 12 roadwheels per vehicle. The curves are softest at about 2 inches of travel and stiffen rapidly at deflections above and below that point. The shorter the roadarm, the more rapid the increase in stiffness.

The 30-inch diameter roadwheel curves, shown in Figure 14d, attain their softest point at the static position and increase rapidly for deflections above and below static. At 10 inches of travel the suspension becomes very stiff, much stiffer than that of the existing suspension. The maximum roadarm length is 32 inches, and there are 10 roadwheels per vehicle.

An optimally shaped stiffness curve is softest at the static position and is fairly steep (stiffens rapidly) for deflections below and above static. A relatively stiff suspension is needed at these deflections to control pitch and bounce oscillations and return the vehicle to its normal or static position, without the vehicle frequently bottoming out.

The 14- and 20-inch diameter wheel suspensions exhibit a fairly steep stiffness for deflections below static, but are too soft for deflections above static. An auxiliary or bump spring would be required in addition to the torsion bar to sufficiently stiffen the suspension against deflection above the static position.

The 26- and 30-inch roadwheels both exhibit the desired curve shape with the stiffness increasing rapidly for deflections above and below static. Roadarms of lengths less than 12 inches should not be used with the 30-inch roadwheel, because the stiffness becomes excessive at 10 inches of travel.

---

*The maximum roadarm lengths for the larger diameter wheels (20, 26, and 30 inch) are not included in the stiffness versus deflection curves because they are too long for practical use.

For the wheel diameters considered in phase one (equating static stiffnesses), general trends can be cited which affect the stiffness curve shape. As the wheel diameters increase, it is seen that: (1) the total stiffness tends to decrease for deflections below static and increase for deflections above; (2) the amount of available rebound deflection (deflection below static) tends to increase; and (3) the softest point on the stiffness curves shifts toward the static position, indicating that, as the wheel diameter increases, the static and bump (10 inches of travel) deflections are becoming equidistant from the horizontal position of the roadarm. Finally, as the roadarm length increases, for each wheel diameter the stiffness curve tends to flatten out.

Load deflection curves are shown in Figure 15 for four roadwheel-roadarm combinations (one for each size roadwheel) used in the phase one analysis. The curves indicate that the wheel load increases more rapidly as deflection and wheel diameter increase, reflecting the increase in stiffness with increasing roadwheel diameter, and the decreasing number of roadwheels.

The vehicle frequency (rigid body heave on the suspension) as a function of roadwheel deflection is shown in Figure 16 for the same roadwheel and roadarm combinations used in the load deflection curves (Figure 15). Higher frequencies occur as the wheel diameter increases for deflections above static. Further, the lowest frequency that occurs over the service range shifts toward the static position as the wheel diameter increases.

The second phase of this study equated the existing total stiffness at 10 inches of travel, (20.515 kips per inch) for the same four roadwheel sizes.

Figure 17a shows the resulting stiffness curves for the 14 inch roadwheel. The suspensions shown are as stiff as the existing suspension at 10 inches of travel but are extremely stiff at static and contain little if any rebound capability. Curves of this type are undesirable because the ride quality at the static position would be very poor. The curves attain their lowest stiffness at approximately the same deflection as in phase one, but the magnitude is considerably higher.

The 20 inch roadwheel curves, shown in Figure 17b, are similar in shape to the 14 inch roadwheel curves except that they are initially softer and contain more rebound deflection capacity. The softest points on the curves occur at about 4 inches of deflection.

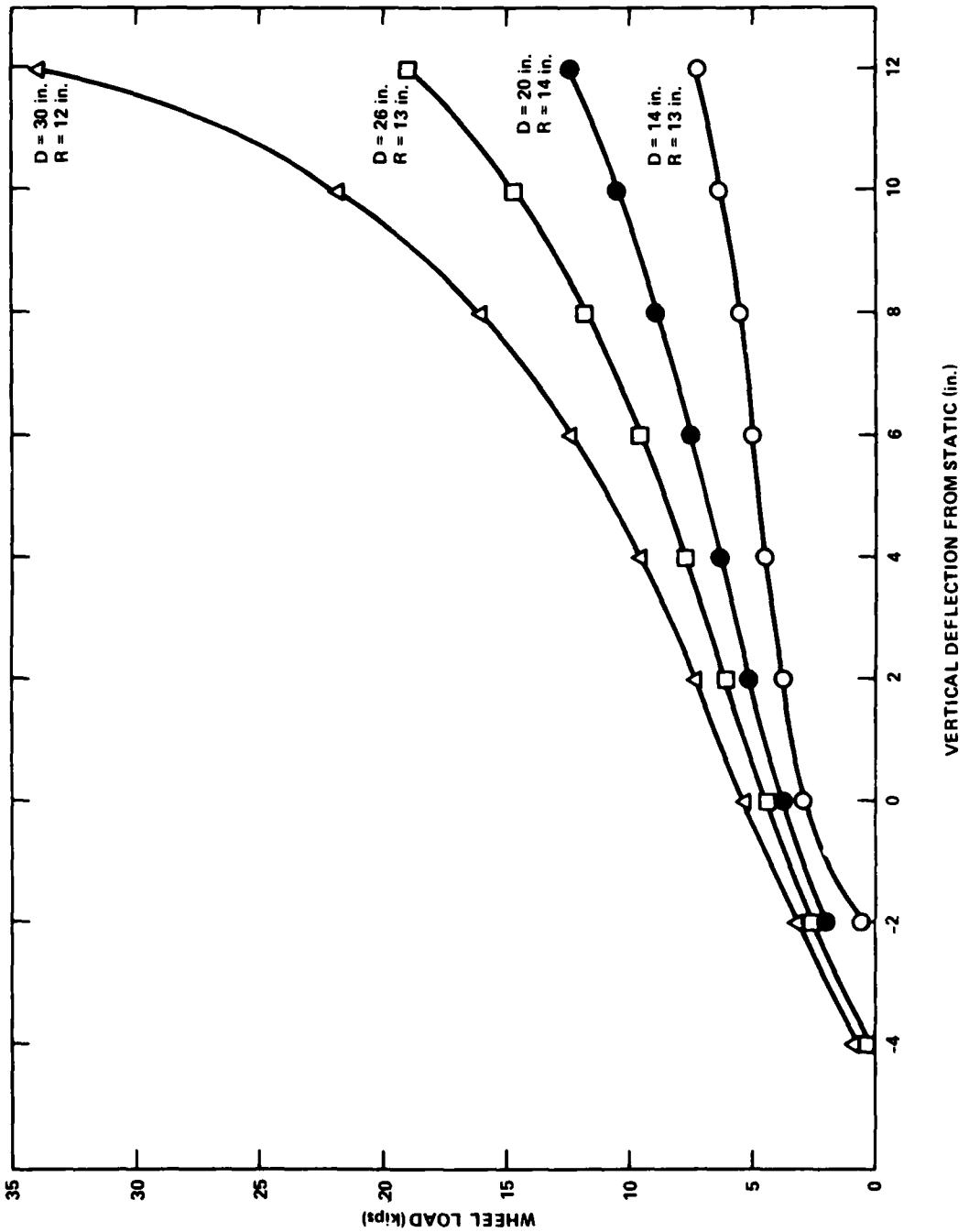

Figure 15 - Wheel Load versus Deflection with Stiffnesses Equated at Static Condition

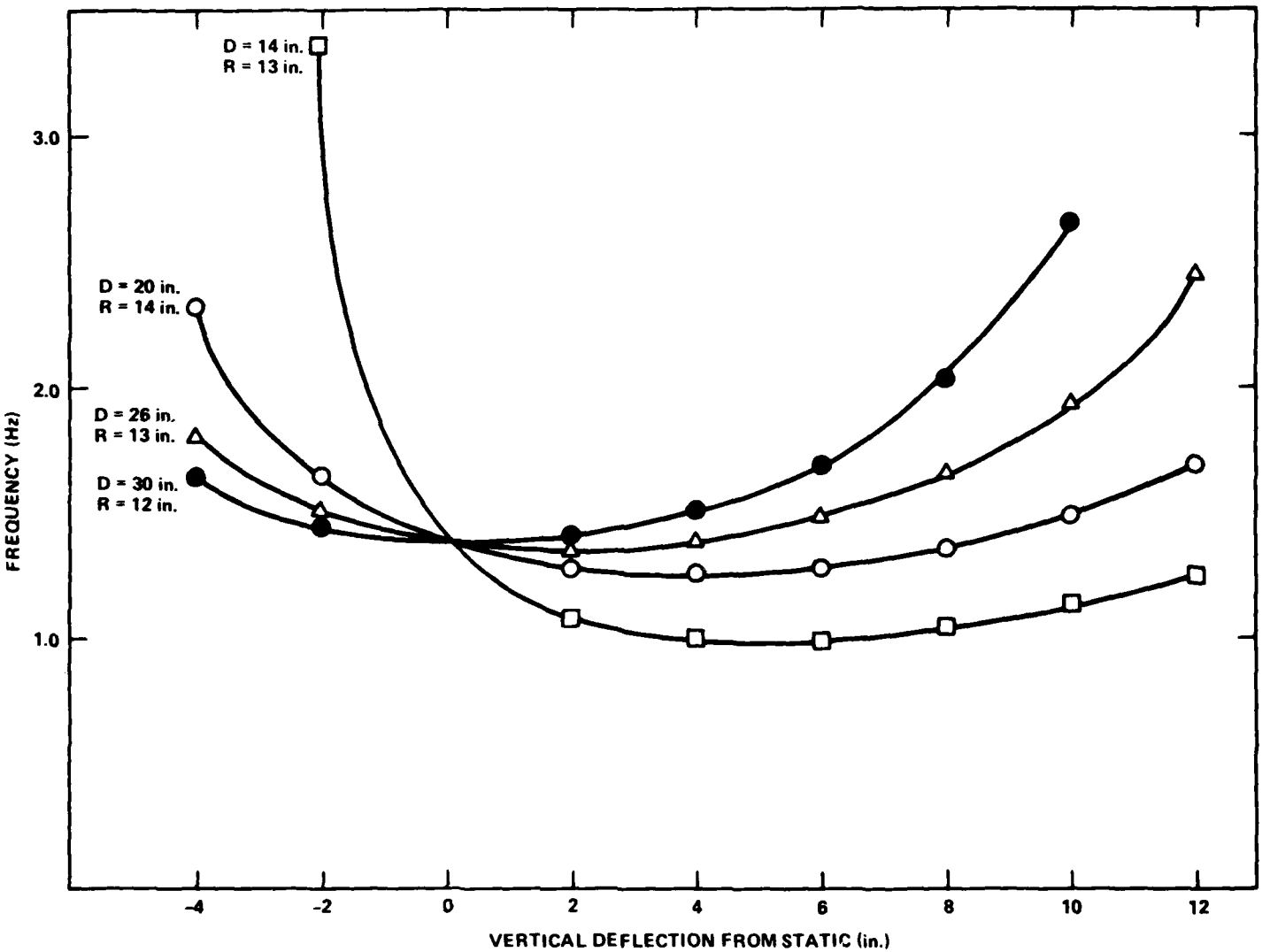

Figure 16 - Frequency versus Deflection with Stiffnesses Equated at Static Condition

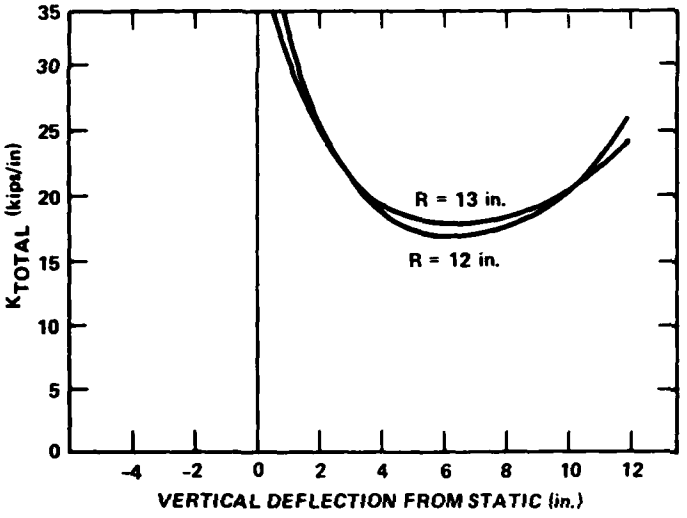

Figure 17a - 14-Inch Diameter

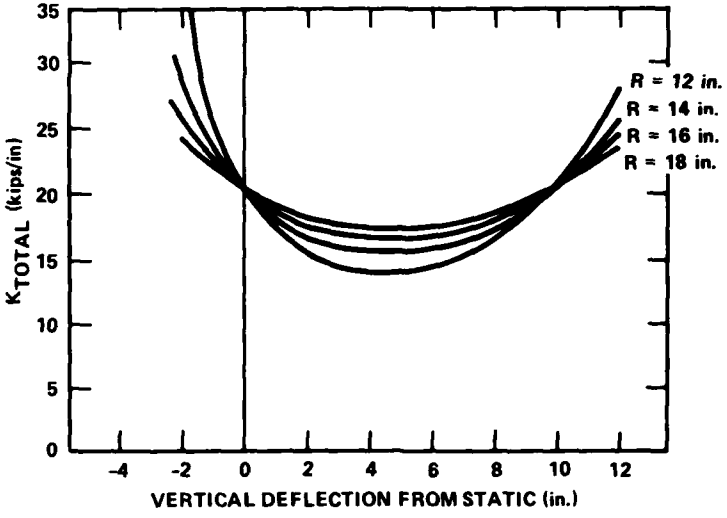

Figure 17b - 20-Inch Diameter

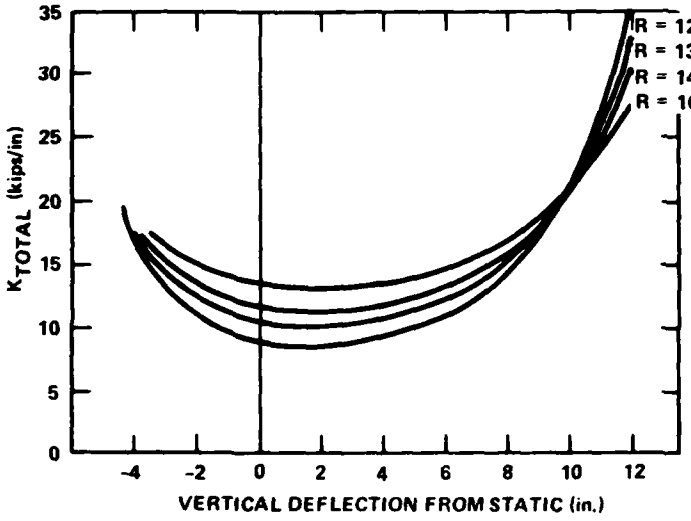

Figure 17c - 26-Inch Diameter

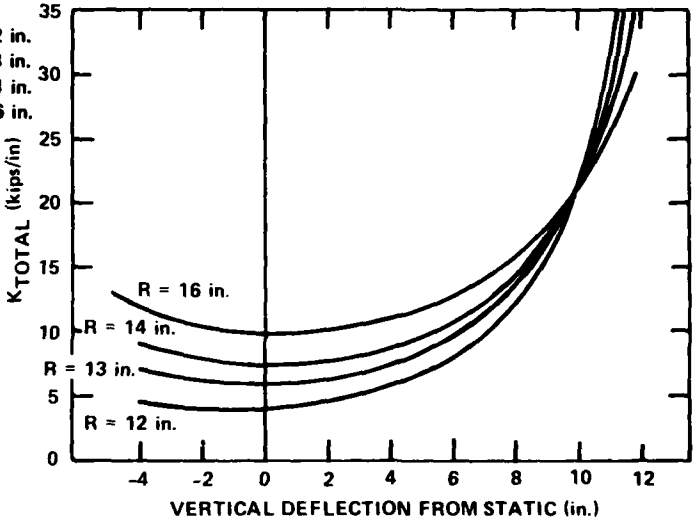

Figure 17d - 30-Inch Diameter

Figure 17 - Spring Rate versus Deflection with Stiffnesses Equated at 10-Inches of Travel

The 26 inch wheel diameter curves shown in Figure 17c are less stiff and contain much more rebound capacity than the 20 inch wheel curves. The curves attain their lowest point at about 2 inches of travel. As the roadarm length decreases the stiffness decreases and rebound capacity increases.

The 30 inch wheel diameter curves shown in Figure 17d are much softer and quite a bit flatter about static deflection than the 26-inch diameter curves. The curves attain their lowest point at the static position. As is true with the 26 inch curves, as the roadarm length decreases, the stiffness decreases and rebound capacity increases. The curves are very flat below static deflection and would, therefore, not be very effective in controlling pitch and bounce oscillations. Further, actual torsion bar dimensions may not be obtainable for such soft stiffness curves, because the bar diameter would have to be large enough to resist the increased wheel load and the length would have to be long enough to attain the required rotational spring rate, possibly longer than the width of the vehicle.

Load deflection curves are shown in Figure 18 for the same four roadwheel and roadarm combinations that were used in phase one. The curves indicate that for changes in deflection below static, change in wheel load increases at a faster rate as the wheel diameter is decreased. For deflections above static, change in wheel load increases at a faster rate as the wheel diameter is increased. This reflects the initial flattening and final steepening of the stiffness curves as the wheel diameter is increased.

Vehicle frequency versus deflection curves are shown in Figure 19 for the same roadwheel and roadarm combinations. Higher frequencies at static occur as the wheel diameter decreases, with the lowest frequency of each curve shifting to the right as the wheel diameter decreases.

The results of these two phases give an indication of how the stiffness curves are affected by changes in roadarm length and wheel diameter. The curves also indicate the change in ride characteristics to be expected by changing to either smaller or larger roadwheels with respect to that of the existing vehicle, when using a torsion bar type of suspension.

Ride quality assessment, in terms of the vehicle vertical spring stiffness-deflection relationship, may not be strictly valid for tandem roadwheels due to the walking beam effect of this configuration. However, it is believed that since the

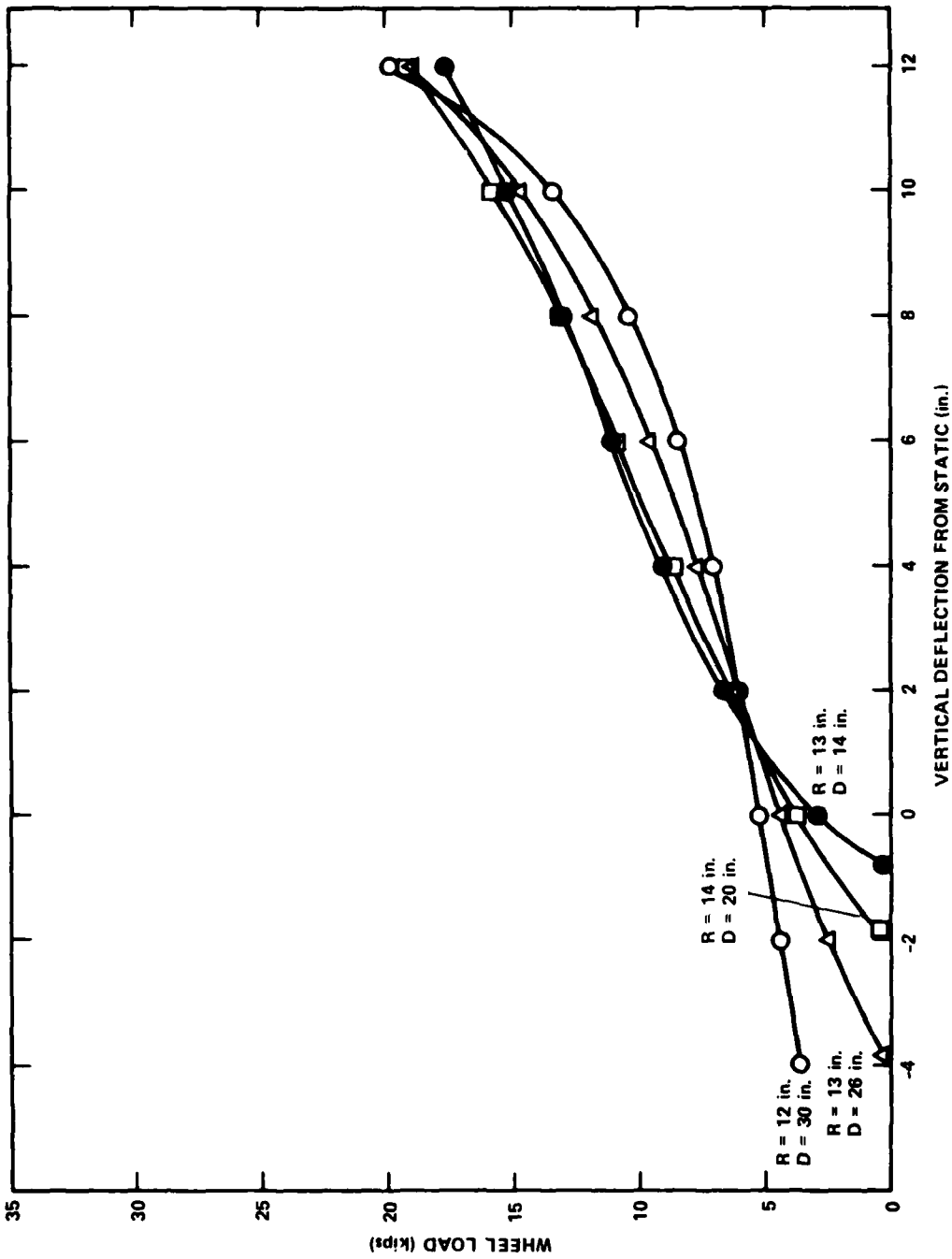

Figure 18 - Wheel Load versus Deflection with Stiffnesses Equated at 10-Inches of Travel

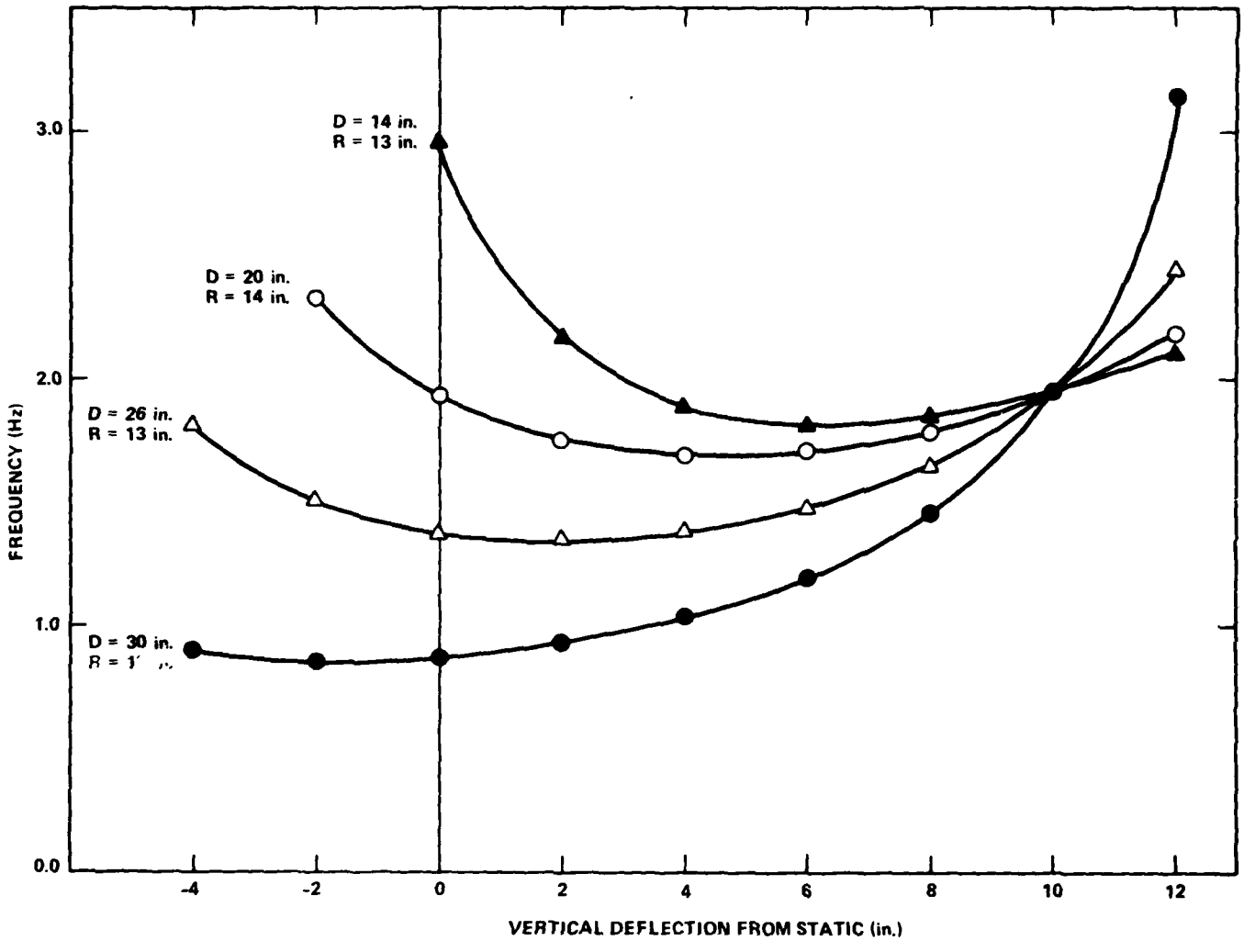

Figure 19 - Frequency versus Deflection with Stiffnesses Equated at 10-Inches of Travel

roadarm lengths and the angles they make with respect to horizontal in the tandem configuration are similar to the single configuration, a similar spring stiffness-deflection relationship will be produced.

To compliment the vertical stiffness study, the effect of wheel diameter on total suspension weight will be briefly investigated for certain roadwheel and roadarm combinations selected from the phase one stiffness curves using the torsion bar type suspension and neglecting any effects on ride quality.

EFFECT OF WHEEL DIAMETER ON SUSPENSION WEIGHT AND BUOYANCY GAIN

A relative weight study was performed between selected roadwheel and roadarm combinations of phase one (one combination from each of the roadwheel diameter sizes) to determine how different size wheel diameters affect the overall suspension weight and potential buoyancy gain. Weight algorithms were developed (see Appendix C) to estimate the weight of each individual component of the suspension for a given wheel diameter and roadarm length. A plot of suspension weight versus wheel diameter can be developed to indicate the weight of the suspension system associated with wheels of varying diameter. Small roadwheels can result in considerable buoyancy gain, but seem to have an adverse effect on ride quality as indicated by the spring stiffness deflection curves; consequently larger roadwheels tend to give better ride quality, as indicated by the spring stiffness-deflection curves, but take away any potential buoyancy gain and present a buoyancy loss. Plots of total additional buoyancy gain (or loss) and net buoyancy gain (total additional buoyancy gain minus total additional weight gain) were developed as a function of wheel diameter.

To develop these plots, a total vehicle stiffness curve must be obtained so that a roadarm and torsion bar assembly can be designed. The total weight of the vehicle is assumed to remain constant; any savings in suspension weight is assumed to be made up somewhere else, such as in armor weight. To offer a valid comparison, stiffness curves generated under the same constraints were selected from the first phase analysis disregarding any effect on ride quality (total stiffness equated to existing total stiffness at static).

The weight algorithms were used to approximate the suspension weights for wheel diameters of 20 inches or greater. A smaller diameter wheel would have to employ the wheel flange as the hub, similar to the 14-inch diameter wheel shown in Figure 6. Wheel diameters of 20 inches or larger would be made similar to the existing configuration shown in Figure 3 with separate wheel and hub units.

Buoyancy gains (or losses) associated with each wheel diameter were obtained by calculating the change in volume on both sides of the vehicle resulting from either raising or lowering the sponson from its original (existing) position, see Figure 13. As mentioned before, a buoyancy gain can be realized for the existing vehicle "as is" by fairing in the discontinuity of the existing sponson (Volume 2). The net buoyancy gain is the difference between the total buoyancy gain and the additional suspension weight and was calculated as explained previously.

The additional suspension weight and buoyancy gain for the 14-inch diameter roadwheel are the same as given in Table 1 and Figure 13 because this is the same suspension design used in Appendix A.

The other suspension weights (for 20-, 26-, and 30-inch diameter wheels), which were calculated from the weight algorithms (see Appendix B), are felt to be accurate to within $\pm$5 percent of the actual suspension weight. Figure 20, illustrates the change in total suspension weight as a function of roadwheel diameter. As is evident from the plot, total suspension weight is essentially insensitive to wheel diameter. As the wheel diameter decreases, the weight per station decreases, but the number of stations increases and consistently compensates for the decrease in suspension weight.

Figure 21 shows the effect of wheel diameter on buoyancy gain. The curve is nearly linear and indicates a constant increase in buoyancy gain as the wheel diameter decreases. The buoyancy gain is the volume obtained by raising or lowering the sponson to accommodate a particular wheel diameter.

The net buoyancy gain, the change in total suspension weight subtracted from the buoyancy gain, is also nearly linear, see Figure 22, indicating the negligible change in suspension weight compared to the buoyancy gain.

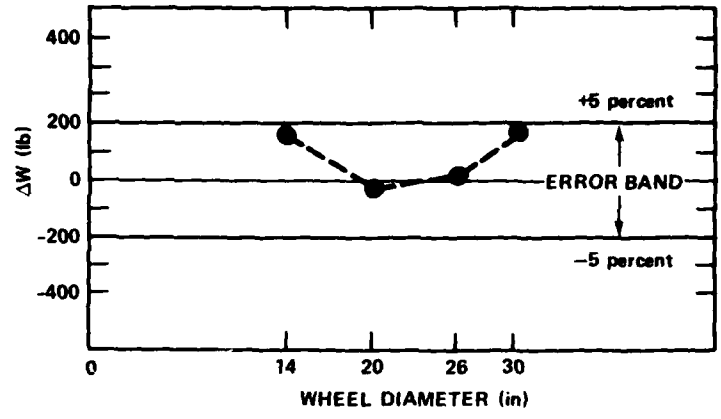

Figure 20 - Change in Total Suspension Weight versus Wheel Diameter

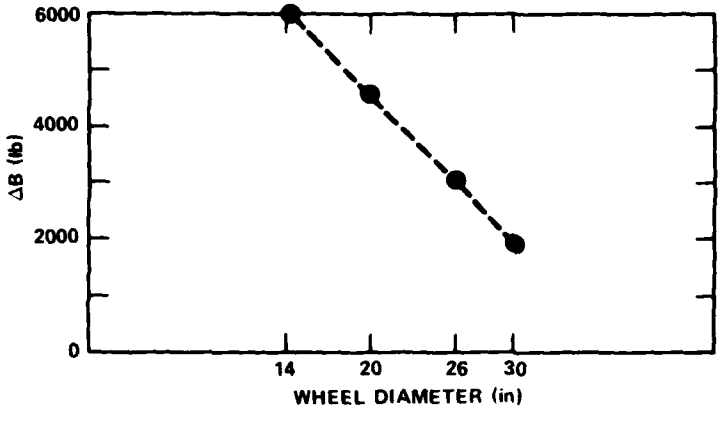

Figure 21 - Change in Buoyancy Gain versus Wheel Diameter

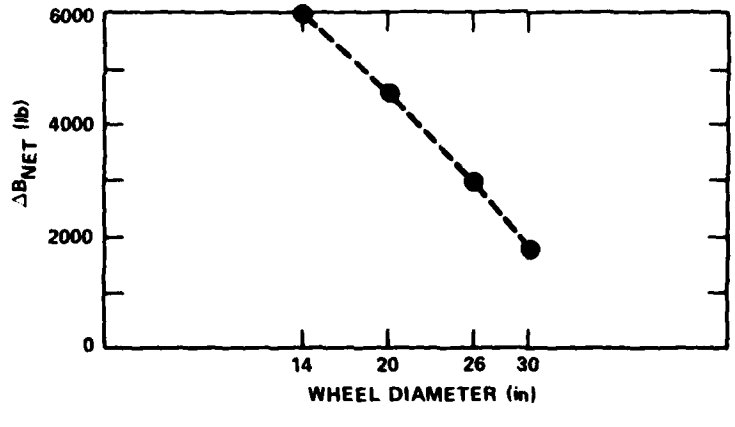

Figure 22 - Net Buoyancy versus Wheel Diameter

SUMMARY AND CONCLUSIONS

Small roadwheels for future vehicles were investigated by designing them for the LVTP7 which was used as a point of reference. The small roadwheel suspension, designed for the LVTP7, was shown to be structurally and mechanically feasible for possible implementation on a future vehicle. The major benefits, obtained from using small roadwheels rather than the large existing roadwheels, include (1) a considerable internal volume gained by enclosing the increased wheel clearance volume (a benefit which can be immediately realized); and (2) a better ground pressure distribution can also be expected when using smaller roadwheels. Other changes, such as vehicle ride quality and handling, can be evaluated with full-scale testing. These benefits must be assessed while considering the tradeoffs associated with this change, which include: (1) the geometric changes to be made to the track width, (2) the location with respect to the hull and/or torsion bar protrusion to accommodate the increased width of the small roadwheels, and (3) the involved wheel replacement. These changes, in themselves, from the present design are not unattainable and could be accomplished, should the gain in buoyancy (or reduced silhouette) be deemed worth the necessary changes.

The major effect small roadwheels could have is to change the ride quality of the vehicle if employed with a torsion bar only or tube over bar type suspension. Use of a torsion bar suspension with smaller, roadwheels was shown to develop an undesirable stiffness-deflection curve for the vehicle indicating that the torsion bar type suspension should be implemented with some type of bump springs or the use of a hydropneumatic suspension if small roadwheels are used. Further, if the restriction that the vehicle ground clearance remain constant is relaxed, the shape of the stiffness versus deflection curve will change accordingly. A lower ground clearance would enhance the performance of small roadwheels and reduce the degree of surge and heave coupling. The drawbacks of small roadwheels will now be briefly summarized individually: (1) loads applied to the small diameter roadwheels require the wheel width to increase to maintain an acceptable load per inch of tire width. As a result, the wider wheel is not compatible with the bearing pads on the existing LVTP7 track blocks; (2) to be compatible with the bearing surface of the track, the track blocks for any future vehicle employing small roadwheels would have to be reconfigured for any new wheel width which is different from the existing width.

(3) the torsion bar must be recessed or the track moved outboard to accommodate the single roadwheel design. This can be easily incorporated into a future design as previously described; (4) due to the basic configuration of the small roadwheel, an awkward and involved wheel changing is encountered. Because there is no independent wheel hub the bearings must be repacked and the lubricant drained at each wheel changing, making field maintenance difficult.

The tandem roadwheel set to be adapted to a future design would require considerable modification. The track must be moved outboard to accommodate the roadarms between the wheels and hull in addition to recessing the torsion bar. Additionally, the amount of torsional restraint needed (if any) between the upper and lower roadarms is uncertain and would require in-service testing for this determination. The tandem configuration also carries with it a higher weight and an increased parts inventory and cannot be evaluated on an existing vehicle without extensive modifications to the suspension system of an existing vehicle.

The vehicle stiffness curve parametric study indicates a possible ride quality degradation associated with single small roadwheels when they are suspended solely from torsion bars. The stiffness curves equated at the static position have the desired shape for large roadwheels, and if auxiliary bump springs are used (in addition to torsion bars) with the small roadwheels, the stiffness curves, equated at the static position, can also attain the desired shape for small roadwheels as well. Bump springs would, in effect, steepen the stiffness curves for deflections above static. The use of hydropneumatic suspension units would also enable small roadwheels to be used directly on the vehicle with this type of suspension because the stiffness versus deflection curve for this type suspension can be designed into the unit excluding more of the geometric constraints that are imposed on a torsion bar type suspension design.

Ride quality assessment in terms of the vehicle spring stiffness-deflection relationship for tandem roadwheels may not be strictly valid, due to the walking beam effect of the tandem roadwheel configuration. However, it is believed that since the upper roadarm lengths and the angles they make with respect to the horizontal in the tandem configuration are similar to the single configuration, a similarly undesirable spring stiffness-deflection relationship will be produced.

Because the required modifications to adapt single small roadwheels to future tracked vehicles appears more promising and requires less deviation from existing

design practices from a mechanical point of view, a logical approach would be to fabricate a pair of single small roadwheels to be placed on the vehicle for evaluation (using the design for evaluation) to verify design procedures and make any design improvements, if necessary. Further, after the first pair of roadwheels is evaluated, and any necessary modifications made, a complete set of small roadwheels can then be fabricated and placed on a test vehicle for evaluation of ride quality, handling, river egress, and general performance over various terrain surfaces.

ACKNOWLEDGMENTS

The authors wish to express their appreciation to the following individuals for their support and guidance given throughout this study: Mr. Ernest D. Wolfe, of the Systems Development Department, who was the Marine Corps project manager for this effort, Messrs Alfred L. Disenbacher, Milton O. Critchfield, and Jeffery E. Beach, of the Structures Department, who provided suggestions and technical support; Messrs. A. Perry Clark and Milton J. Russell, of the Central Instrumentation Department, who provided guidance and suggestions for the mechanical aspects of the small roadwheel design, as well as drafting support; and Ms. Wenona Marques for her invaluable secretarial support in preparing this report.

APPENDIX A

ROADARM DESIGN FOR USE WITH SMALL ROADWHEELS

This appendix contains strength calculations for the suspensions to be used with small roadwheels which will be subjected to the same design constraints, vertical wheel deflection, and vehicle ground clearance, as the existing suspension.

The roadwheel assembly for evaluation will be placed on an existing vehicle, as was shown in Figure 2. The roadarm design to be used with the roadwheel for evaluation will incorporate the existing tube over bar torsion assembly "as is," with no changes or modifications made to it, except for the initial re-indexing to scale-down the wheel load. Complete design details of the design for evaluation can be obtained from DTNSRDC drawings E11-3674-1, 2, 3, and 4.

The roadarm to be used with the wide flanged roadwheel is designed with the torsion bar recessed to conform to the existing suspension and track geometry (assuming the track bearing problem can be resolved), and contains characteristics of a torsion "bar only" assembly to be used in place of the existing tube over bar torsion assembly.

The roadarms designed in this appendix are subjected to biaxial bending and torsional moments, as well as shear and axial forces. Equations of these moments and forces in the plane of the cross section were derived as a function of location along the axis (centerline) of the roadarm, rotation of the roadarm with respect to the horizontal (θ), and attitude of the roadarm away from or toward the hull (α). The roadwheel and roadarm assembly was assumed to be subjected to both a vertical and a horizontal wheel load.

The vertical and horizontal wheel loads act in the right-handed mutually orthogonal X'Y'Z' coordinate system whose origin is located at the load application point as shown in Figure A.1. The X'-axis extends along the centerline of the track at the wheel track interface. The vertical wheel load P_v, acts through the centerline of the track directly beneath the wheel spindle along the Y'-axis. The horizontal wheel load P_h, acts outboard along the Z'-axis at the wheel track interface (worst case loading condition). The X'Y'Z' coordinate system (and hence the vertical and horizontal wheel loads) does not rotate as the roadarm rotates about the torsion bar, but does translate as the roadwheel and track deflect upward.

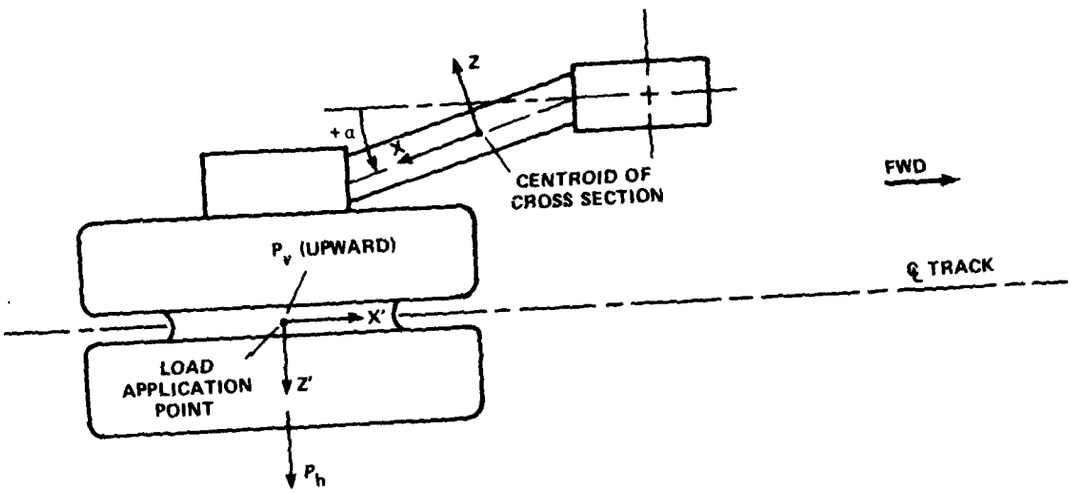

Figure A.1a - View Looking Downward

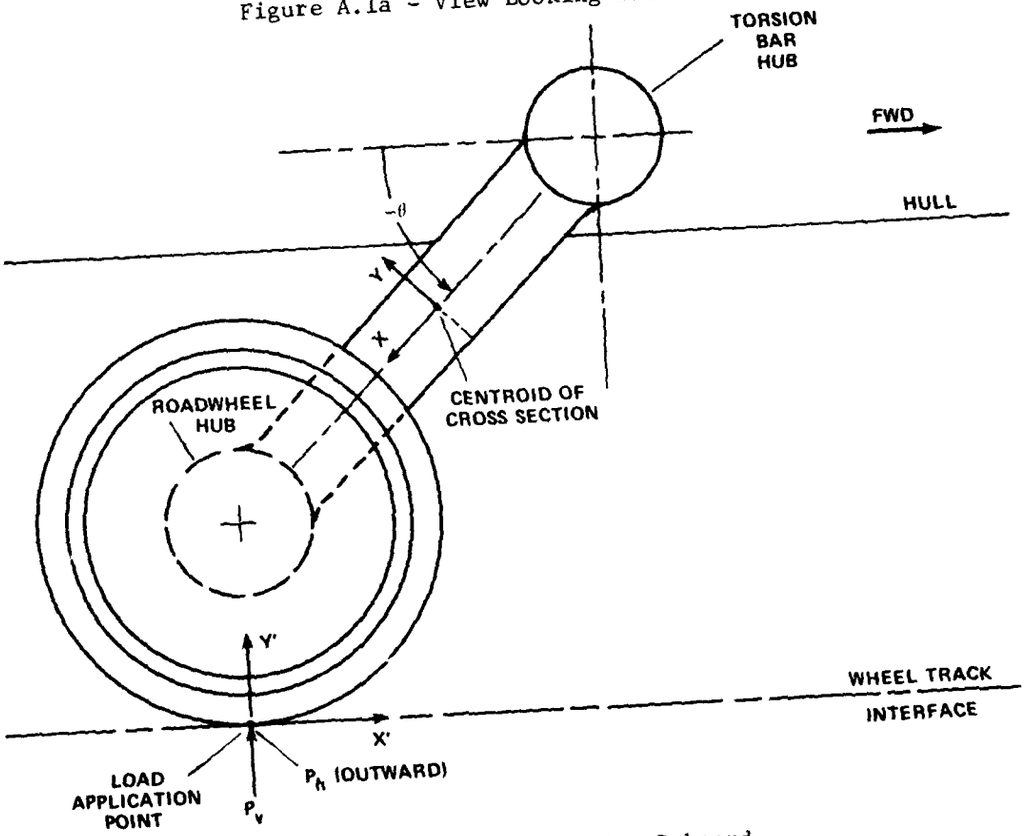

Figure A.1b - View Looking Inboard

Figure A.1 - Vertical and Horizontal Wheel Loads
Acting on Roadwheel

A ratio of horizontal to vertical wheel load of 0.3 was computed as illustrated in Reference 3 for a 52,000 pound tracked combat vehicle. Although the wheel loads calculated from this reference seemed quite high (higher than the existing suspension could withstand), the ratio of the wheel loads was assumed to be a good representation of the actual loading condition. The magnitude of the vertical force (and, therefore, the horizontal force) change as a function of roadarm rotation, as will be evident in Equation (A.11).

The roadarm consists of a cast member with two hubs at either end; the torsion bar hub, which fits over the torsion bar assembly and the roadwheel hub into which the roadwheel spindle is shrunk fit.

The forces and moments at any given cross section of the roadarm between these two hubs act in the right-handed mutually orthogonal XYZ coordinate system whose origin is located at the centroid of the cross section, as shown in Figure A.1. The X-axis extends along the axis of the roadarm, and the cross section is in the YZ plane. The XYZ coordinate system moves along with the roadarm as the roadarm rotates about the torsion bar through angle θ.

When the roadarm is horizontal, θ = 0 degree, the coordinates X_o, Y_o, and Z_o locate the centroid of the cross section from the load application point, as shown in Figure A.2. With appropriate section properties of the member's cross section, stress components can be calculated by using the following equations for forces and moments acting at the centroid of any given cross section of the roadarm between these two hubs, as shown in Figure A.3

$$V_x = P_v \cos \alpha \sin \theta + P_h \sin \alpha \tag{A.1}$$

$$V_y = P_v \cos \theta \tag{A.2}$$

$$V_z = P_v \sin \alpha \sin \theta - P_h \cos \alpha \tag{A.3}$$

$$M_x = P_v \cos \theta \, (-Z_o \cos \alpha - X_o \sin \alpha) + P_h \cos \theta \, (Y_o \cos \alpha) \tag{A.4}$$

$$M_y = P_h X_o - P_h Y_o \sin \theta + P_v Z_o \sin \theta \tag{A.5}$$

$$M_z = P_v \cos \theta \, (-Z_o \sin \alpha + X_o \cos \alpha) + P_h \cos \theta \, (Y_o \sin \alpha) \tag{A.6}$$

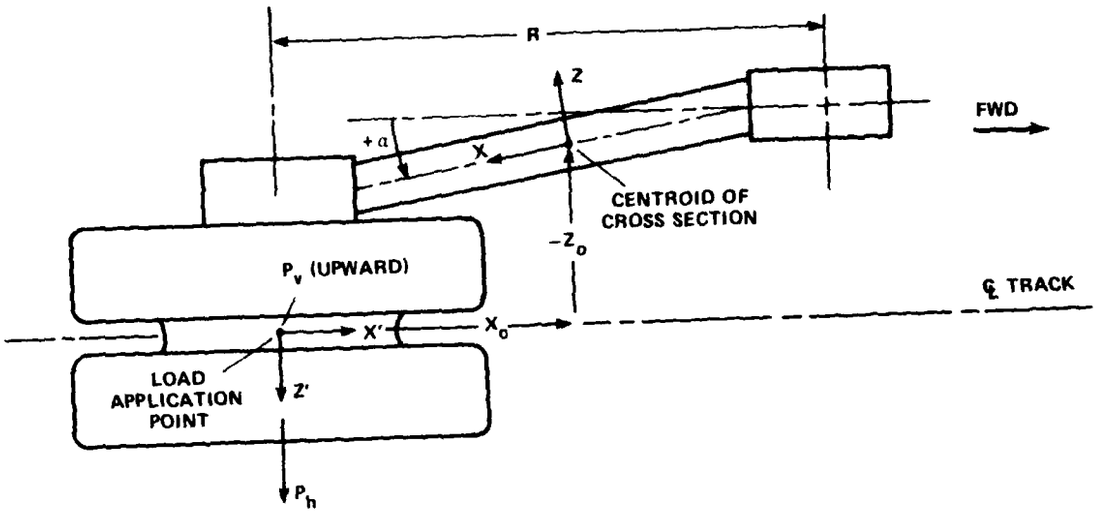

Figure A.2a - View Looking Downward

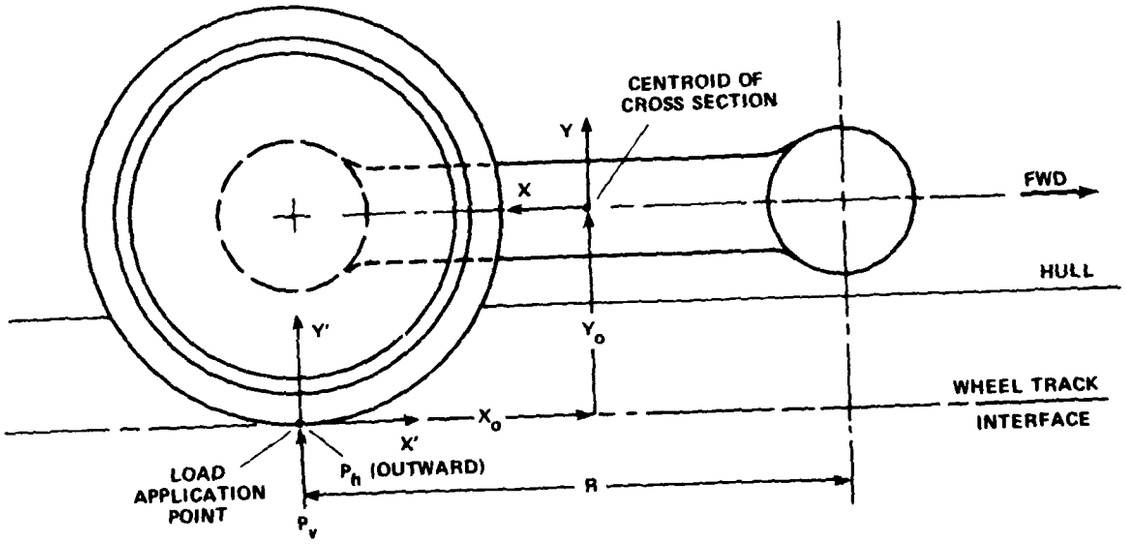

Figure A.2b - View Looking Inboard

Figure A.2 - Coordinates X_o, Y_o, and Z_o, Locating a Cross Section on Roadarm from Roadwheel Load Application Point when θ = 0 Degree

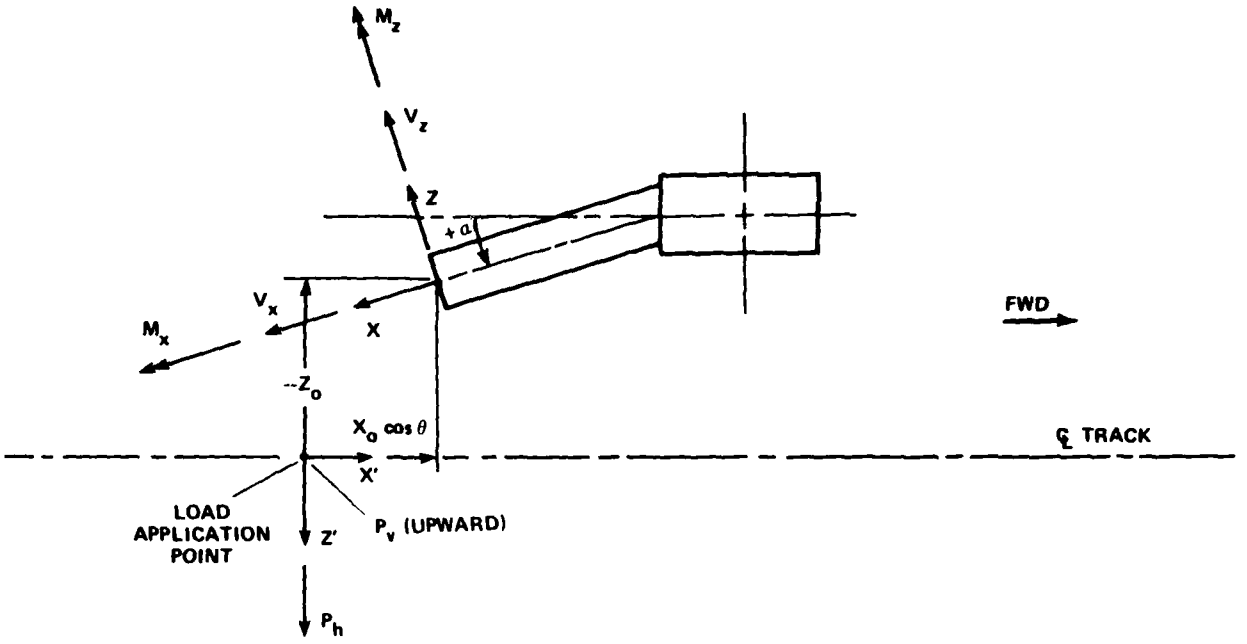

Figure A.3a - View Looking Downward

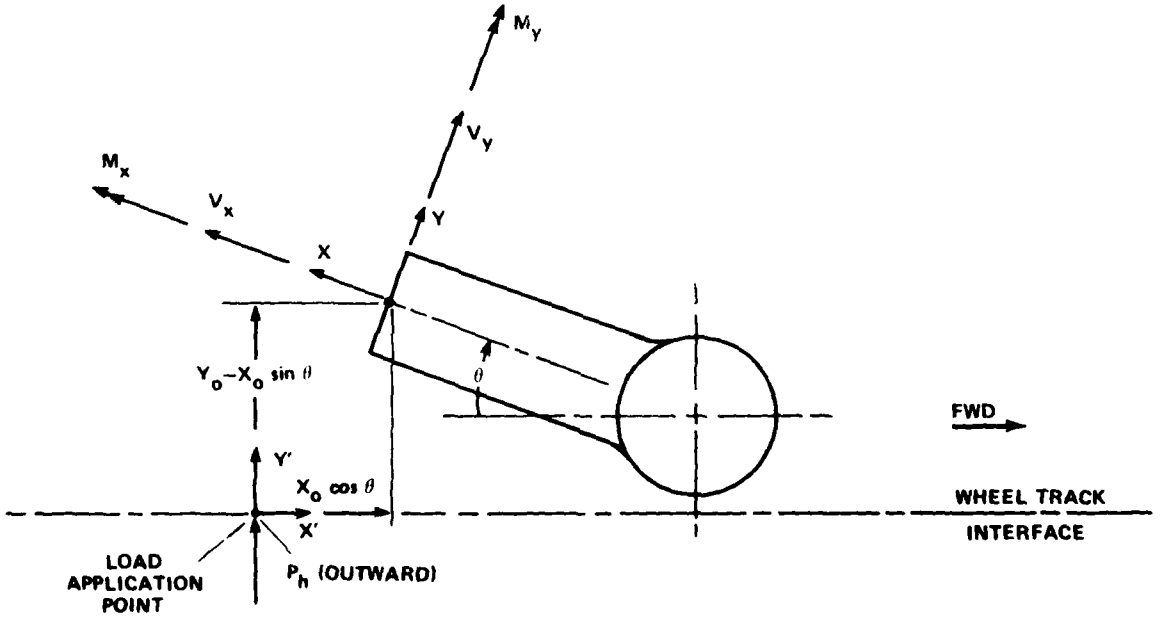

Figure A.3b - View Looking Inboard

Figure A.3 - Forces and Moments Acting on Roadarm Cross Section

where P_v = vertical wheel load

P_h = horizontal wheel load

α = roadarm angle of inclination (+ away from vehicle)

θ = roadarm angle of rotation (+ CW from horizontal)

X_o, Y_o, Z_o = coordinates locating cross section at θ = 0 degree

V_x = axial force in x direction

V_y = shear force in y direction

V_z = shear force in z direction

M_x = torsional moment about x axis

M_y = bending moment about y axis

M_z = bending moment about z axis

To effectively resist the applied forces and moments and to provide a simple design which can be easily fabricated, a prismatic member of rectangular cross section was selected for the portion of the roadarm between the torsion bar hub and the roadwheel hub. These two hubs are assumed to effectively restrain the warping deformation associated with torsional loadings. The torsion bar hub dimensions were kept the same as the existing hub dimensions in both designs; to facilitate placement of the hub onto the existing torsion bar (in the design for evaluation) and because a bar only torsion bar also employs a trunnion to attach the bar to the roadarm, the same hub dimensions were also used for the wide flanged wheel roadarm design.

The hub at the roadwheel end of the roadarm was basically sized by the bearings selected and the diameter of the spindle which extends through both the bearings and the hub.

To determine the final dimensions of the rectangular cross section, a parametric type of stress analysis was performed by varying the width and depth of the member to obtain a design of minimum weight within the factors of safety employed.

Strength calculations for the tandem set configurations are omitted here because they result in excessive weight and incompatibility with the vehicle. They can be analyzed similar to the procedure outlined.

It should be noted that the force and moment equations, and consequently the stress components, are basically in terms of the vertical wheel load P_v; the horizontal wheel load is assumed to be 0.3 P_v. However, the vertical wheel load is also a function of the torsion bar spring rate and suspension system geometry.

Because the existing torsion bar assembly will be used in the evaluation tests, the torsional spring rate must be evaluated and incorporated into the force and moment equations in terms of the vertical load P_v, as follows.

EXISTING TORSION BAR ANALYSIS

The existing torsion bar assembly is a tube-over-bar type of arrangement which, in effect, connects a torsion bar and tube in series to resist the applied vertical wheel load. The torsion tube is rigidly connected to the hull at one end and to the torsion bar at the other end which, in turn, is attached to the roadarm as shown in Figure A.4. For the two torsion members connected in series the equivalent torsional spring rate can be expressed in terms of the individual bar and tube spring rates as

$$k_{eq} = \frac{k_{BAR}\ k_{TUBE}}{k_{BAR} + k_{TUBE}} \tag{A.7}$$

$$k_{BAR} = \frac{\pi\ d^4\ G}{32\ L_B} \tag{A.8}$$

$$k_{TUBE} = \frac{\pi\ (D_T^4 - d_t^4)\ G}{32\ L_T} \tag{A.9}$$

where k_{BAR} = torsional spring rate of the bar

k_{TUBE} = torsional spring rate of the tube

L_B = active length of bar

L_T = active length of tube

d = diameter of bar

D_T = outside diameter of tube

d_t = inside diameter of tube

G = shear modulus of rigidity

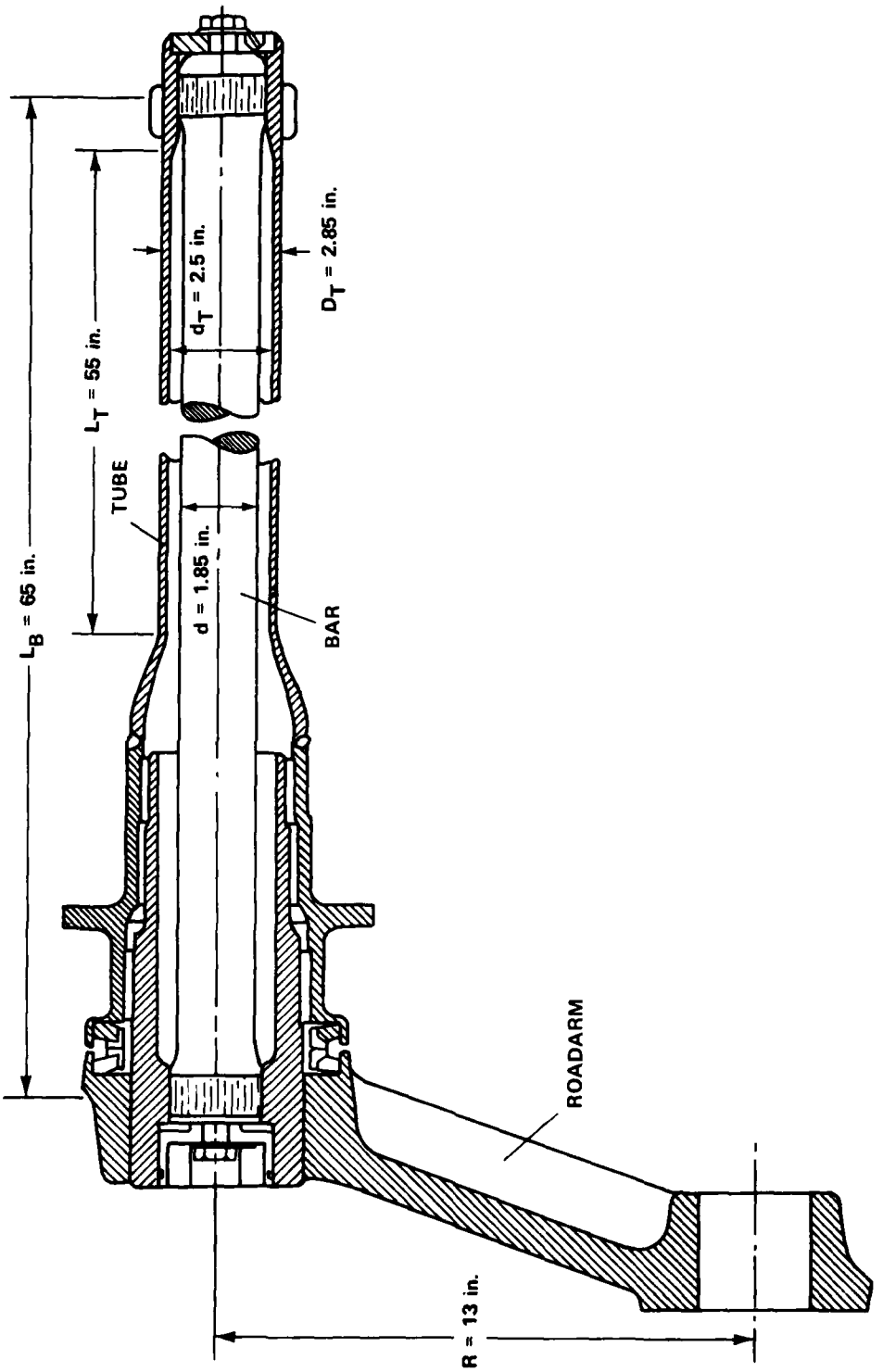

Figure A.4 - Existing Tube-Over-Bar Suspension Assembly

The typical suspension layout shown in Figure A.5 illustrates the parameters used in this discussion and their sense of direction.

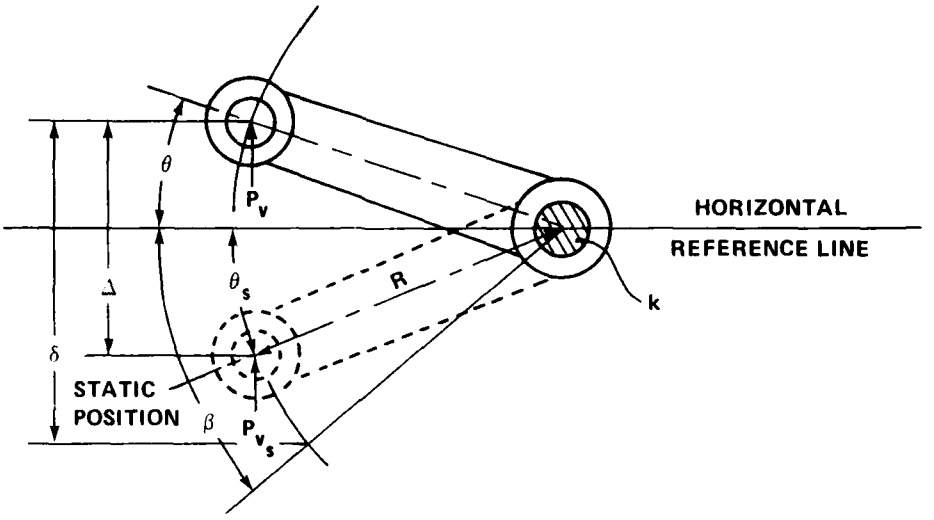

Figure A.5 - Typical Suspension Layout

The torque applied to the torsion bar assembly is equal to the windup angle $(\theta+\beta)$ multiplied by the equivalent torsional spring rate k_{eq}, and is also equal to the vertical wheel load P_v times the moment arm R cos θ.

$$T = P_v (R \cos \theta) = k_{eq} (\theta+\beta) \qquad (A.10)$$

where β = angle between roadarm and horizontal reference line under zero load. Positive below reference line (radians); β = 0.698 radians for existing suspension.

δ = vertical deflection of the end of the roadarm from the zero load position. Positive upward (inches).

Δ = vertical deflection of the end of the roadarm from the static load position. Positive upward (inches).

θ = roadarm rotation from horizontal reference line under load P_v. Positive above reference line (radians).

θ_s = roadarm rotation from horizontal reference line under static load P_s. Positive above reference line (radians).

k = rotational spring rate of torsion bar (inch kips per radian).

P_v = vertical wheel load. Positive upward (kips).

P_{v_s} = vertical wheel load at the static (rest) position. Positive upward (kips).

R = length of roadarm (inches).

The vertical wheel load can, therefore, be expressed as a function of the torsional spring rate and roadarm rotation as

$$P_v = \frac{k_{eq}\ (\theta+\beta)}{R \cos \theta} \tag{A.11}$$

Because each torsion member is subjected to the same applied torque, the shear stress in the bar and tube can be expressed, respectively, as:

$$\tau_{BAR} = \frac{16\ T}{\pi\ d^3} = \frac{16}{\pi\ d^3}\ [k_{eq}\ (\theta+\beta)] \tag{A.12}$$

$$\tau_{TUBE} = \frac{16\ T\ D_T}{\pi\ (D_T^4-d_t^4)} = \frac{16\ D_T}{\pi\ (D_T^4-d_t^4)}\ [k_{eq}\ (\theta+\beta)] \tag{A.13}$$

Based on the material properties of the torsion bar and tube, the rotation to cause shear failure in the torsion bar assembly can be calculated. From material type and hardness specified in Reference 4, the material yield stress was found to be approximately 280 kips per square inch.

The bar of the existing torsion bar assembly is prestressed before installation to increase the elastic capacity of the bar by introducing residual stresses. Based on a torque elastic-plastic[5,6] analysis (see Appendix B) and the degrees of preset, the maximum allowable shearing stress was calculated to be 177 kips per square inch using Coulomb's maximum shearing stress criteria[6,7] of one-half the yield stress. The service limit of rotation of the existing assembly was taken to be 26.1 degrees, which corresponds to a vertical roadwheel deflection of 10 inches from the static vehicle load position (10 inches being the maximum allowable wheel travel before bottoming out on the sponson), and an applied vertical wheel load of 14.7 kips.

ROADARM DESIGN FOR USE WITH ROADWHEEL DESIGN FOR EVALUATION

The roadarm to be used with the roadwheel design for evaluation, having a wheel width equal to the existing wheel width, is positioned parallel to the hull. The angle of inclination toward or away from the vehicle, α, is, therefore, equal to zero. The most highly stressed state occurs at a cross section near the torsion bar hub. Because this is a design for evaluation of the small roadwheel, to verify these design procedures, a factor of safety of 2.0 was employed in the roadarm design on those stresses occurring at a vertical wheel displacement of 10 inches.

After substituting the appropriate values of X_o, Y_o, Z_o, an α, into Equations (A.1) through (A.6), forces and moments acting on the cross section shown in Figure A.6 can be given, with $P_h = 0.3\ P_v$ as:

$$V_x = P_v \sin\theta$$

$$V_y = P_v \cos\theta$$

$$V_z = -0.3\ P_v$$

$$M_x = 9.382\ P_v \cos\theta$$

$$M_y = (3.863 - 9.382 \sin\theta)\ P_v$$

$$M_z = 12.875\ P_v \cos\theta$$

Roadarm section properties can be calculated as:

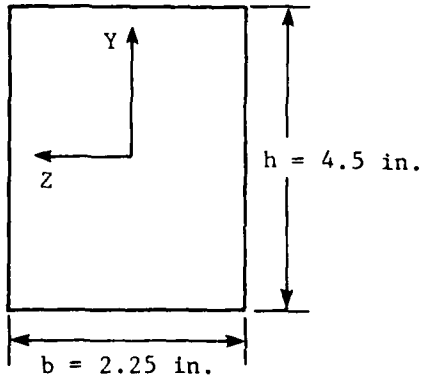

$$SM_y = \frac{1}{6} b^2 h = 3.797 \text{ in.}^3$$

$$SM_z = \frac{1}{6} bh^2 = 7.594 \text{ in.}^3$$

$$A = bh = 10.125 \text{ in.}^2$$

$$C_w = \frac{b^3 h^3}{144} = 7.208 \text{ in.}^6$$

$$J = b^3 h \left[\frac{1}{3} - 0.22203 \left(\frac{b}{h}\right) + 0.0265 \left(\frac{b}{h}\right)^2\right]^* = 11.735 \text{ in.}^4$$

$$\beta_w = \left(\frac{GJ}{EC_w}\right)^{1/2} = 0.791 \text{ in.}^{-1}$$

$$L_{eff} = 10.375 \text{ in.}$$

*Quadratic approximation for J is given in Reference 8.

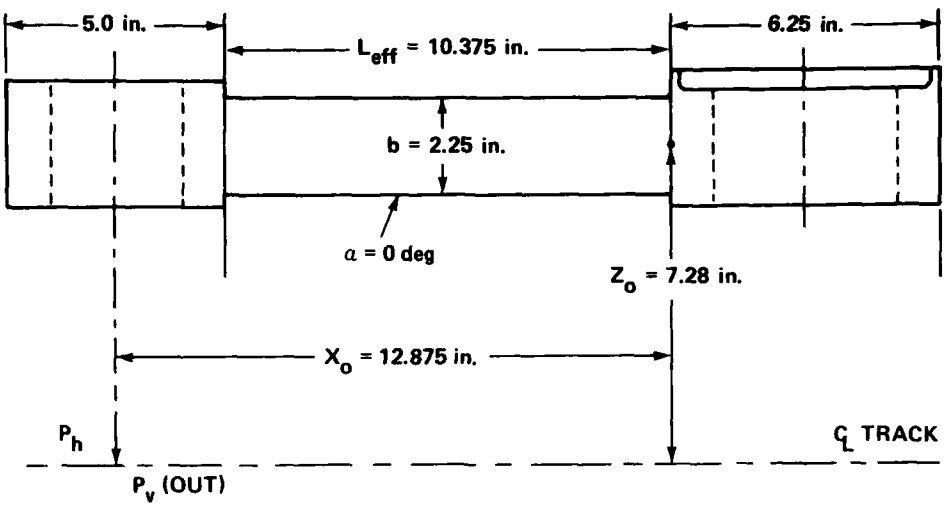

Figure A.6a - Roadarm View Looking Downward

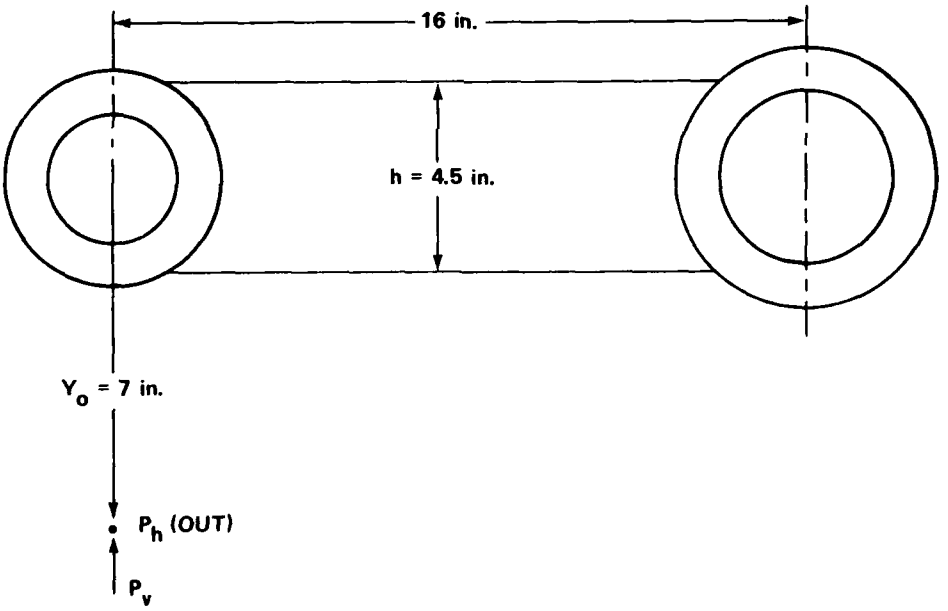

Figure A.6b - Roadarm View Looking Inboard

Figure A.6 - Location of Most Highly Stressed Cross Section of Roadarm to be Used with the Roadwheel for Evaluation

where SM_y = section modulus about y axis

SM_z = section modulus about z axis

A = area of cross section

C_w = warping constant

GJ = torsional rigidity

G = modulus of rigidity

E = Young's modulus of elasticity

L_{eff} = effective length of member between hubs

The individual stress components at this cross section can then be calculated as*

1. Longitudinal stress due to M_z (bending)

$$\sigma_{M_z} = \frac{M_z}{SM_z} = +1.696\ P_v \cos \quad \text{(A.14)}$$

2. Longitudinal stress due to M_y (bending)

$$\sigma_{M_y} = \frac{M_y}{SM_y} = P_v\ (1.017\text{-}2.471 \sin \quad) \quad \text{(A.15)}$$

3. Longitudinal stress due to V_x (axial)

$$\sigma_{A_x} = \frac{V_x}{A} = 0.099\ P_v \sin \quad \text{(A.16)}$$

---

*St. Venant torsional shear stresses are not included because they are equal to zero at the restrained ends of the member; but are nonzero at points away from the ends.

4. Shearing stress due to V_y (maximum at z axis, y=0)*

$$\tau_{Vy} = \frac{3}{2}\frac{V_y}{A} = 0.148\ P_v \cos\theta \qquad (A.17)$$

5. Shearing stress due to V_z (maximum at y axis, z=0)*

$$\tau_{Vz} = \frac{3}{2}\frac{V_z}{A} = -0.044\ P_v \qquad (A.18)$$

The stresses resulting from restrained torsion of a rectangular cross section can be given as[8]

6. Longitudinal stress due to M_x (warping)

$$\sigma_w = \frac{Ebh}{4}\frac{d^2\gamma^{**}}{dx^2} = \frac{Ebh}{4}\left(\frac{M_x\beta_w}{GJ}\tanh\frac{\beta_w L}{2}\right) = 4.1612\ P_v \cos\theta \qquad (A.19)$$

7. Shear stress due to M_x (maximum across thickness b)

$$\tau_{wb} = \frac{Eb^2h}{16}\frac{d^3\gamma}{dx^3} = \frac{Eb^2h}{16}\frac{M_x\beta_w^2}{GJ} = 1.8532\ P_v \cos\theta \qquad (A.20)$$

8. Shear stress due to M_x (across depth)***

$$\tau_{wh} = \frac{Eb^2h}{16}\frac{d^3\gamma}{dx^3} = \frac{Eb^2h}{16}\frac{M_x\beta_w^2}{GJ} = 1.8532\ P_v \cos\theta \qquad (A.21)$$

---

*The factor 3/2 in this equation is a shape factor--the ratio of maximum shear stress to average shear stress acting over a rectangular cross section.

**γ = the angle of twist per unit length of the roadarm.

***Because no equation for the shear stress along depth h is given in Reference 8, its value is bounded by conservatively estimating its value to be equal to the shear stress acting along width b (which is maximum acting on cross section).

The longitudinal stress components can be combined as shown in Figure A.7. Because the wheel load on the smaller wheel is reduced by 12/18, the ratio of existing number of roadwheels to the number of small roadwheels per vehicle, and the length of the roadarm is increased from 13 to 16 inches; β, the angle the roadarm makes with the horizontal under zero load, must be changed accordingly; this can be done by re-indexing the torsion bar. By rearranging terms in Equation (A.11), β can be expressed as:

$$\beta = \frac{P_{v_s} R \cos \theta_s}{k_{eq}} - \theta_s \qquad (A.22)$$

where P_{v_s} = load per wheel at static position = $\frac{52.77}{18}$ kips = 2.888 kips

R = length of roadarm = 16 inches

k_{eq} = torsional stiffness of existing tube over bar assembly = 148.7 inch-kips per radian

θ_s = angle roadarm makes with horizontal under a static vehicle load = -0.6974 radians

Solving Equation (A.22), β equals 0.936 radians. The vertical load, P_v, can now be substituted into the resulting stress equations in terms of the torsional parameters, k_{eq}, β, and R. The direct longitudinal stresses at each corner of the cross section can be obtained by algebraically adding the individual axial, bending and warping stress components acting at each corner as shown in Figure A.7. Looking along the roadarm axis toward the torsion bar hub, corner 1 is the lower right corner of the cross section; corner 2, the lower left; corner 3, the upper left; and corner 4, the upper right. The stresses at each corner of the cross section can now be expressed as:

$$\sigma_1 = \sigma_{A_x} - \sigma_{M_y} + \sigma_{M_z} + \sigma_W$$

$$= \frac{k_{eq}\ (\theta+\beta)}{R \cos \theta} (5.8567 \cos \theta + 2.5697 \sin \theta - 1.0173) \qquad (A.23)$$

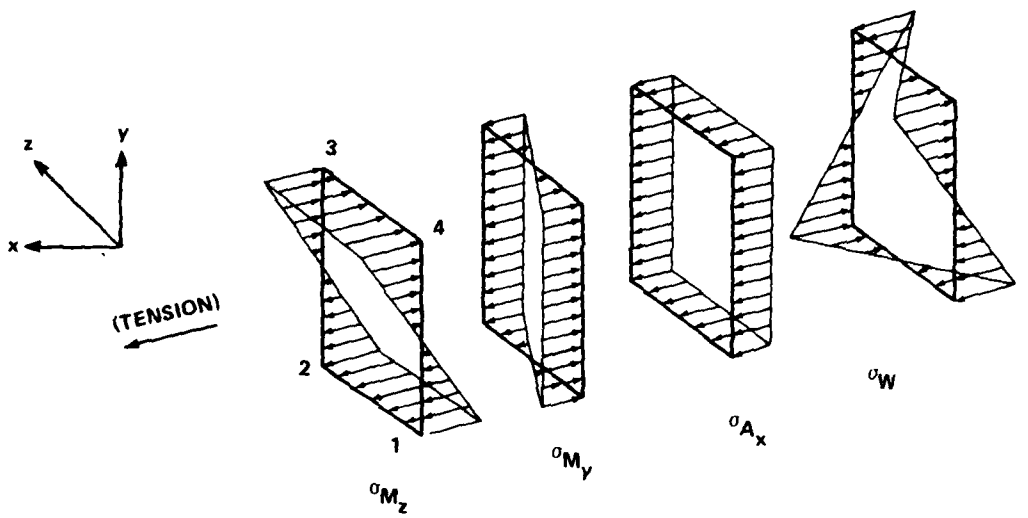

Figure A.7a - Longitudinal Stress Profiles

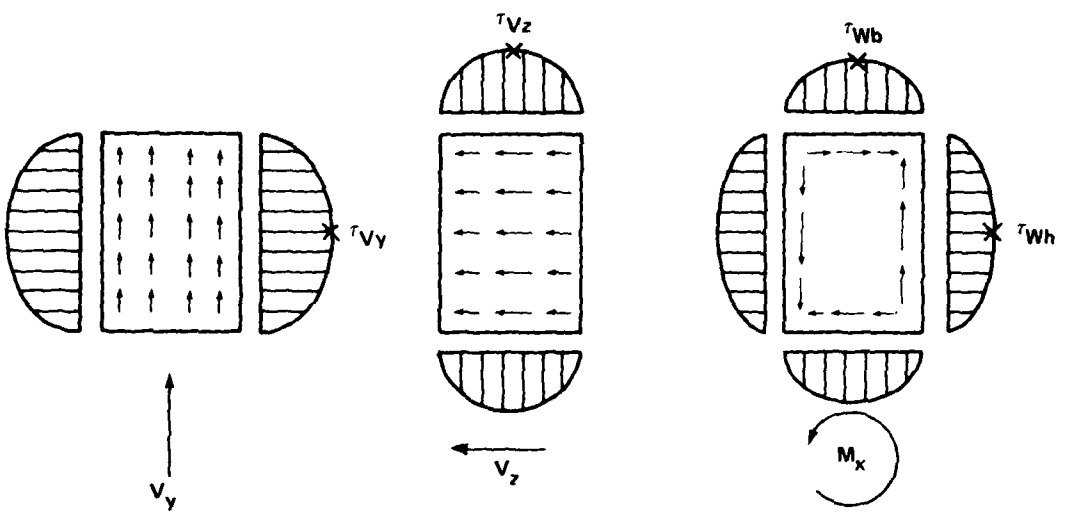

Figure A.7b - Shear Stress Profiles

Figure A.7 - Longitudinal and Shear Stress Profiles at Cross Section of Small Roadwheel Roadarm

$$\sigma_2 = \sigma_{A_x} + \sigma_{M_y} + \sigma_{M_z} - \sigma_W$$

$$= \frac{k_{eq}\ (\theta+\beta)}{R \cos \theta} (-2.4657 \cos \theta - 2.3721 \sin \theta + 1.0173) \qquad \text{(A.24)}$$

$$\sigma_3 = \sigma_{A_x} + \sigma_{M_y} - \sigma_{M_z} + \sigma_W$$

$$= \frac{k_{eq}\ (\theta+\beta)}{R \cos \theta} (2.4657 \cos \theta - 2.3721 \sin \theta + 1.0173) \qquad \text{(A.25)}$$

$$\sigma_4 = \sigma_{A_x} - \sigma_{M_y} - \sigma_{M_z} - \sigma_W$$

$$= \frac{k_{eq}\ (\theta+\beta)}{R \cos \theta} (-5.8567 \cos \theta + 2.5697 \sin \theta - 1.0173) \qquad \text{(A.26)}$$

where k_{eq} = 148.7 inch-kips per radian

R = 16 inches

β = 0.9356 radians

and are plotted as a function of roadarm rotation in Figure A.8.

The vertical line at the roadarm rotation angle of, approximately, 0 degree indicates the point at which the roadarm has reached 10 inches of vertical deflection from the statically loaded position. At this point of rotation, corner 4 exhibits the highest stress state with a factor of safety of 2.0 on yield.

The shear stresses acting on the cross section are also combined and presented as a function of the torsion bar assembly characteristics and the roadarm rotation θ. The shear stress profiles resulting from the applied loads are shown in Figure A.9.

After substituting the vertical wheel load P_v in terms of the torsional parameters, k_{eq}, β, and R, into the resulting stress equations, the individual shear stresses acting along each edge of the cross section can be added to express the resulting shear stresses as:

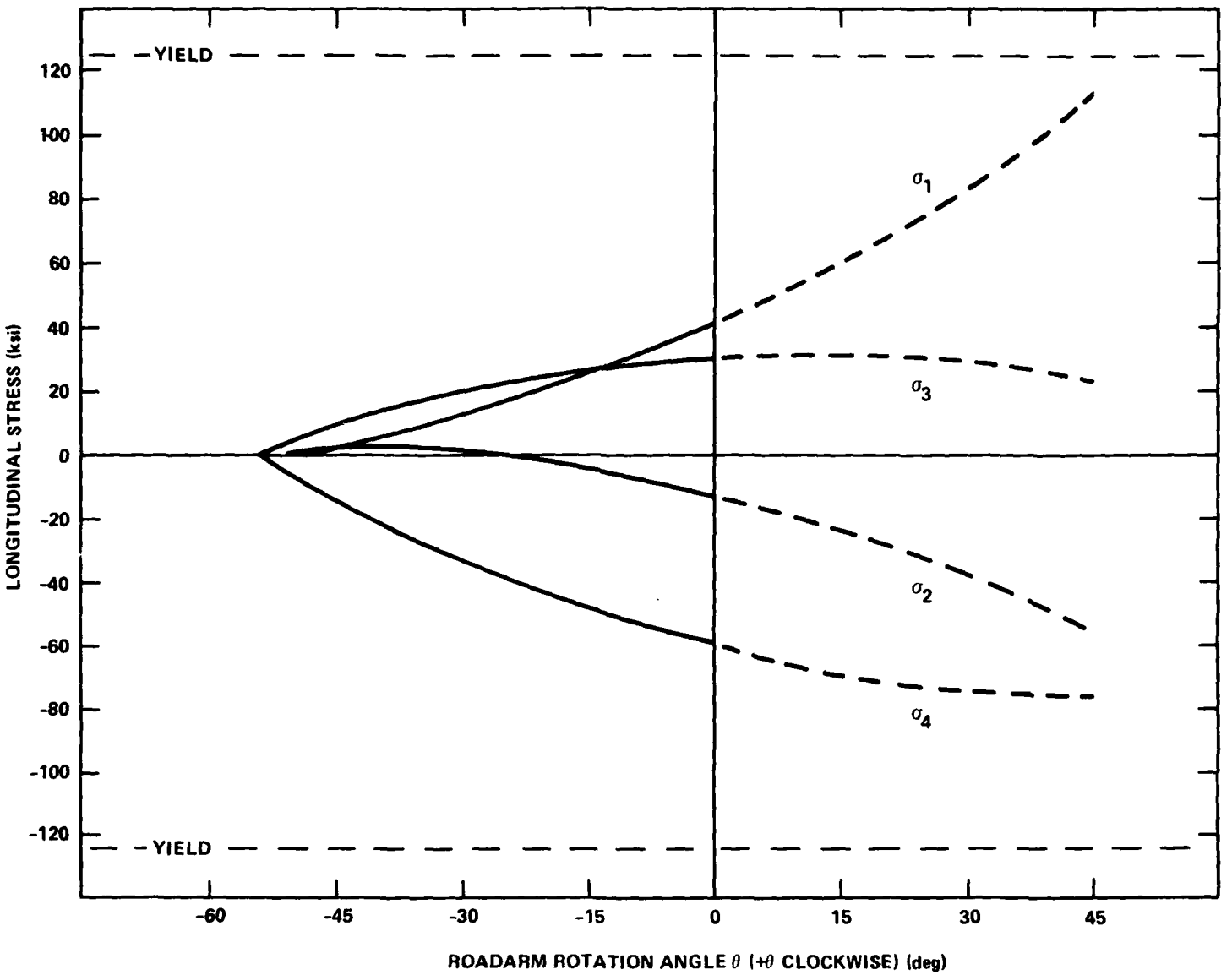

Figure A.8 - Longitudinal Corner Stresses as a Function of Roadarm Rotation (Design for Evaluation)

$$\tau_{TOP\ EDGE} = \tau_{Vz} - \tau_{Wb}$$

$$= \frac{k_{eq}\ (\theta+\beta)}{R \cos \theta} (-1.8532 \cos \theta - 0.0444) \qquad (A.27)$$

$$\tau_{BOTTOM\ EDGE} = \tau_{Vz} + \tau_{Wb}$$

$$= \frac{k_{eq}\ (\theta+\beta)}{R \cos \theta} (1.8532 \cos \theta - 0.0444) \qquad (A.28)$$

$$\tau_{INBOARD\ EDGE} = \tau_{Vy} - \tau_{Wh}$$

$$= \frac{k_{eq}\ (\theta+\beta)}{R \cos \theta} (1.7051 \cos \theta) \qquad (A.29)$$

$$\tau_{OUTBOARD\ EDGE} = \tau_{Vy} + \tau_{Wh}$$

$$= \frac{k_{eq}\ (\theta+\beta)}{R \cos \theta} (-2.0013 \cos \theta) \qquad (A.30)$$

where k_{eq} = 148.7 inch-kips per radian

R = 16 inches

β = 0.9356 radian

and are plotted as a function of roadarm rotation in Figure A.9.

The vertical line at the roadarm rotation angle of, approximately, 0 degree indicates the point at which the roadwheel has deflected vertically 10 inches from the statically loaded position. At this point the outboard edge exhibits the highest stress state with a factor of almost 3.5 on the maximum allowable shear stress of 1/2 yield.

ROADARM DESIGN FOR USE WITH WIDE FLANGED ROADWHEEL

The roadarm to be used with the wide flanged roadwheel is positioned with respect to the hull at an angle of inclination α of 0 degree.

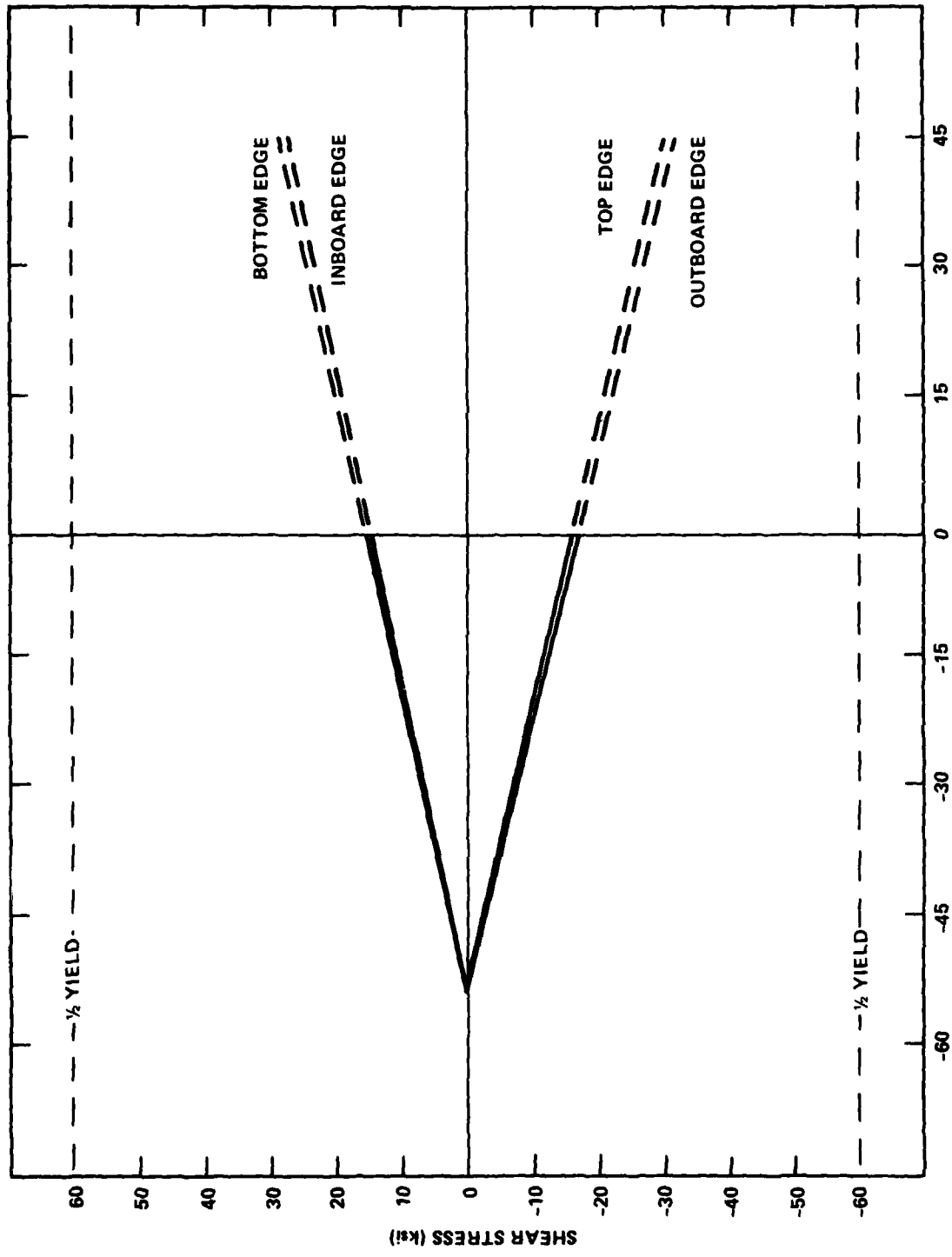

Figure A.9 - Shear Stresses as a Function of Roadarm Rotation (Design for Evaluation)

The vertical (and horizontal) wheel load in this case is expressed as a function of the "bar only" torsion bar characteristics rather than the existing t[illegible] over bar characteristics. The torsion bar is also recessed 1.65 inches to be com[illegible]ible with the track guide to hull dimension. Because this type of cross section has not been evaluated through actual testing, a factor of safety of 2.0 was employed, as in the design for evaluation, on those stresses occurring at a vertical wheel displacement of 10 inches. The most highly stressed cross section occurs at a point near the torsion bar hub. Once this cross section has been evaluated through testing, to assess the analytical assumptions, a more weight efficient roadarm may be obtainable.

Only the results of this design will be presented here, because the procedure is identical to that of the design for evaluation. The only difference between the two designs, as mentioned before, are the length of the roadarm (13 inches), the roadarm rotation angles under static and zero wheel loads, θ_s and β (-0.9114 and 1.2622 radians, respectively), and the rotational spring rate of the torsion bar, k_{BAR} (66.57 inch-kips per radian). The cross sectional dimensions are b = 2 inches and h = 4 inches, and the effective length of the roadarm is 7.375 inches. The section properties can be calculated as before.

Figure A.10 shows the location of the most highly stressed cross section of the roadarm in terms of X_o, Y_o, Z_o, and α. From these parameters the forces and moments, and hence the stresses, acting on the cross section can be determined in terms of the vertical wheel load P_v.

To express these stresses in terms of only the roadarm rotation, the torsion bar characteristics β and k were obtained from the torsion bar design procedure given in Appendix B. For this torsion bar design, the length of the bar was taken to be 82 inches, because it is anchored on the opposite side of the vehicle and, the total vertical stiffness at static was equated to the total vertical stiffness of the existing suspension at static. Finally, the shear stress in the bar was designed to the same factor of safety against failure as the existing torsion bar, at maximum vertical travel (10 inches).

The longitudinal stresses can be combined, as in the previous design (see Figure A.7). After substituting the vertical wheel load P_v, in terms of the torsion bar characteristics previously calculated, into the stress equations, the direct

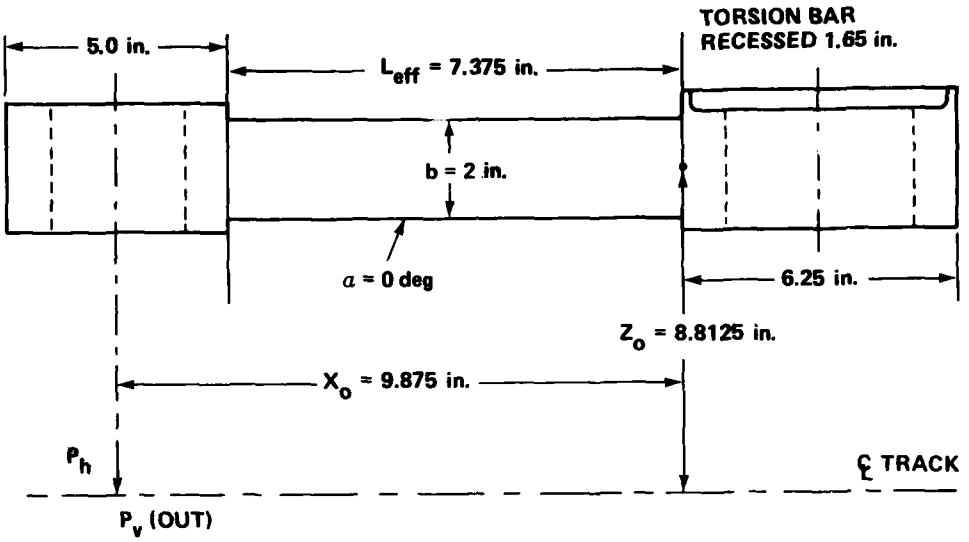

Figure A.10a - Roadarm View Looking Downward

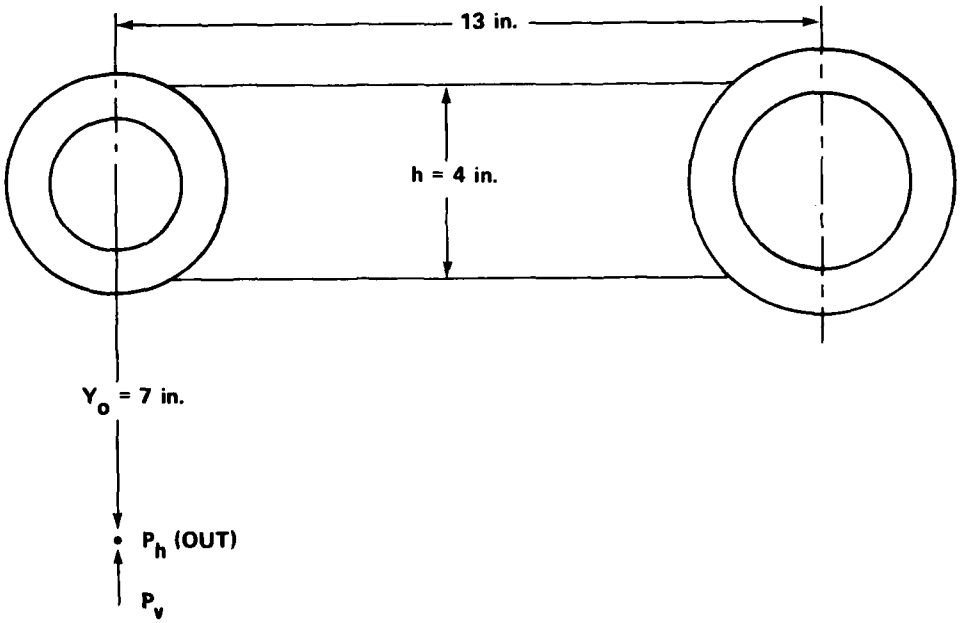

Figure A.10b - Roadarm View Looking Inboard

Figure A.10 - Location of Most Highly Stressed Cross Section of Roadarm to be Used with Wide Flanged Roadwheel

longitudinal stresses at each corner of the cross section can be obtained by algebraically adding the individual axial, bending, and warping stress components acting at each corner, as shown in Figure A.7. The corners are numbered the same as in the previous design. The combined corner stresses can now be expressed as:

$$\sigma_1 = \sigma_{A_x} - \sigma_{M_y} + \sigma_{M_z} + \sigma_W$$

$$= \frac{k\ (\theta+\beta)}{R \cos \theta} (8.7274 \cos \theta + 4.2172 \sin \theta - 1.1109) \qquad (A.31)$$

$$\sigma_2 = \sigma_{A_x} + \sigma_{M_y} + \sigma_{M_z} - \sigma_W$$

$$= \frac{k\ (\theta+\beta)}{R \cos \theta} (-5.0242 \cos \theta - 3.9672 \sin \theta + 1.1109) \qquad (A.32)$$

$$\sigma_3 = \sigma_{A_x} + \sigma_{M_y} - \sigma_{M_z} + \sigma_W$$

$$= \frac{k\ (\theta+\beta)}{R \cos \theta} (5.0242 \cos \theta - 3.9672 \sin \theta + 1.1109) \qquad (A.33)$$

$$\sigma_4 = \sigma_{A_x} - \sigma_{M_y} - \sigma_{M_z} - \sigma_W$$

$$= \frac{k\ (\theta+\beta)}{R \cos \theta} (-8.7274 \cos \theta + 4.2172 \sin \theta - 1.1109) \qquad (A.34)$$

where $k = 66.57$ inch-kips per radian

$R = 13$ inches

$\beta = 1.2622$ radians

and are plotted as a function of roadarm rotation in Figure A.11.

The vertical line at a roadarm rotation angle of, approximately, 0 degree indicates the point at which the roadwheel has attained 10 inches of vertical deflection from the statically loaded position. At this point of rotation, corner 4 exhibits the highest combined stress state with a factor of safety of 2.0 on yield.

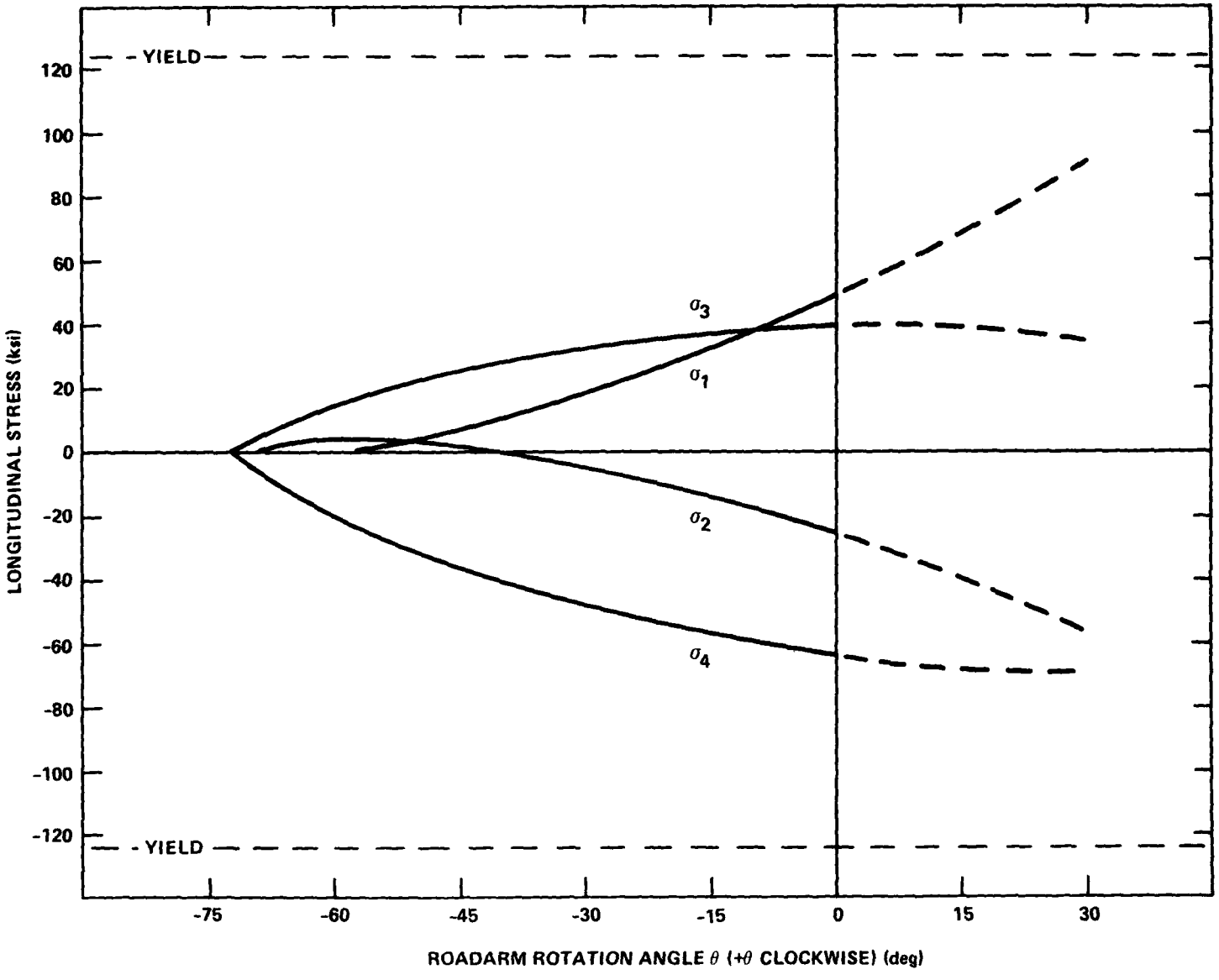

Figure A.11 - Longitudinal Corner Stresses as a Function of Roadarm Rotation (for Wide Flanged Roadwheel)

The shear stresses acting along each edge of the cross section are similarly combined (see Figure A.7) and, after substituting the vertical wheel load P_v, (in terms of the torsion bar characteristics previously calculated) into the resulting stress equations, the combined shear stresses acting along each edge of the cross section can be expressed as:

$$\tau_{TOP\ EDGE} = \tau_{Vz} - \tau_{Wb}$$

$$= \frac{k\ (\theta+\beta)}{R \cos \theta} (-3.0691 \cos \theta - 0.0563) \qquad (A.35)$$

$$\tau_{BOTTOM\ EDGE} = \tau_{Vz} + \tau_{Wb}$$

$$= \frac{k\ (\theta+\beta)}{R \cos \theta} (3.0691 \cos \theta - 0.0563) \qquad (A.36)$$

$$\tau_{INBOARD\ EDGE} = \tau_{Vy} - \tau_{Wh}$$

$$= \frac{k\ (\theta+\beta)}{R \cos \theta} (2.8816 \cos \theta) \qquad (A.37)$$

$$\tau_{OUTBOARD\ EDGE} = \tau_{Vy} + \tau_{Wh}$$

$$= \frac{k\ (\theta+\beta)}{R \cos \theta} (-3.2566 \cos \theta) \qquad (A.38)$$

where $k = 66.57$ inch-kips per radian

$R = 13$ inches

$\beta = 1.2622$ radians

and are plotted as a function of roadarm rotation in Figure A.12.

The vertical line at the roadarm rotation angle of, approximately, 0 degree indicates the point at which the roadwheel has deflected vertically 10 inches from the statically loaded position. At this point the outboard edge exhibits the highest stress state with a factor of safety of 3.0 on the maximum allowable shear stress, which is 1/2 yield.

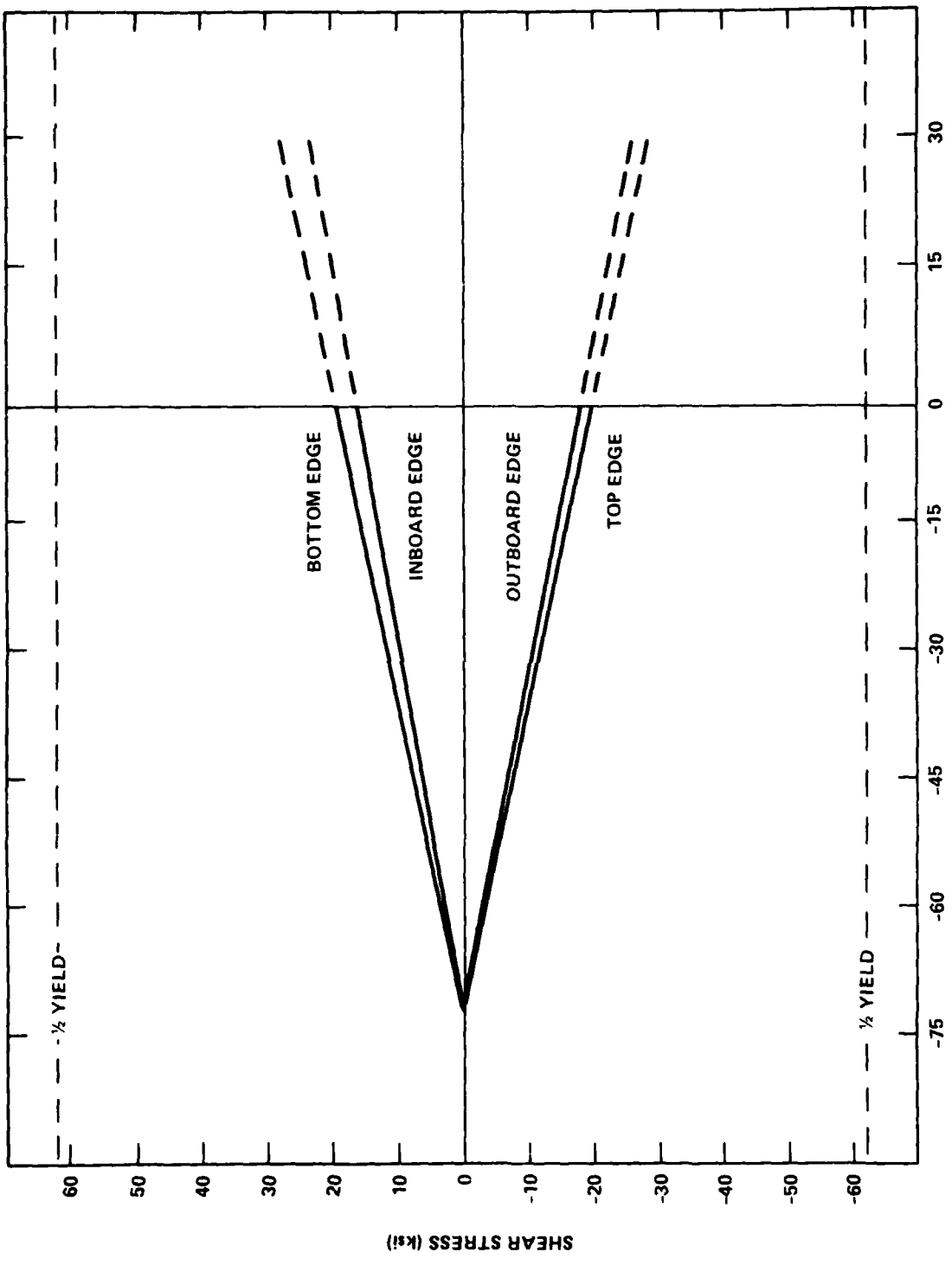

Figure A.12 - Shear Stresses as a Function of Roadarm Rotation (for Wide Flanged Roadwheel)

APPENDIX B

PROCEDURES FOR DEVELOPING STIFFNESS CURVES AND DESIGNING TORSION BAR AND TUBE-OVER-BAR SUSPENSIONS

The first section of this appendix outlines the procedure and presents equations which were used to develop the stiffness versus deflection curves presented in the text for various roadwheel and roadarm combinations.

The appendix also includes an analysis of the existing torsion bar preset to determine the amount of reserve strength stored in the bar after presetting and to show how the factor of safety, used in Appendix A, was arrived at.

This torsion bar presetting analysis is then incorporated into a torsion bar or torsion tube over bar design procedure for a specified suspension geometry, spring rate, and factor of safety.

The equations which were used to develop the stiffness curves are, in part, based on the geometry of the suspension system. A typical suspension layout is shown in Figure A.5 where the variables used in this study are defined.

Based on Figure A.5, the load and deflection characteristics of a torsion bar suspension can then be given as

$$P = \frac{k\ (\theta+\beta)}{R\ \cos\ \theta} \tag{A.11}$$

$$\Delta = R\ (\sin\ \theta - \sin\ \theta_s) \tag{B.1}$$

$$\delta = R\ (\sin\ \theta + \sin\ \beta) \tag{B.2}$$

and the vertical stiffness of an individual suspension unit $K = dP/d\delta$, as[3]

$$K = \frac{k}{R^2}\left[\frac{1+(\theta+\beta)\ \tan\ \theta}{\cos^2\ \theta}\right] \tag{B.3}$$

The individual vertical stiffness is nonlinear and for a given wheel diameter can be plotted as a function of θ, or Δ for given values of k, β, and R.

To preserve the vehicle ground clearance for a particular roadwheel-roadarm combination, the distance between the roadwheel-track interface and the horizontal reference line must be the same as that of the existing vehicle.

The existing vehicle in the static position has a roadarm position θ_s, of -0.3351 inches radians (-19.2 degrees), a roadarm length of 13 inches and a wheel diameter of 26 inches. The distance between the wheel to track interface and the horizontal reference line (17.275 inches) can be obtained by substituting these values into Equation (B.3).

$$\frac{D}{2} - R \sin \theta_s = 17.275 \tag{B.4}$$

Using this equation, the angular rotation of a roadarm in the static position θ_s can be obtained for any given roadwheel and roadarm combination such that the vehicle ground clearance remains unchanged.

Also, in the static position, the vehicle gross weight is assumed to be evenly distributed among each of the roadwheels N (the vehicle gross weight is 52.77 kips). Equation (A.11) can, therefore, be rewritten to reflect the static condition as:

$$P_s = \frac{52.77}{N} = \frac{k\ (\theta_s+\beta)}{R \cos \theta_s} \tag{B.5}$$

The number of roadwheels N can be determined for a given wheel diameter, such that the angle of attack of the existing track envelope is preserved and the wheels are realistically configured.

With the total static vertical stiffness specified, the torsion bar characteristics, k and β, can be obtained by solving Equations (B.5) and (B.6) simultaneously with $\theta = \theta_s$ in Equation (B.6). Then, the total stiffness versus rotation curve can be generated by substituting varying values of θ into Equation (B.6).

$$K_{TOTAL} = NK = \frac{Nk}{R^2}\left[\frac{1+(\theta+\beta)\ \tan \theta}{\cos^2 \theta}\right] \tag{B.6}$$

When the total vertical stiffness is specified at some point of deflection other than the static position, another variable is introduced (the roadarm rotation θ corresponding to that point of deflection) and an additional equation (Equation (B.1)) must be used to solve for k and β.

The total stiffness versus deflection curve can be obtained for a given roadwheel and roadarm combination by substituting values of Δ, the deflection above static, into Equation (B.1), solving for the corresponding roadarm rotations θ and substituting these values of θ along with k and β already determined into Equation (B.6) to solve for the total stiffness at that deflection.

Whether a certain stiffness curve is actually obtainable in terms of actual tube and bar component dimensions (within the size limitations of the vehicle) will be discussed next.

EXISTING TORSION BAR PRESET ANALYSIS

Before a specific stiffness curve can be selected as a possible suspension candidate, the rotational spring rate k, previously calculated, must be defined in terms of actual torsion bar (or tube over bar) dimensions to determine if such a spring rate is actually obtainable. Some values of k are unrealistic in that there are no combinations of diameter and length, within the size limitations of the vehicle, which would give the desired value of k. As mentioned before, if the wheel load is small enough, a "bar only" torsion bar can be designed of sufficient strength to be used alone. As the wheel load increases, a "tube over bar" torsion bar is needed for suspensions requiring a low equivalent spring rate, k_{eq}.

In either case, before installation, the bar is usually prestressed in the direction of service loading to just past the yield point of the material. A slight permanent set is produced and after unloading some residual stresses remain. Prestressing, in effect, extends the materials elastic limit because the residual stresses remaining after prestressing must be overcome before additional stresses can develop.

To aid in the design of other torsion bars and to determine how far the bars need to be wound up during presetting, the existing bar was analyzed to determine the factor of safety between the actual service shear stress at 10 inches of travel (maximum travel) and the point at which the bar would experience additional yielding while in service. Yielding while in service was selected as an upper bound for the factor of safety, because any additional yielding (in addition to the preset) would produce undesirable permanent rotational set and alter the suspension characteristics from which they were originally intended.

To calculate the residual stresses remaining in a torsion bar after presetting, the relationship between shearing stress and shearing strain must be known throughout the range of windup. The shear stress-strain relationship of the existing torsion bar was unavailable but was assumed to be representative of an elastic perfectly plastic material (no strain hardening capability). The equations presented here can be used for any bilinear shear stress-strain diagram, as shown in Figure B.1. The shear stress at yield is assumed to be one-half of the tensile yield stress, i.e., τ_{yp} = 140 ksi.

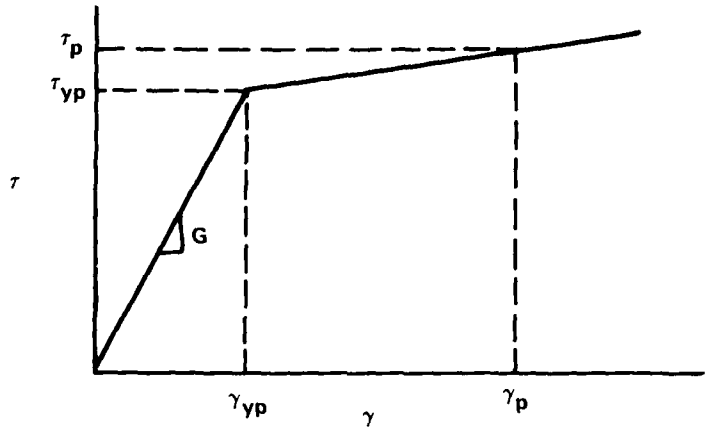

Figure B.1 - Shear Stress-Strain Diagram

The existing bar is 65 inches long and 1.85 inches in diameter. The torque required to initiate yielding can be calculated from Equation (B.7) to be 174.05 inch-kips.

$$T_{yp} = \frac{\pi d^3}{16} \tau_{yp} \tag{B.7}$$

where d = bar diameter and τ_{yp} = shear stress at yield (assumed to be 1/2 σ_y) = 140 ksi. The amount of windup required to initiate yielding can then be calculated from Equation (B.8) to be 0.8554 radians (49.01 degrees).

$$\phi_{yp} = \frac{T_{yp}}{k_{BAR}} \tag{B.8}$$

After attaining a rotation of 0.8554 radians, the outer fibers begin to go plastic as the inner plastic core is reduced. The total amount of windup to prestress the bar of the existing suspension, ϕ_p is 1.5219 radians (87.2 degrees).

Reference 3 recommends a maximum applied shear strain, γ_{max} of 0.022 radians during the presetting operation of torsion bars made of through hardened material of hardness near Rockwell C50. In terms of γ_{max}, the maximum recommended windup for the existing bar can be calcaluted from Equation (B.9) to be 1.5459 radians (88.58 degrees), which is, approximately, the preset windup angle.

$$\phi_{max} = \frac{2\ L_B\ \gamma_{max}}{d} \tag{B.9}$$

The torque which must be applied to produce the desired windup for presetting can be given as[5]

$$T_{PRESET} = \frac{2\ \pi\ L_B^3}{\phi^3} \int_o^{\gamma_p} \gamma^2\ \tau\ d\ \gamma \tag{B.10}$$

where the right side of this equation represents the moment of inertia with respect to the shear stress τ axis of the area under the shear stress-strain diagram shown in Figure B.2.

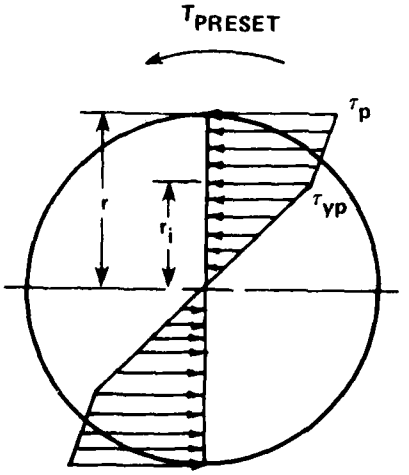

Figure B.2 - Shear Stress Distrubition
Showing Partial Yielding
under Preset Torque

Points γ_{yp} and γ_p, shown on the shear strain axis of Figure B.1, represent the yield shear strain and preset shear strain, respectively, and points τ_{yp} and τ_p, shown on the shear stress axis, represent the yield shear stress and preset shear stress, respectively.

After integrating, and substituting $\phi_p = 2\ L_B\ \gamma_p/d$, Equation (B.10) can be rewritten as:

$$T_{PRESET} = \frac{\pi d^3}{48}\left[\tau_{yp}\ (4-a^3)+(\tau_p-\tau_{yp})(3-a-a^2-a^3)\right] \qquad (B.11)$$

where $a = \gamma_{yp}/\gamma_p$.

Solving Equation (B.11), with $\tau_p = \tau_{yp}$ (no strain hardening), the torque required to preset the existing torsion bar can be calculated to be 220.3 inch-kips. Under this applied torque the outer portion of the bar cross section is subjected to a constant yield stress τ_{yp}, while the inner core remains elastic. Figure B.2 illustrates this shear stress distribution over the cross section where r_i, the intermediate radius, locates the elastic-plastic boundary.

The preset torque Equation (B.11) can also be obtained by integrating the shear stress distribution, shown in Figure B.2, over the entire cross sectional area. The resulting expression will be the same as Equation B.11 with $a = r_i/r$. This is expected, because during twisting of a round bar, the cross sections remain plane, so that the shear strain at any point is proportional to the radius.

When the bar is unloaded, as if an equal and opposite torque were applied, the torsional shear stresses follow Hooke's law to produce the elastic linear stress distribution shown in Figure B.3.

To produce the same torque, T_{PRESET}, the linearly elastic shear stress distribution shown in Figure B.3 is integrated over the entire cross sectional area of the bar and the shear stress at the surface of the bar is found to be slightly greater than the presetting surfaces shear stress by an amount $\Delta\tau$. This relationship can be given as:

$$T_{PRESET\ UNLOAD} = \frac{\pi d^3}{16}\ (\tau_p+\Delta\tau) \qquad (B.12)$$

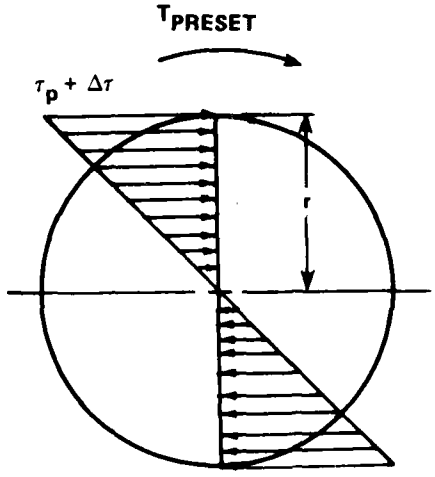

Figure B.3 - Elastic Linear Shear Stress Distribution when Preset Torque is Unloaded

Because the shear stress distributions shown in Figures B.2 and B.3 both represent the same applied torque T_{PRESET}, the two shear stress distributions can be superimposed to obtain the unloaded bar with the residual shear stress distribution shown in Figure B.4. The residual surface shear stress can be expressed as:

$$\Delta\tau = \frac{\tau_{yp}(4-a^3)}{3} + \frac{(\tau_p-\tau_{yp})}{3}(3-a-a^2-a^3) - \tau_p \qquad (B.13)$$

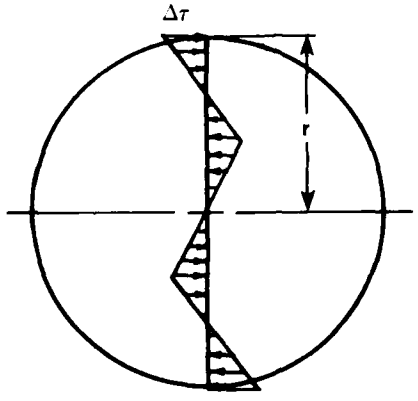

Figure B.4 - Residual Shear Stress Distribution Remaining in Bar after Presetting Operation

The elastic range has, in effect, been extended due to the presence of the residual stresses, because the bar now behaves elastically if torques less than or equal to the preset torque are reapplied in the same direction.

The magnitude of the residual shear stress $\Delta\tau$, in the outer fibers of the existing preset bar, can be calculated from Equation (B.13), with $\tau_p = \tau_{yp} = 140$ ksi and $a = \gamma_{yp}/\gamma_p = 0.562$, to be 38.38 ksi. The elastic range of the existing torsion bar has, therefore, been extended to $\tau_{yp} + \Delta\tau$, or 178.38 ksi.

The factor of safety can now be determined as the ratio of the maximum allowable shear stress (177.15 ksi) and the maximum shear stress attained in the bar while in service $\tau_{BAR_{10}}$, which occurs at 10 inches of travel. From Equation (A.12), $\tau_{BAR_{10}}$ can be calculated to be 138 ksi, and the factor of safety (F.S.), from Equation (B.13) is then determined to be 1.29 on additional "yield."

$$F.S. = \frac{\tau_p + \Delta\tau}{\tau_{BAR_{10}}} \tag{B.14}$$

This factor of safety is employed in all subsequent designs of torsion bar suspensions.

TORSION BAR OR TORSION TUBE OVER BAR DESIGN

A torsion bar or torsion tube over bar can be designed with the same factor of safety as the existing bar, for the specific suspension characteristics (D, R, k_{eq}, β, θ_s, θ_{10}) which were previously determined. If a torsion "bar only" is desired, the length of the bar is fixed at, approximately, 82 inches, because it must be anchored on the opposite side of the vehicle; and $k_{BAR} = k_{eq}$. If a tube-over-bar is needed (usually for heavier wheel loads), values of L_B and k_{BAR} must be assumed and a trial and error procedure must be employed. In either case, the service shear stress in the bar at 10 inches of travel can be computed from Equation (A.12) where the diameter of the bar is obtained from k_{BAR} (Equation (A.8)).

To design the bar with the same factor of safety as the existing bar (or with a different factor of safety), Equation (B.14) can be used to solve for the value of $\Delta\tau$ required to achieve the desired factor of safety. Substitution of $\Delta\tau$ into Equation (B.13) and solving for "a", will locate the elastic-plastic boundary in terms of the intermediate radius r_i, because $a = r_i/r$. If a strain hardenable material is being used, "a" must be solved for iteratively, by entering the shear stress strain

curve with a value of γ_p, picking off the corresponding value of τ_p, solving Equation (B.13) for a value of "a", and then solving for $\gamma_p = \gamma_{yp}/a$, until the preset strains match. A value of "a" greater than or equal to 1.0, actually has no physical meaning other than indicating the bar need not be preset at all, because the in-service shear stresses are not exeeding the shear stress yield point within the factor of safety specified.

As stated before, Reference 3 recommends a maximum applied shear strain γ_{max} of 0.022 radians during presetting of torsion bars made of through hardened material of hardness near Rockwell C50. This value of γ_{max} prevents the bar from being unnecessarily damaged, because most of the cross section has been yielded and very little additional torque capacity can be achieved. A value of "a" less than or equal to 0.55 ($a = \gamma_{yp}/\gamma_p = \tau_{yp}/G\gamma_p = 140/(11500)\ (0.022) = 0.55$) indicates that too much of the cross section of the bar must be yielded to attain the specified factor of safety. In such a case, k_{BAR} must increase (by increasing d and/or decreasing L_B). If a "bar only" is being analyzed, the bar cannot be designed of sufficient strength, and a tube-over-bar design should be attempted.

If the value of "a" is between 0.55 and 1.0, the bar can be preset to attain the specified factor of safety. Because the preset shear strain is known, $\gamma_p = \gamma_{yp/a}$, the preset stress τ_p can be obtained from the shear stress strain diagram and the torque required to preset the bar can then be calculated from Equation (B.11).

If a tube over bar is being designed, the design continued to determine the dimensions of the tube such that the tube will fit over the bar, have sufficient strength, and satisfy Equation (A.7) for k_{eq}. The length of the tube is assumed to be 10 inches shorter than the length of the bar, such that, when assembled, the tube over bar torsion assembly will resemble that of the existing suspension shown in Figure A.3. The dimensions of the tube can now be obtained by solving two simultaneous equations. Because the equivalent spring rate k_{eq} and the spring rate of the bar (initially assumed) are known, the spring rate of the tube can be solved for by using Equation (A.7) in terms of the quantity $(D_T^4 - d_T^4)$ where D_T and d_T are the outside and inside diameters of the tube, respectively,

$$\frac{1}{k_{eq}} = \frac{1}{k_{BAR}} + \frac{1}{k_{TUBE}} \qquad (A.7)$$

and with Equation (A.9) the quantity $(D_T^4-d_T^4)$ can be solved for implicitly as

$$(D_T^4-d_T^4) = \frac{32\ L_T}{\pi\ G}\left(\frac{k_{eq}\ k_{BAR}}{k_{BAR}-k_{eq}}\right) \tag{B.15}$$

The second equation needed, relates the shear stresses in the bar and the tube at any given roadarm rotation. For consistency, the same relation between tube and bar stresses will be used as that of the existing tube and bar, that is, $\tau_{TUBE} = 2/3\ \tau_{BAR}$.

Therefore, combining Equations (A.12) and (A.13), and solving for D_T, the outer tube diameter yields

$$D_T = \frac{2}{3}\ \frac{(D_T^4-d_T^4)}{d^3} \tag{B.16}$$

Once the outer tube diameter is solved, the inner tube diameter d_t, and tube spring rate k_{TUBE}, can also be determined. A final check on the design is to see if the calculated inner tube diameter is greater than the bar diameter. If it is not, the process is repeated with different values of L_B and k_{BAR} until an acceptable solution is obtained. If the wheel load is high, and the desired equivalent spring rate k_{eq} is low, there may not exist an acceptable solution. This condition would require a large diameter bar to be strong enough and a length long enough to obtain the specified value of k_{eq}. Because the bar length in a tube over bar configuration is limited to about 75 inches (82 inches for a "bar only") an acceptable solution may not be obtainable. This is the procedure that was employed to determine if the suspension characteristics, given in Figures 12 and 15 of the text, were realizable (e.g., could a bar or tube over bar be found which satisfies the previous constraints of vehicle weight per wheel, geometry, safety factor, etc.). These were the suspensions then used to estimate the weights for the weight study, presented in the text.

APPENDIX C

WEIGHT ALGORITHMS USED IN WHEEL DIAMETER VERSUS SUSPENSION WEIGHT STUDY

This appendix contains the weight algorithms, suspension component weights, and vehicle buoyancy gains that were used in the "effect of wheel diameter on suspension weight and vehicle buoyancy gain" study presented in the text.

The weight algorithms listed in Table C.1 were used to approximate the

TABLE C.1 - WEIGHT ALGORITHMS

WHEEL WEIGHTS EQUATIONS

A. RUBBER $W_R = 23468 \left(\frac{1}{255+26.5(D-14)}\right)\left(\frac{D-1.25}{2}\right)$

B. WHEEL RIM AND WEB

$$W_W = \left[(0.373)\left(\frac{D}{2}-1.375\right)\left[\left(\frac{W}{N}\right)\left(\frac{1}{255+26.5(D-14)}\right)+0.25\right] + (2)(0.298)\left(\frac{D}{4}+1.062\right)\left(\frac{D}{2}-5.875\right)\right] N$$

C. HUB AND SPINDLE $W_H = 35N$

D. WEAR RING

$$W_S = \left(\frac{D}{2}-2.375\right)(1.545)\,N$$

TORSION BAR WEIGHT EQUATIONS

A. BAR $W_B = \frac{\pi d^2}{4}(L_B)(0.281)\,N$

B. TUBE $W_T = \frac{\pi(D_T^2-d_T^2)}{4}(L_T)(0.281)\,N$

C. TRUNNION AND ANCHORS $W_{TA} = 40N$

ROADARM WEIGHT EQUATION $W_{RA} = (88.256+bh(L_{eff}-1.325h\sin\phi))(0.281)\,N$

suspension weights for wheel diameters of 20 inches or greater, and are felt to be accurate to within ±5 percent of the actual suspension weight.

The actual dimensions of the suspension components used to calculate the weights are listed in Table C.2. The dimensions of all four roadarms were obtained from the

TABLE C.2 - DIMENSIONS OF SUSPENSION COMPONENTS

Roadwheel			Roadarm					Torsion Bar				
N	D (in)	L_A (in/lb)	b (in)	h (in)	L_{eff} (in)	R (in)	α (deg)	L_B (in)	d (in)	L_T (in)	D_T (in)	d_T (in)
18	14	255	2.0	4.0	7.375	13	0.0	82	1.48	-	-	-
14	20	414	2.0	4.25	8.1679	14	-23.62	82	1.76	-	-	-
12	26	573	2.5	4.5	8.8434	13	-20.87	65	1.85	55	2.85	2.5
10	30	679	2.625	5.43	5.7111	12	-23.98	75	1.95	65	2.73	2.23

NOTE:
N = number of roadwheels per vehicle
D = diameter of roadwheel
L_A = allowable load per inch of nominal tire width
b = width of roadarm rectangular cross section
h = depth of roadarm rectangular cross section
L_{eff} = effective length of roadarm
R = length of roadarm from centers of hubs
α = inclination of roadarm toward or away from vehicle
L_B = active length of bar
d = diameter of bar
L_T = active length of tube
D_T = outside diameter of tube
d_T = inside diameter of tube

design procedure outlined in Appendix A for a rectangular cross section (the existing roadarm was redesigned with a rectangular cross section for comparison). The torsion bar dimensions were obtained from the design procedure in Appendix B.

Table C.3 lists the individual weights of the suspension obtained by using the

TABLE C.3 - SUSPENSION SYSTEM WEIGHT BREAKDOWN

Wheel Diameter (Inches)	14	20	26	30
Wheels (Rubber, Rim, Hub, Spindle, Wear Ring) (lb)	1872	1815	1921	1915
Torsion Bars (lb)	1434	1345	1342	1567
Roadarms (lb)	745	696	638	594
Total Weight (lb)	4051	3856	3901	4076
ΔW (lb)	150	-45	0	175

weight algorithms. The change in weight ΔW represents the change in weight relative to the existing suspension weight.

Buoyancy gains (or losses) associated with each wheel diameter are listed in Table C.4 and were obtained by calculating the change in volume on both sides of the

TABLE C.4 - BUOYANCY (GAIN OR LOSS)

Wheel Diameter (Inches)	14	20	26	30
Volume 1 (lb)	1446	742	-	-510
Volume 2 (lb)	2606	2108	1630	1304
Volume 3 (lb)	2040	1750	1408	1168
Total ΔB (lb)	6092	4620	3038	1962
Net Buoyancy Gain $\Delta B - \Delta W$ (lb)	5942	4665	3038	1787

vehicle resulting from either raising or lowering the sponson from its original (existing) position (see Figure 11). As mentioned before, a buoyancy gain can be realized for the existing vehicle "as is" by fairing in the discontinuity of the existing sponson (Volume 2).

The total buoyancy gain is divided up into three sections, or volumes, (as in Figure 11). The first volume being the change in height of the forward sponson section. The second volume is the result of fairing in the discontinuity between the forward and aft sections of the sponson. The third volume is a further elongation of the aft sponson section to just forward of the water jets. The net buoyancy gain is the difference between the total buoyancy gain and the additional suspension weight.

REFERENCES

1. "Tank Design and Development," Detroit Arsenal, Warren, Michigan (1954).

2. "Tires, Solid Rubber, and Wheels, Solid Rubber Tires," Military Specification, MIL-T-3100B (22 Apr 1963).

3. "Engineering Design Handbook," Automotive Series, U.S. Army Material Command Headquarters (Apr 1967).

4. Marks, L. S. and Z. Baumeister, Editors, "Mechanical Engineers' Handbook," 7th Edition, McGraw-Hill Book Co., Inc., N.Y. (1967).

5. Timoshenko, S., "Strength of Materials Part II: Advanced Theory and Problems," D. Van Nostrand Co., Inc., N.Y. (1956).

6. Singer, F., "Strength of Materials," 2nd Edition, Harper and Row Publishers, Inc., N.Y. (1963).

7. Boresi, A. P. et al., "Advanced Mechanics of Materials," 3rd Edition, John Wiley and Sons, Inc., N.Y. (1978).

8. Just, D. J. and W. J. Walley, "Torsion of Solid and Hollow Rectangular Beams," Journal of the Structural Division (Sep 1979).

AD-A111 513 DAVID W TAYLOR NAVAL SHIP RESEARCH AND DEVELOPMENT CE--ETC F/G 19/3
INVESTIGATION OF SMALL ROADWHEELS FOR USE ON TRACKED VEHICLES.(U)
OCT 81 D P KIHL, R A SWANEK
UNCLASSIFIED DTNSRDC-81/061 NL

Copies	
12	DTIC

Copies	Cod
1	11
1	112
20	112
1	17
1	170
1	173
1	173
5	173
5	173
1	173
1	173
10	521
1	522
1	522

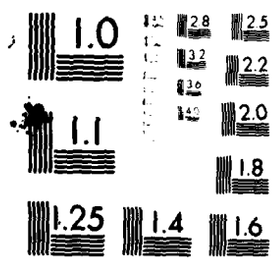

INITIAL DISTRIBUTION

ISTRIBUTION

e

Ellsworth

O'Neill

Wolfe

Murray

Eynon

Stavovy

Dinsenbacher
Kihl
Swanek

Critchfield

Beach

ports Distribution

classified Lib (C)

classified Lib (A)